Mode of Action of Trabectedin in Human Mixoid Liposarcoma Growing in Immunodeficient Mice: Evidence that the Drug Acts by Displacing FUS-CHOP Chimeric Protein From its Target Promoters

Thesis

Mode of action of trabectedin in human mixoid liposarcoma growing in immunodeficient mice. Evidence that the drug acts by displacing FUS-CHOP chimeric protein from its target promoters.

Open University, UK

Discipline of Life Sciences

by

Silvana Di Giandomenico

Master Degree in Molecular Biology

Mario Negri Institute for Pharmacological Research, Milan, Italy

September 2012

Date of Submission: 27 September 2012
Date of Award: 29 November 2012

ProQuest LLC.
789 East Eisenhower Parkway
P.O. Box 1346
Ann Arbor, MI 48106 – 1346

Mode of action of trabectedin in human mixoid liposarcoma growing in immunodeficient mice. Evidence that the drug acts by displacing FUS-CHOP chimeric protein from its target promoters.

Thesis submitted for the degree of Doctor of Philosophy

Open University, UK

Discipline of Life Sciences

Silvana Di Giandomenico

Mario Negri Institute for Pharmacological Research, Milan, Italy

September 2012

ABSTRACT

Trabectedin (ET-743, Yondelis) is a marine alkaloid isolated from the tunicate Ecteinascidia turbinata, cytotoxic against a variety of tumor cell lines in vitro and human tumor xenografts in vivo. It has been approved by EMEA for the 2nd line therapy of soft tissue sarcomas in 2007 and for the 2nd line therapy of ovarian cancer in 2009. Myxoid liposarcoma (ML) is a specific histological subtype within the family of adults soft tissue sarcomas. Specifically >90% of usual myxoid/round cell liposarcomas (ML/RCLS) are characterized by the chromosomal translocation t(12;16) (q13; p11), which produces the FUS-CHOP oncogene. Different chimera subtypes seem to respond differently to trabectedin in clinical setting. To elucidate the mechanisms behind the differential sensitivity to trabectedin, tumor myxoid liposarcomas type II and type III were xenografted

in nude mice, treated with trabectedin (0.15 mg/kg was injected i.v.) and the binding of FUS-CHOP to some of its target promoters was monitored by Chromatin immuno precipitation to verify the drug ability to displace the binding.We found that trabectedin was more effective on type II than type III ML xenografts. The response to trabectedin in Type II xenografts was associated with partial regression and pathological response. Type III ML xenografts appeared much less sensitive to trabectedin and tumors did not regress. Molecular analysis revealed that trabectedin was able to remove FUS-CHOP type II and III from its own gene targets 24 hours after treatment. 72 hours after treatment, FUS-CHOP Type III was attached to its targets whereas FUS-CHOP Type II remained unbound. The results suggest that the different of type II and type III to trabectedin are related to a different duration of the drug ability to display FUS-CHOP from DNA.

"Considerate la vostra semenza:

Fatti non foste per viver come bruti ma per seguir virtute e canoscenza"

La Divina Commedia, Inferno/Canto XXVI - vv. 118-120; Dante Alighieri

ACKNOWLEDGEMENTS

I lovingly dedicate this thesis to my loved and missed grandfather, Vito De Palma, who was a great scientist and who taught me the love for Science

Completing my PhD degree is probably the most challenging activity of my life. The best and worst moments of my doctoral journey have been shared with many people. It has been a great privilege to spend several years in the Department of Oncology at Mario Negri Institute of Milan, and its members will always remain dear to me.

There are a number of people without whom this thesis might not have been written, and to whom I am greatly indebted.

To my mother and father, who represented a source of inspiration to me throughout my life, a very special thank you for supporting me in my determination to find and realize my potential, and to make this contribution to our world.

I owe my loving thanks to my dear husband Server for his unconditional support both practically and emotionally throughout my degree. Without his encouragement, understanding and patience, which are greatly appreciated, would be impossible for me to start and finish my Ph.D study.

Foremost, I would like to express my sincere gratitude to Prof. Maurizio D'Incalci for the continuous support of my Ph.D study and research, for his patience, motivation and

knowledge. His guidance helped me in all the time of research and writing of this thesis. I could not have imagined having a better advisor and mentor for my Ph.D study.

I thank my friends in Mario Negri, in particular, I am grateful to Roberta Frapolli for supporting and enlightening me during my Ph.D research and for the great time I spent with her working on my project which was an important opportunity for my scientific growth.

I warmly thank Giulia Taraboletti for her guidance in the angiogenesis analysis and for her essential assistance in reviewing my thesis.

I wish to express my warm and my gratitude to Elisa De Stanchina for being so supported before and during my Ph.D Study.

Lastly my sincere thank goes to Dr Stephen Nimer for offering me the opportunities to work in his Laboratory and leading me working on diverse exciting projects. I also thank my labmate in Nimer's Lab, Goro Sashida for the stimulating discussions and for all the fun we have had in 2 years.

PREFACE

The work described herein was performed at the Mario Negri Institute for pharmacological Research in Milan, Italy from 2009 to 2012.

The work was performed under the supervision of Prof. Maurizio D'Incalci (director of studies), Dr. Roberta Frapolli (third monitor part) and Prof. Ian Judson (external supervisors).

DECLARATION

This thesis has not been submitted in whole or in part for a degree or diploma or other qualifications to any other university.

The experimental work described here was performed by myself. Collaborations to perform specific parts of the project were clearly indicated in the "Results" and "Materials and Methods" chapter.

Table of Contents

Chapter 1:

INTRODUCTION

Sarcomas are a heterogeneous group of rare solid tumours of mesenchymal cell origin with distinct clinical and pathological features, and are divided into major categories: sarcoma of tissue (including fat, muscle, nerve and nerve sheath, blood vessels, and other connective tissues) and sarcomas of bone [1].

1.1 Soft tissue sarcomas (STS)

Soft tissue sarcomas (STS) are the most frequent type of sarcomas; the annual incidence in Itay for 2 011 was approximately 3000 cases per year [2].

In the last two decades our knowledge about the molecular pathogenesis of these tumours has increased dramatically, whereas little progress has been made on the therapy with the exception of the gastrointestinal sarcoma (GIST) driven by activating mutations of the proto-oncogene KIT, and thus sensitive to Imatinib [3], [4].

The most common primary sites are head and neck (9%), torso (18%), upper extremity (13%), retroparitoneum (13%), thigh, buttock and groin (46%). The anatomic site of the primary disease is important for treatment and for outcome (figure 1). STS metastasize to the lungs and others; tumours arising in the abdominal cavity usually metastasize to the liver and peritoneum [3].

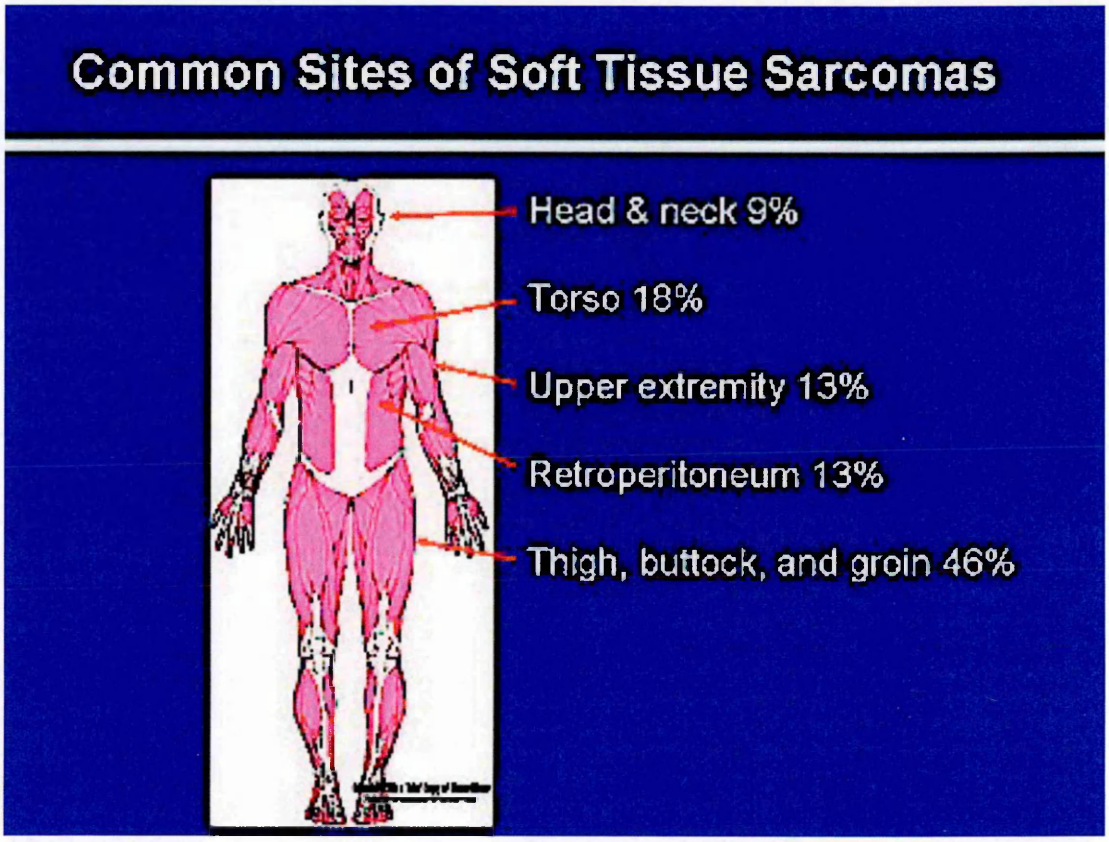

Figure 1: common sites of Soft Tissue Sarcoma (modified from http://www.medscape.org/viewarticle/572 942)

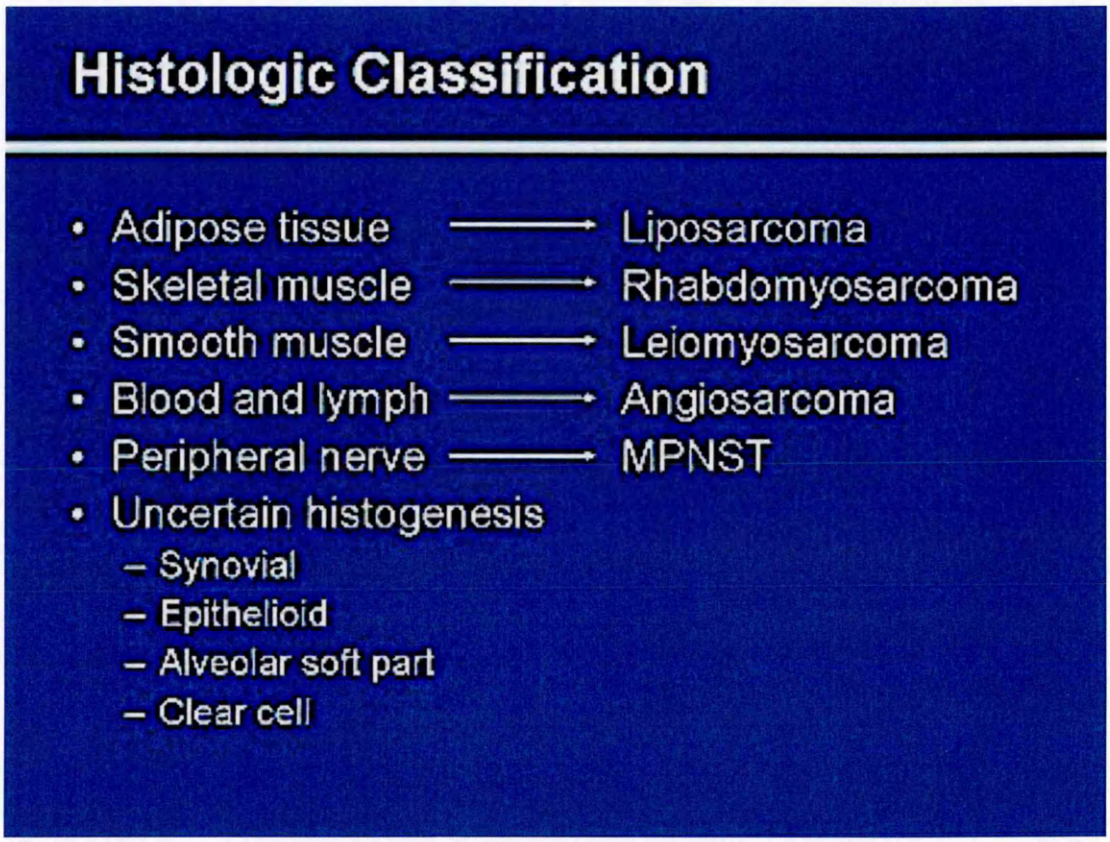

Figure 2: histological classification (modified from http://www.medscape.org/viewarticle/572 942)

In recent years, molecular genetic testing has been useful to segregate sarcomas into two major genetic group: (a) sarcomas with specific genetic alterations and simple karyotypes including fusion genes due to reciprocal translocations (e.g. FUS-CHOP in myxoid liposarcomas) and specific mutations (e.g., KIT mutations in GISTs); and (b) sarcomas with nonspecific genetic alterations and complex unbalanced karyotypes, reflected by numerous genetic losses and/or gains [3, 4]. Chromosomal translocations are the majority of specific genetic alterations associated with sarcomas. Most of the chromosomal translocations have been cloned, and most of the fusion genes have been identified (Table 1). These fusion genes encode chimeric proteins that are important for the biology of the tumours, behaving in most cases as transcription factors that alter the transcription of multiple downstream genes and pathways. The resulting oncoproteins can provide useful diagnostic and prognostic information.

Soft tissue sarcomas (STS) with complex genomic profiles (50% of all STS) are predominantly composed of spindle cell/pleomorphic sarcomas, including leiomyosarcoma, myxofibrosarcoma, pleomorphic liposarcoma, pleomorphic rhabdomyosarcoma, malignant peripheral nerve sheath tumour, angiosarcoma, extraskeletal osteosarcoma, and spindle cell/pleomorphic unclassified sarcoma (previously called spindle cell/pleomorphic malignant fibrous histiocytoma). These neoplasms show, characteristically, gains and losses of numerous chromosomes or chromosome regions, as well as amplifications. Many of them share recurrent aberrations (e.g., gain of 5p13-p15) that seem to play a significant role in tumour progression and/or metastatic dissemination [3, 4].

TUMOR	ABERRATION	GENES INVOLVED
Other Sarcomas		
Alveolar soft part sarcoma	der(17)(X;17)(p11;q25)	*ASPL-TFE3*
Angiomatoid fibrous histiocytoma	t(2;22)(q33;q12) t(12;16)(q13;p11)	*EWS-CREB1* *TLS-ATF1*
Clear cell sarcoma	t(12;22)(q13;q12) t(2;22)(q33;q12)	*EWS-ATF1* *EWS-CREB1*
Congenital/infantile – fibrosarcoma	t(12;15)(p13;q25)	*ETV6-NTRK3*
Dermatofibrosarcoma protuberans	t(17;22)(q22;q13) and derivative ring chromosomes	*COL1A1-PDGFB*
Desmoid fibromatosis	Trisomy 8 or 20; loss of 5q	*CTNNB1* or *APC* mutations
Epithelioid sarcoma (proximal type)	Bi-allelic inactivation of 22q11.2	*INI1*
Extrarenal rhabdoid tumor	Bi-allelic inactivation of 22q11.2	*INI1*
Extraskeletal myxoid chondrosarcoma	Rearrangements of 9q22	*CHN*
Sporadic GIST Familial GIST (Carney-Stratakis syndrome)	Activating kinase mutations KREBS cycle mutation	*KIT* or *PDGFRA* *SDH* subunit mutations
Inflammatory myofibroblastic tumor	Rearrangements of 2p23	*ALK*
Leiomyosarcoma	Complex alterations	Unknown
Low-grade fibromyxoid sarcoma	t(7;16)(q34;p11)	*TLS-BBF2H7*
Malignant peripheral nerve sheath tumor	Complex alterations	Unknown
Synovial sarcoma	t(X;18)(p11;q11) t(X;18)(p11;q11)	*SYT-SSX1* *SYT-SSX2*
Tenosynovial giant cell tumor/pigmented villonodular synovitis (TGCT/PVNS)	t(1;2)(p13;q35)	*CSF1*

Table 1: Morphologic diagnosis based on microscopic examination of histologic sections remains the gold standard for sarcoma diagnosis. However, several ancillary techniques are useful in support of morphologic diagnosis, including immunohistochemistry, classical cytogenetics, and molecular genetic testing. Molecular genetic testing has emerged as a particularly powerful ancillary testing approach because many sarcoma types harbor characteristic genetic aberrations, including single base-pair substitutions, deletions and amplifications, and translocations. Most molecular testing uses fluorescence in situ hybridization (FISH) approaches or polymerase chain reaction (PCR)-based methods. [3].

Since the choice of treatment is determined by the grade of the tumour, it is essential to have a careful review of the biopsy tissue by a pathologist who is experienced in diagnosing sarcomas. Complete staging and treatment planning by a multidisciplinary team of cancer specialists is required to determine the optimal treatment for patients with this disease. In most cases, a combined modality approach of preoperative or postoperative radiation therapy is used, rather than the radical surgical procedures that were used in the past. The role of chemotherapy is less defined. Because of the evolving nature of treatment options for sarcomas, all patients with such lesions should be included in a clinical trial whenever possible [3] .

1.2 Liposarcomas

Liposarcoma, the malignancy of adipocytes (figure 3), was first described by Virchow in the 1860s. It is the most common soft tissue sarcoma, comprising approximately 17% of all sarcomas, and 3% of all liposarcomas occur in the head and neck region, usually in the neck and cheek areas [5].

Because of the rarity of STS most studies deal with the whole group of STSs. The causes of STS are only poorly understood. The pathogenesis is based on various inherited and environmental factors and also, on pre- existing conditions [6, 7]. Among environmental factors exposure to ionizing irradiation, alkylating agents, arsenical pesticides and medications, vinyl chloride, immunosuppressive drugs, human immunodeficiency virus (HIV), herpes virus type 8 and anabolic steroids are described as risk factors. Exposure to chemicals such as phenoxyherbicides, dioxin and chlorophenol represent possible risk factors [8, 9]. Inherited conditions associated with STSs are Li-Fraumeni syndrome, neurofibromatosis type-1, Gardner's syndrome, retinoblastoma, Werner's syndrome and nevoid basal cell carcinoma syndrome (Gorlin's syndrome). Pre-existing medical conditions such as long-standing lymphoedema (Stewart-Treves syndrome) can also cause STS. Several cases with trauma preceding development of STS have been reported in the literature but there is no proof of a causal relationship [9, 10].

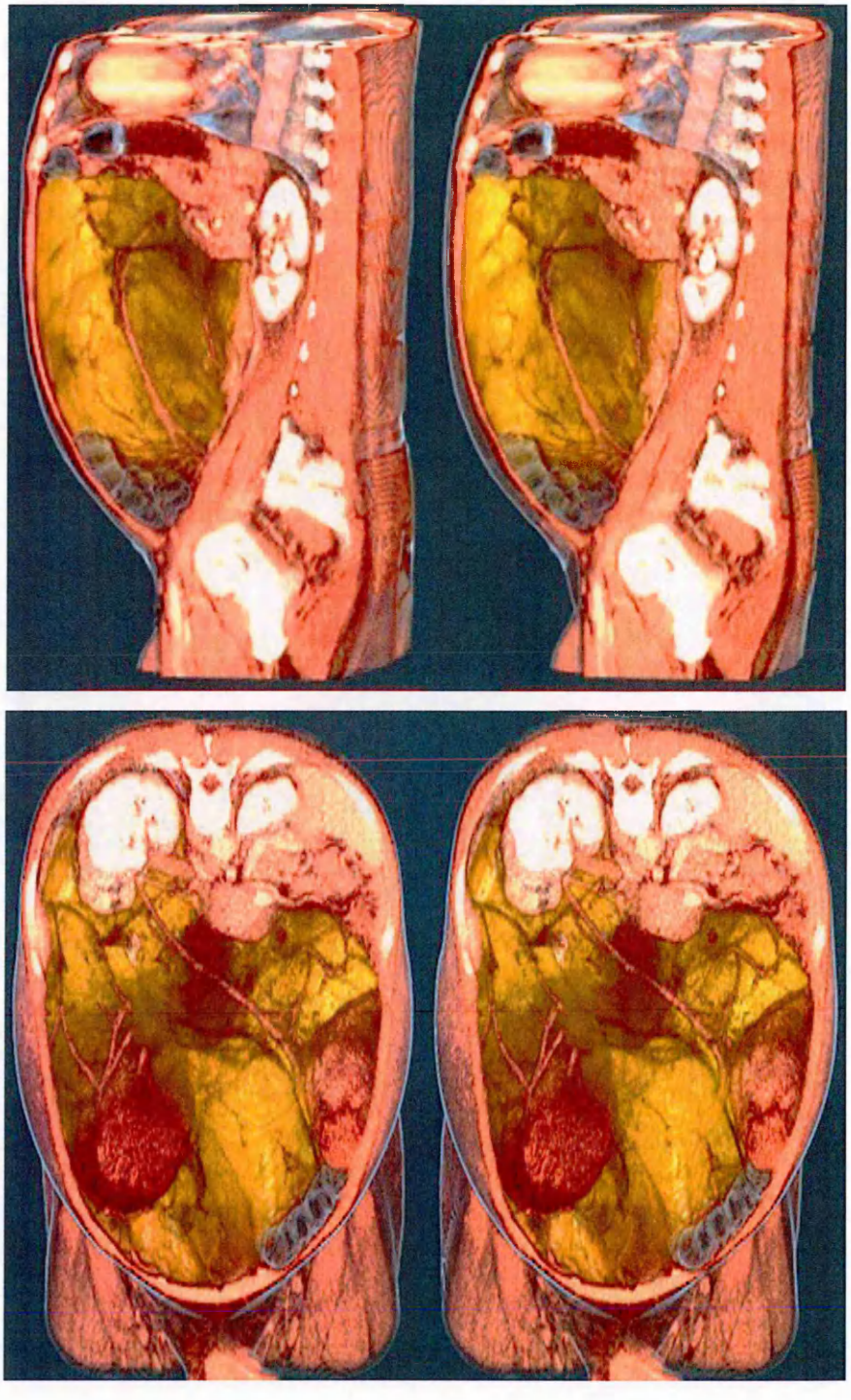

Figure 3: Volume Rendering of an abdominal CT scan with I.V. contrast. Late venous phase. Large abdominal liposarcoma with solid structures (no metastases). All the abdominal organs are dislocated. Noteworthy: The right kidney is malrotated and its ureter is elongated in an arch extending to the left side. (modified from http://www.flickr.com/photos/voxel12 3/4670052 2 17/)

1.2 .1 Diagnosis

1.2 .1.1. Clinical presentation

The localization of the tumour for clinical manifestation is very important. The presentation of liposarcoma on the extremities and superficial trunk is often a deep-seated mass, frequently of large size, painless or with mild or moderate pain and functional disturbances. Retroperitoneal liposarcomas tend to be diagnosed later, with more serious bowel symptoms such as gradual abdominal enlargement, pain, anorexia, vomiting and intestinal or urinary obstruction .

1.2 .1.2 Radiology

Computed tomography (CT) or magnetic resonance imaging (MRI) is used to perform radiology but MRI is preferred because of its high intrinsic contrast resolution and multiplanar imaging possibilities. The different LS subtypes have different magnetic resonance (MR) appearance and diagnostic pitfalls.[11]

It is difficult to distinguish the well-differentiated liposarcomas (WDLSs) of the extremities from lipomas, but the most important features that can suggest malignancy are: 1) male sex, 2) high age, 3) large size, 4) presence of thickened septa and nodular and/or globular areas of non-adipose tissue within the fatty lesion composing 25% or more of the volume [11, 12].

Dedifferentiated liposarcomas (DDLSs) occur within a WDLS. The radiological features suggesting dedifferentiation are areas of focal, nodular non-lipomatous region greater than 1 cm in size within a WDLS [12].

Myxoid liposarcomas (ML) often have a characteristic appearance with a large, well-defined and multi-lobulated lesion, localized intra and/ or intermuscularly. The high water content of the lesion gives atypical appearance on MRI. Adipose tissue in the

lesion, that constitutes less than 10% of the lesion and is often seen in septa or as small nodules in the lesion, is an important diagnostic feature [12].

Pleomorphic liposarcomas (PLSs) and round cell liposarcomas (RCLSs) have a non-specific soft tissue tumour appearance on MRI, with prominent heterogeneity and, often, areas of necrosis and hemorrhage. Small amounts of fat in the lesion suggest the diagnosis.

1.2 .1.3 Biopsy options

A pretreatment biopsy to diagnose and grade a sarcoma is highly preferred. Biopsy should be performed by an experienced surgeon (or radiologist) and may be accomplished by open incisional or needle technique. Different biopsy techniques are used in the pre-operative diagnosis, depending on the site, size and depth of the lesion [13]. Most of the sarcoma centers uses core-needle biopsy or longitudinally oriented incisional biopsy for extremity masses. Using Fine needle aspiration (FNA) allows to reduce the small risk of seeding sarcoma cells to the surrounding. Fine needle aspiration is also useful for diagnosing intra-abdominal, retroperitoneal and mediastinal masses.

The disadvantage of using FNA is that the cellular samples are small and it can be difficult to ascertain the tumour grade and histological type. For surgical planning, it is, however, most important to decide whether the lesion represents a soft tissue tumour and whether the tumour is benign or malignant [14]. A 90% diagnostic accuracy of differentiating a benign lesion from a liposarcoma has been reported with FNA cytology. An experienced cytopathologist is essential for this method to be successful, as is well-functioning collaboration between the radiologist, orthopedic surgeon and cytopathologist [15, 16].

1.2 .1.4 Method to detect and identify difference types of FUS-CHOP

Initially Fluorescent *in situ* Hybrizidation (FISH) is used to detect the chimera, then reverse transcription-polymerase chain reaction (RT-PCR) is used to identify the difference types of *FUS-CHOP* fusion gene transcripts, pathognomonic for ML. This method helps to differentiate between ML and other myxoid variants of STSs, such as myxoid malignant fibrous histiocytoma (MFH), myxofibrosarcoma, predominantly myxoid WDLS of the retroperitoneum, and intramuscular myxoma [17].

1.2 .2 Treatment

1.2 .2 .1. Surgery

The surgical procedure is considered the most important treatment modality. Ideally, the biopsy site should be excised en bloc with the definitive surgical specimen. Radical excision/entire anatomic compartment resection is not routinely necessary. Surgical clips should be placed to mark the periphery of the surgical field and other relevant structures to help guide potential future radiation therapy. If closed suction drainage is used, the drains should exit the skin close to the edge of the surgical incision (in case re-resection or radiation is indicated).

Wide local excision with clear margins is important for local tumour control [18]. Until 2006 the margins were reported as:

- "*Intralesional margin*": the dissection passed within the lesion and microscopic or macroscopic tumour was left at the margin of the resection.
- "*Marginal margin*": the lesion was removed in one piece but the dissection was through the pseudocapsule or reactive tissue surrounding the lesion.
- "*Wide margin*": the tumour was removed en bloc completely surrounded by a cuff of normal tissue but the dissection was within the involved compartment.
- "*Myectomy*" : the muscle in which the tumour was located was removed without opening its fascia.
- "*Compartmental resection*" was performed when the tumour involved compartment, beyond the fascial septa of the involved compartment, was removed en bloc.

Since 2006 there has been a modification in the classifications of margins as follows:

- *"Positive margin*": a gross tumour or microscopic tumour is left at the margin, which is reported.

- *"Negative margin"*: no microscopic tumour at the margin. The extent of the margin is reported.

More than 20 mm of normal tissue around the tumour, or fascia completely surrounding the tumour is classified as "wide margin" [3, 18].

1.2.2.2 Radiotherapy (RT)

The goal of RT is to kill tumour cells selectively, without irreversibly injuring adjacent normal tissue. This is done by exploiting two abnormal aspects of tumour behavior: decreased ability for repair and increased susceptibility to ionizing radiation damage. Tumours are generally less able than normal tissue to repair DNA damage, owing to defective repair mechanisms. Tumour cells are also comparatively more radiosensitive than normal tissues, as they are more frequently in radiosensitive cell-cycle phases. Thus, dividing the radiation dose into a number of treatment fractions provides two advantages that further exploit the biologic differences between tumour and normal tissue: it allows DNA repair to take place within the normal tissues, and it allows proliferating tumour cells to redistribute through the cell cycle and move into the more radiosensitive phases [19].

Radiotherapy in STS is considered to be an established method for elimination of microscopic tumour [20]. Radiotherapy as an adjunct to limited surgical excision was shown to achieve lower local control than radical resection alone and no differences in overall survival [21-24]. In a prospective randomized trial, it was shown that adjuvant postoperative radiation therapy in combination with conservative surgery improves local control for extremity STSs of both low and high grade in patients with microscopic negative, marginal or minimal microscopic positive surgical margins. No difference was found in overall survival. It is interesting to note that in the low-grade group 40% of lesions were of the radio-sensitive ML type [24].

Most STS that are unresectable do not respond to radiation therapy with sufficient tumour volume regression. Few studies on this subject report a 5-year local control rate of approximately 30–45% for unresected STSs treated with radiotherapy alone, median 61- 64 Gy [25, 26]. Local tumour control was related to tumour size at radiation, and radiation dose. In previous studies, it was reported that patients who received doses of less <63 Gy had a 5-year local control rate of 2 2 % compared with 60% for patients who received doses of 63 Gy or more [24]. Local control at 5 years was 51%, 45% and 9%, respectively, for tumours <5 cm, 5-10 cm and >10 cm. However, there are some reports on high radiation responsiveness in ML, both as case reports in unresected tumours and in a pre-operative setting[27-31].

1.2 .2 .3 Chemotherapy

Chemotherapy has been used in both a palliative setting and as adjuvant therapy for high-grade STSs. If the cancer is disseminated, the aim of chemotherapy is to shrink tumours and reduce the pain and discomfort they cause, but cure is unlikely. While a symptomatic benefit is frequently seen with chemotherapy for advance STS, a survival benefit has not been defined. In the adjuvant setting, several studies have demonstrated that doxorubicin or ifosfamide-based chemotherapy treatment gives benefits in terms of reduced local recurrence rate and distant metastases but no overall survival benefit [32-36]

1.2 .3 Histological subtypes

The different histological subtypes of liposarcoma all have different appearance and clinical behavior . The histopathological low-grade group constitutes of WDLS (grade I) and ML with <5% round cells (grade II) and the high-grade group of ML with >5% round cells (grade III or IV) and DDLS and PLS (grade IV)[37].

1.2 .3.1 Well-differentiated liposarcomas.

Well-differentiated liposarcomas represent 40-45% of all liposarcomas, with a peak incidence between 50 and 60 years [38]. The most common sites are limbs and the retroperitoneum. Four different histological subtypes are recognized, which is of limited practical importance. Sclerosing and inflammatory types are most often seen in the retroperitoneum. Well-differentiated liposarcomas may recur locally but do not metastasize unless they undergo dedifferentiation which is the most common in the retroperitoneum [39, 40].

According to the update based on the new WHO classification of STSs (2 002), the preferred term for lesions arising at surgically amenable locations should be "atypical lipomatous tumour" but for the lesions arising in the retroperitoneum and mediastinum, the term "WDLS" should be used because of their association with significant mortality[39]. Typical WDLS most often presents as large, deep-seated lesions of the thigh followed by lesions in the retroperitoneum. Tumours in the extremities and superficial trunk have disease-related mortality near 0% but in the retroperitoneum they have a high propensity of local recurrences and the disease-related mortality is high, either as a result of uncontrolled local disease or because of dedifferentiation and metastasis [41]. The risk of dedifferentiation of the lesions in extremities is <2 % but in the retroperitoneum it is >2 0% (3). The typical adipocytic (lipoma-like) WDLS has a characteristic morphology with relatively mature fat cells varying in size, enlarged atypical nuclei in varying number, low cellularity, few mitotic figures and minimal fibrous or myxoid zones. Mono- or multi-vacuolated lipoblasts may be found (figure 4). Karyotypic analysis of WDLS/atypical lipomatous tumour has shown the presence of extra ring and/or giant marker chromosomes derived from 12 q (13-15) [41]. Amplification of *MDM2* and *CDK4* from this region is frequently seen in WDLS but *TP53* is very rarely mutated in WDLS (figure 5) [1].

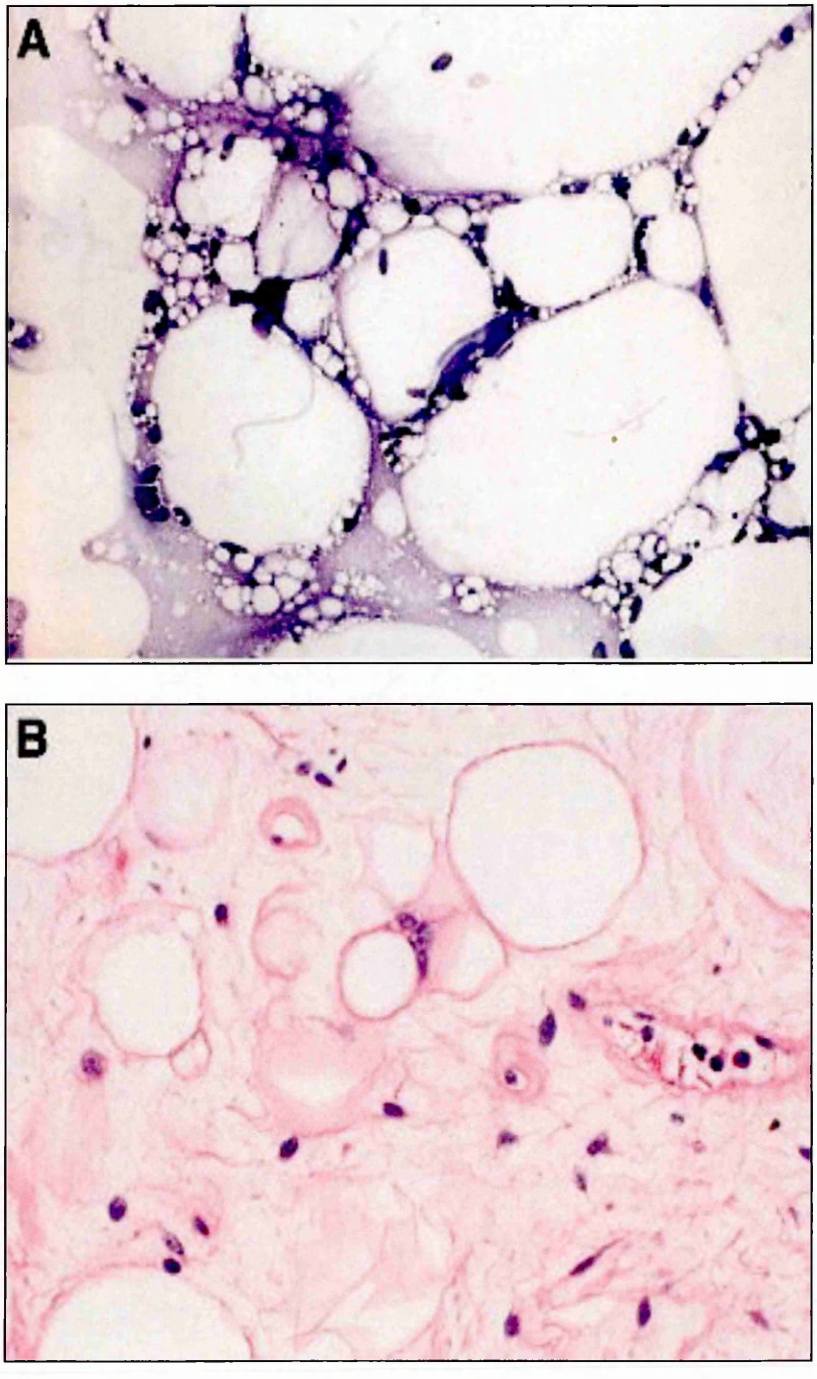

Figure 4 : (A) Aspirate of well-differentiated liposarcoma showing a lipoblast in a background of mature fat (MGG, ×400); and (B) Histology of the same tumour also illustrating a typical lipoblast (H and E, ×400)(modified from Diagnostic Cytopathology , 19 SEP 2 011 DOI: 10.1002 /dc.2 1794)

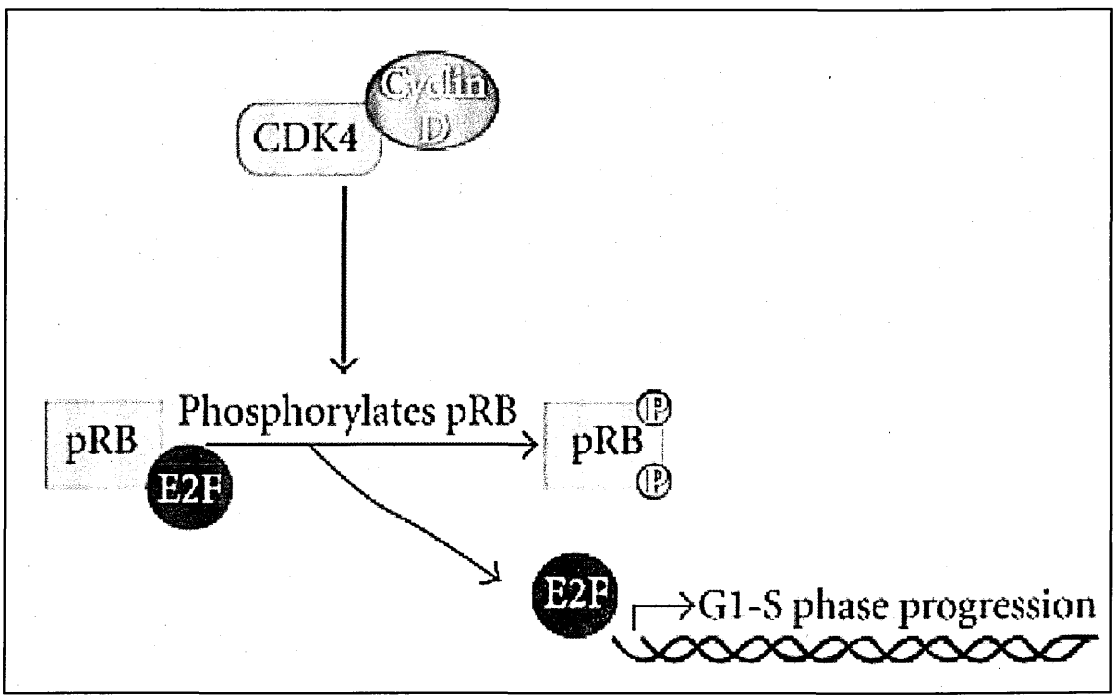

Figure 5: Cyclin dependent kinase CDK4 binds with cyclin D to form active complexes. This results in phosphorylation of Rb and dissociates pRb from the pRb-E2 F complex. E2 F binds DNA to upregulate transcription of genes required to progress to S phase) [42]

1.2 .3.2 Dedifferentiated liposarcomas

Dedifferentiated liposarcoma is a high-grade tumour that occurs most commonly in the retroperitoneum. The dedifferentiation is most probably time-dependent and the majority of the tumours present as de novo lesions [43]. Local recurrence rate after surgery of 41–52 %, distant metastasis rate 15–17%, and a disease-related mortality rate of 2 8–30% have been reported. The tumours located in the retroperitoneum have significantly worse survival than tumours located at other sites [44]. The most common histological features in DDLSs are transition areas from WDLS to non-lipogenic sarcoma, which in most cases resemble high-grade fibrosarcoma or MFH (figure 6).

A minority of lesions contains only areas of low-grade dedifferentiation resembling fibromatosis or well differentiated fibrosarcoma. Independently of the grade of dedifferentiation, the behavior of DDLSs is that of a high-grade malignancy. At a chromosomal level, DDLS frequently displays the same chromosomal abnormality associated with WDLS, i.e. presence of a supernumerary ring or giant chromosome derived from the 12 q (13-15) region [43]. *TP53* mutations, determined by molecular methods, are rare but amplification levels of *MDM2* and *CDK4* are more frequently higher in DDLS than in WDLS (figure 7) [1].

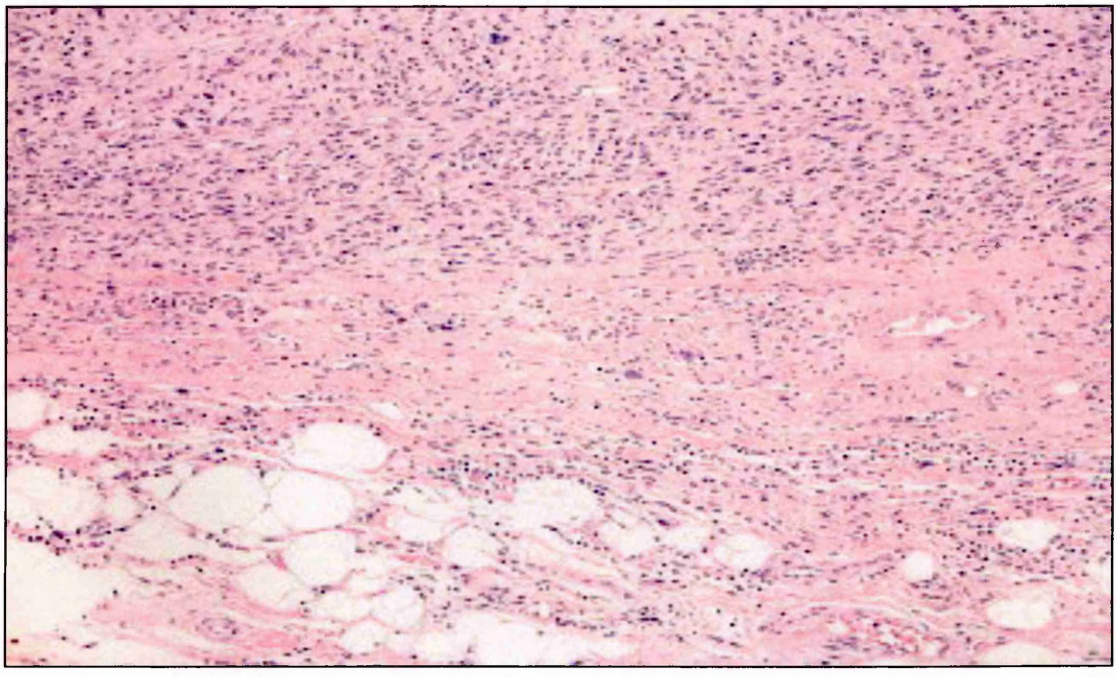

Figure 6: Example of dedifferentiation in a WDL. At the bottom of the picture the large fat vacuoles of the lower grade lesion are present. There is an abrupt transition to the more cellular dedifferentiated component near the top (H and E, ×100).[43]

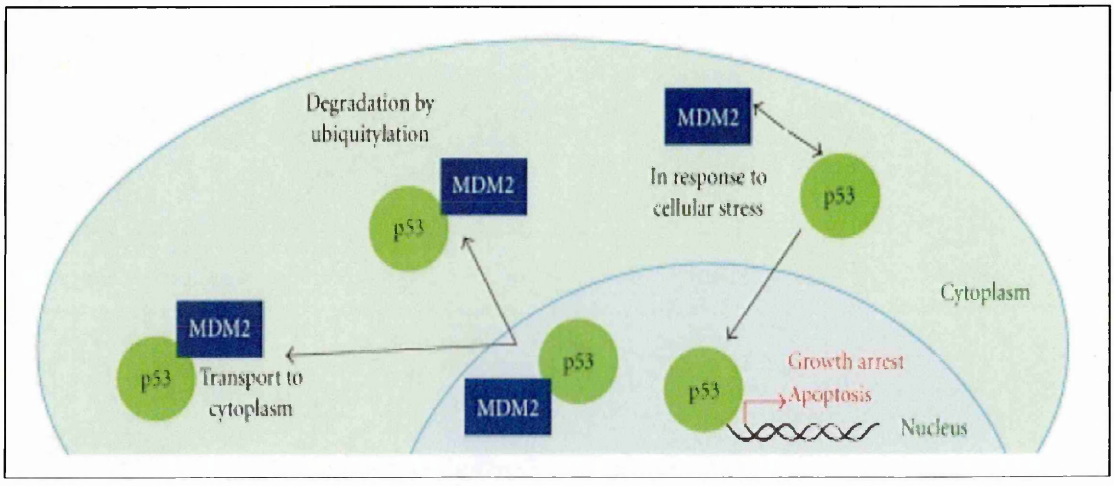

Figure 7: MDM2 binds to the transcriptional activation domain of p53, blocking transcription. MDM2 functions as a ubiquitin ligase, facilitating proteasomal degradation of p53. MDM2 releases p53 in response to cellular stress and p53 translocates to the nucleus where it acts as a transcription factor to enable growth arrest and apoptosis [42].

1.2 .3.3 Pleomorphic liposarcomas

Pleomorphic liposarcoma is the rarest type involving about 10% of liposarcomas [45]. It is a high-grade tumour that may mimic MFH or even carcinoma or melanoma. The diagnosis depends on the identification of, at least focally, lipogenic differentiation and/or lipoblasts that are pleomorphic and multivacuolated with hyperchromatic and scalloped nuclei [45, 46] (figure 8). The tumour suppressor gene *TP53* in PLS is often mutated together with complex chromosomal imbalances, mostly gains but also, though less frequently, losses. This subtype has a high propensity to recur locally and metastasize, and a 5 year local recurrence-free and metastasis-free survival of 50–58% and 48–58%, respectively, has been reported [45, 47].

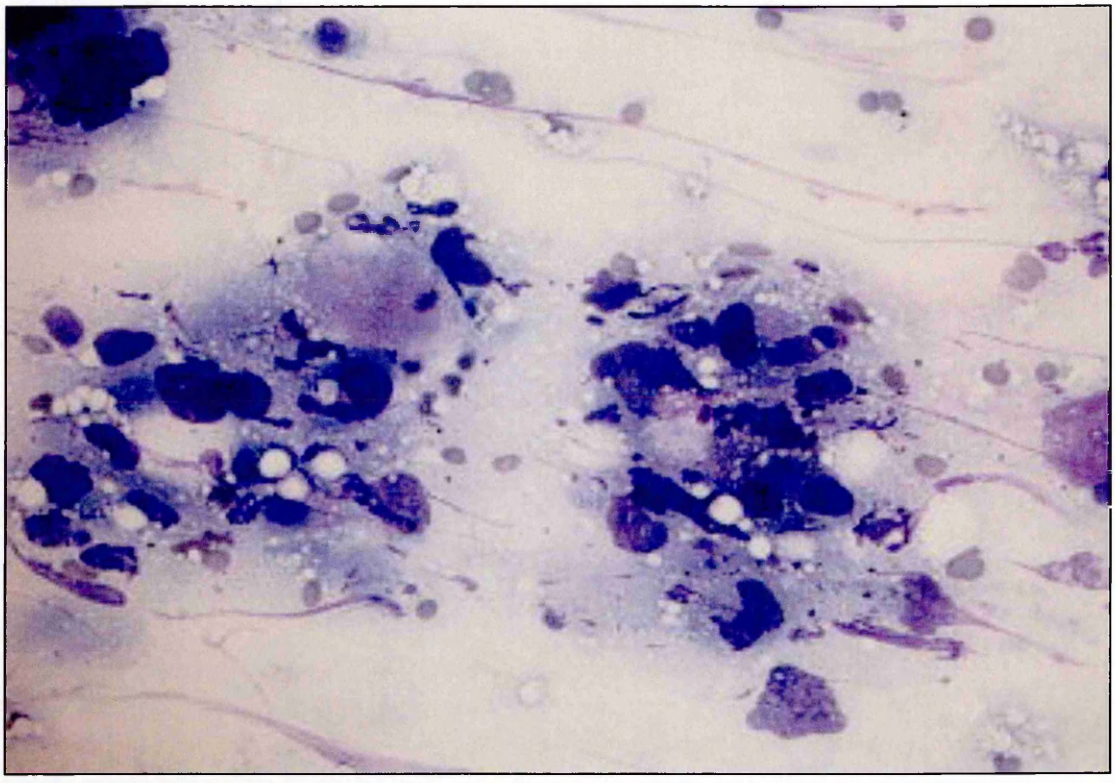

Figure 8: Aspirate from a pleomorphic variant of liposarcoma. The tumour cells are more numerous and have more ominous cytologic features than in other variants of LS. Occasional cytoplasmic vacuoles are the key to their lipogenous lineage (MGG, ×400) [45]

1.3 Myxoid Liposarcoma (ML)

ML is the second most common subtype of liposarcoma and accounts for more than one third of liposarcomas and 10% of all adult soft tissue sarcomas. Microscopically ML is made up of uniform round-oval primitive non-lipogenic cells and variable numbers of uni-multivacuolated lipoblasts intermixed with a well-developed plexiform capillary network and embedded in a myxoid matrix composed of hyaluronic acid. Depending on the proportion of the cellular component to the stroma and the prevalence of immature and mature cellular features ML is divided into a usual or pure subtype, and a round cell or cellular (RC) subtype. Usual ML is the most differentiated form and shows low cellularity, evidence of lipoblast differentiation and a conspicuous vascular network (figure 9) while the RC subtype presents the opposite extreme of the differentiation gamut, and shows high cellularity made up of primitive non-lipogenic cells, little or no intervening myxoid stroma and a capillary vascular pattern that is not easy to visualize (figure 10). Diagnosis of the RC subtype requires >5% hypercellular area [48, 49]. The presence of areas with greater cellularity, round cell (RC) is associated with a worse prognosis. Thirty-one percent of ML patients develop metastasis with bone metastases constituting 56% of these [50]. ML presents inferior survival compared to other low-grade sarcoma subtypes with a 5-year disease survival rate of 85% [51]. ML without RC is particularly radiosensitive with good local control rates with patients treated with adjuvant or neoadjuvant radiotherapy approaching 98% 5-year local control [52].

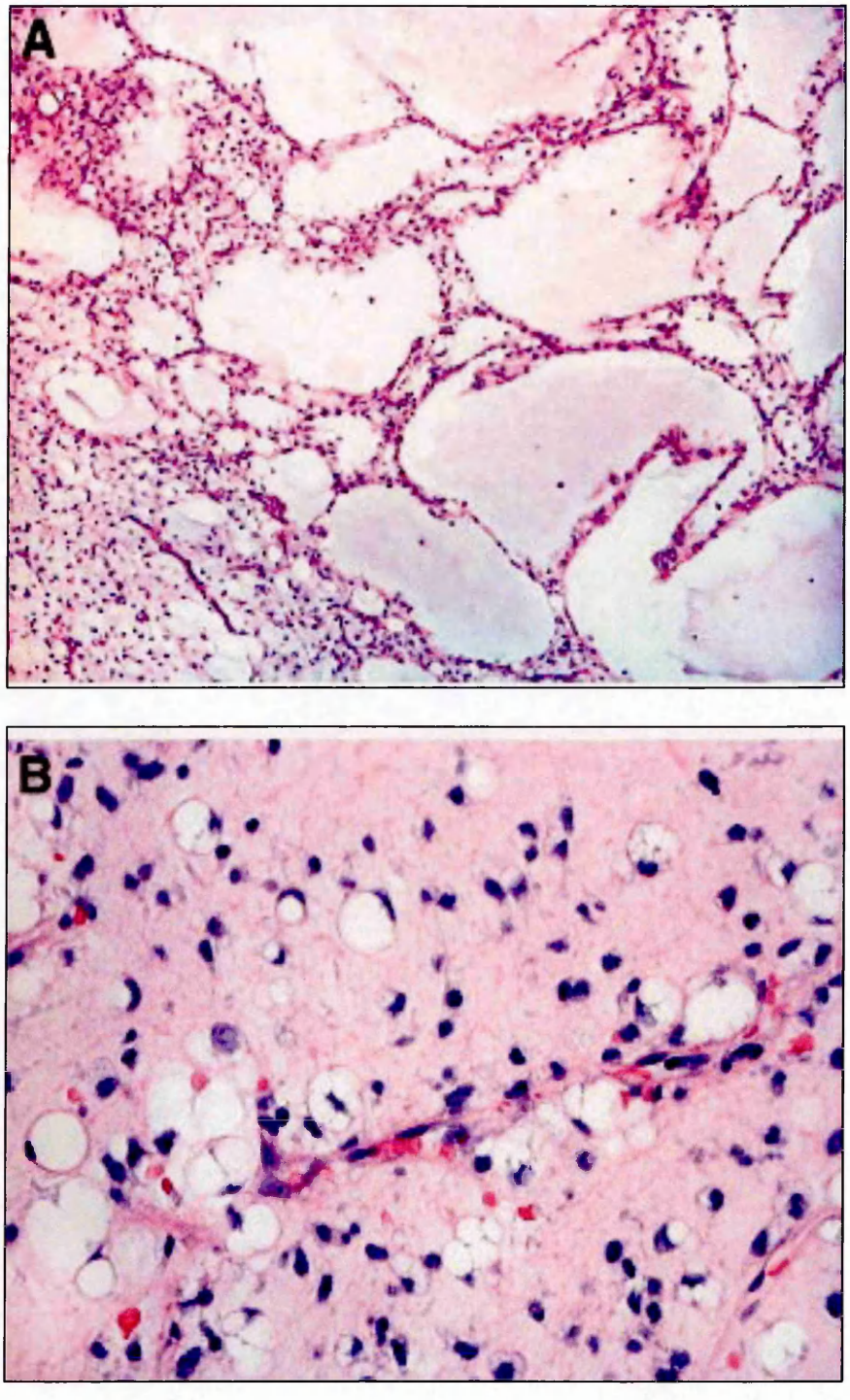

Figure 9: (A) Low power view of myxoid liposarcoma showing large pools of extracellular myxoid material. This pattern is often referred to as a "pulmonary edema" like pattern (H and E, ×40); (B) High power view of ML illustrating a characteristic vascular arcade (H and E, ×2 00) [50]

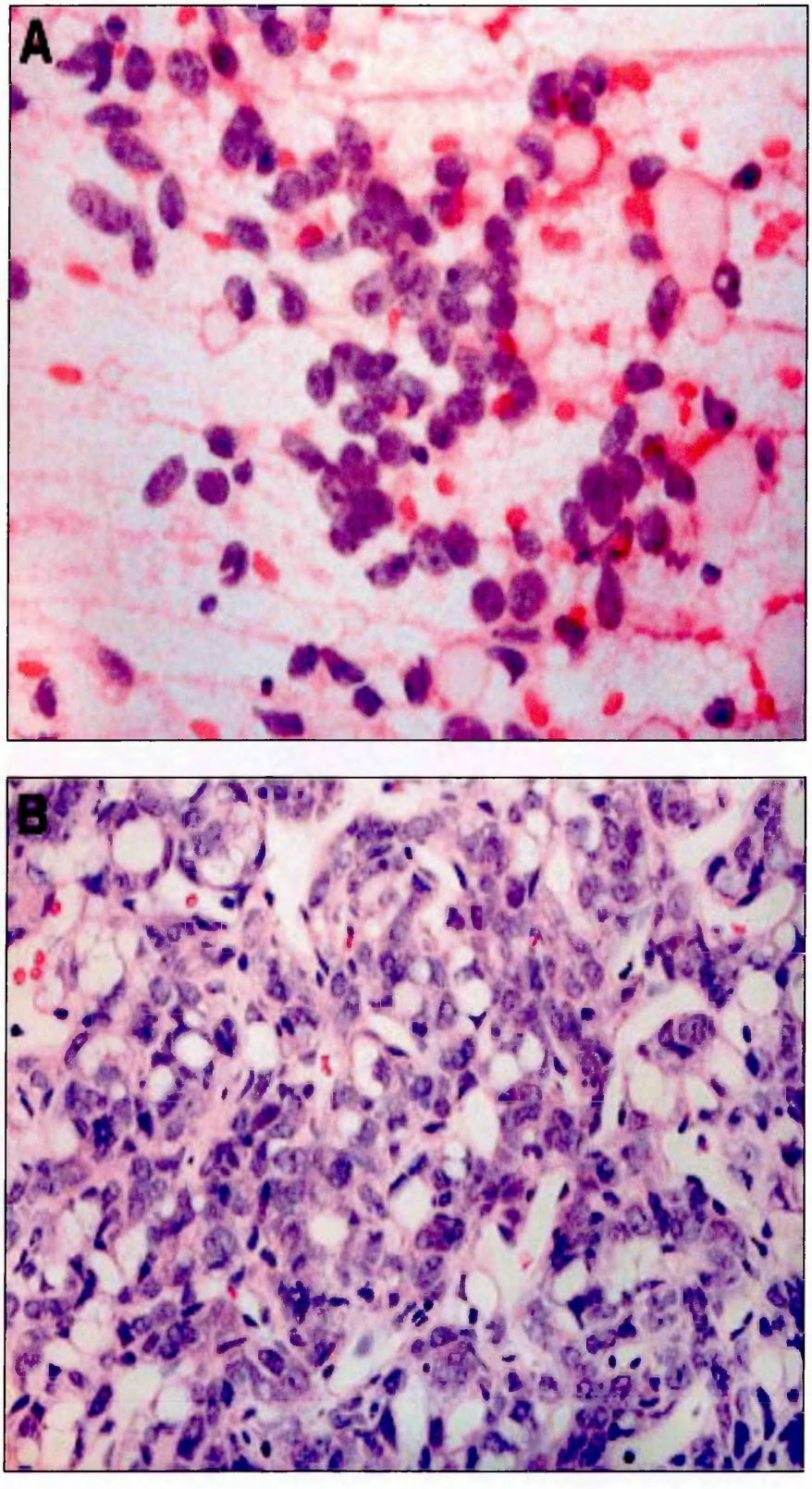

Figure 10: (A) Aspiration of the round cell component of ML/RLS. The cells have a primitive, small round blue cell appearance (H and E, ×400); (B) High power photomicrograph of a "pure" round cell focus of liposarcoma showing a dense cellular proliferation of cells with high N/C ratio (H and E, ×2 00) [53].

1.3.1. Molecular Genetics of Myxoid Liposarcoma

ML is characterized by the recurrent translocation t(12 ;16)(q13;p11) that results in the *FUS-CHOP* gene fusion that is present in over 95% of cases *[53, 54]*. In most cases, the amino terminal domain of *FUS* (also known as *TLS*) is fused to C/EBP homologous protein (*CHOP*, also known as *DDIT3* or *GADD153*) (figure 11) [54]. In rare cases, an alternative translocation event is found t(12 ;2 2)(q13;q12) that results in formation of the novel fusion oncogene where *EWS* takes the place of *FUS*. There is strong evidence for these translocations to be the primary oncogenic event in ML as these tumours have a relatively normal karyotype, the exception being a few recurrent cases of trisomy 8 [55, 56]. There are currently 11 different *FUS-CHOP* chimeras and 4 different known *EWS-CHOP* fusion genes (figure 12) [57]. In the most common variants, a portion of the amino terminus of *FUS* is fused to the entire coding region of *CHOP*. The *FUS-CHOP* transcript type does not appear to have a significant impact upon clinical outcome and RC content, necrosis and p53 expression remain stronger predictors of clinical outcome [53, 58].

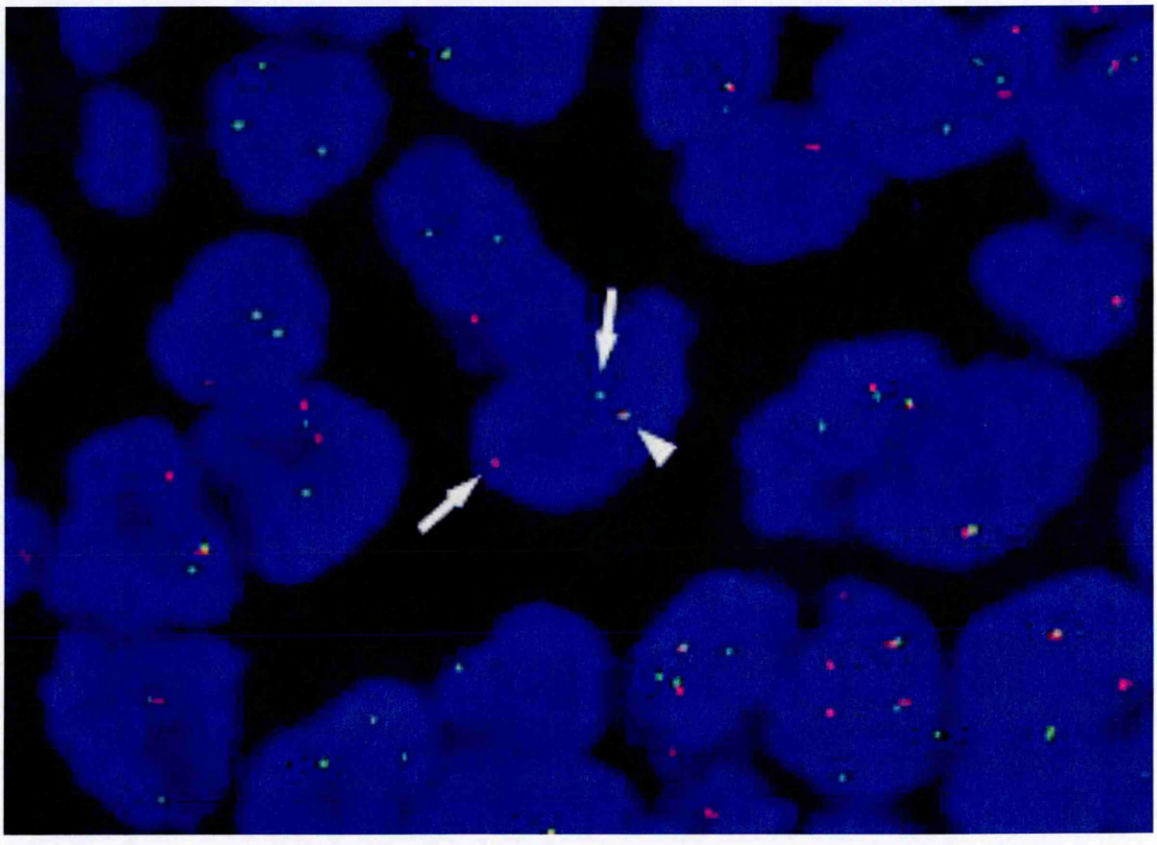

Figure 11: CHOP break apart FISH probe applied to a tumour with a RC component. The tumour cell has one fusion signal (arrowhead) and two break apart signals (arrows), indicating a rearrangement of one copy of the CHOP gene region (12 q13) [49].

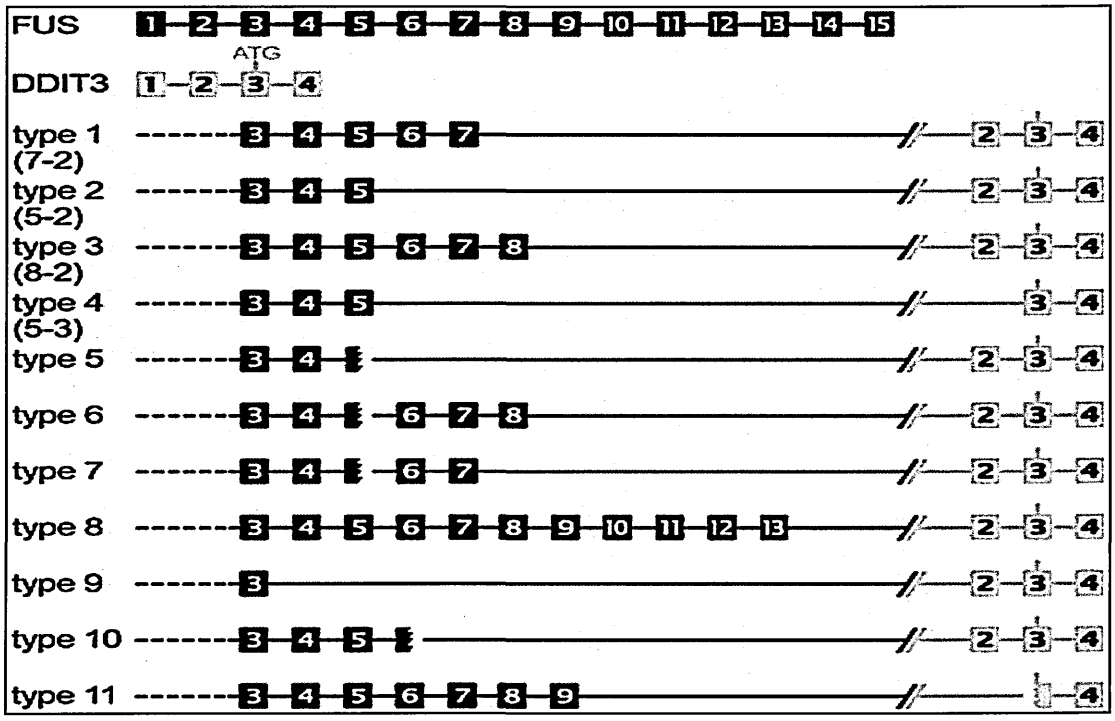

Figure 12: Classification of FUS-CHOP fusions [54]

There is evidence that the fusion transcript type may influence response to therapy although the studies are hindered by sample size [59]. Understanding how the FUS-CHOP fusion causes ML and uncovering any further molecular abnormalities in the disease will aid in development of novel targeted therapies [42, 60].

FUS belongs to the FET family of RNA-binding proteins that consists of FUS, EWS, and TAF15 as well as the closely homologous, Drosophila SARFH [61]. These structurally and functionally related RNA-binding proteins are composed of an SYGQ-rich amino terminus, an RNA recognition motif, a zinc finger motif, and at least one RGG rich repeat region [62]. FET proteins are expressed in most human tissues and appear to be regulated following differentiation in neuroblastoma cells and spontaneously differentiating human embryonic stem cells [62, 63].

Both FUS and EWS have been shown to localize to the nucleus and the cytoplasm, bind RNA, and are also involved in nucleo-cytoplasmic shuttling [63]. The FET family associate with various complexes involved in the induction of transcription, including RNA polymerase II (RNAPII), which regulates transcription and TFIID complexes, that binds DNA as part of the transcriptional machinery [64], implicating both FUS and EWS in transcriptional control. In addition, FUS has recently been shown to repress transcription of RNA polymerase III (RNAPIII), suggesting a broader role in regulation through multiple different mechanisms [65, 66]. Noncoding RNAs are capable of allosterically modifying FUS in response to DNA damage to inhibit the transcription factor CREB-binding protein (CBP) and p300 histone acetyltransferase activity, resulting in transcriptional inhibition at the cyclin D1 promoter in cell lines and shows a further role for FUS in transcriptional control. FUS has also been implicated in the DNA damage response as a downstream target of ATM, which can detect and coordinate DNA repair [42].

The *CHOP* gene, (also known as "C/EBP-homologous protein (CHOP)" and "growth arrest and DNA damage inducible *(GADD 153)*") encodes for a nuclear protein, which is a member of C/EBP family. CHOP is induced in response to endoplasmic reticular stress and is involved in mediating cell death in response to such stress stimuli, e.g. treatment with alkylating agents, ultraviolet (UV) light, nutritional deprivation, oxidative stress and stress that disturb endoplasmic reticulum function. [66]. CHOP also plays a role in regulating differentiation in adipocytes by interfering with the process in response to metabolic stress [67]. One of the important roles of CHOP is to heterodimerize with other members of the family, serving as a dominant negative protein by altering their transcriptional potential [67]. Within the constitutively active FUS-CHOP chimeras, CHOP retains the heterodimerization and DNA-binding domains and it is thus proficient in shortcutting the normal C/EBP activities [67, 68]. Among the activities of this important class of transcription factors, genetic and biochemical experiments established the key role of three members C/EBPα, β, and δ in adipocyte differentiation. C/EBPβ and C/EBPδ play redundant roles in the early phases of commitment, whereas C/EBPα becomes active and important in the later phases leading to terminal differentiation [69, 70].

The C/EBPs belong to the basic-leucine zipper class of transcription factors, six isoforms have been described, all of which act as homo- and/or heterodimers formed via a highly conserved bZIP domain [67]. The bZIP class of leucine zipper is characterized by juxtaposition of a region rich in basic amino acids to a region containing a repeat of hydrophobic amino acids, often leucines. The two regions form an α-helical conformation, one of this two regions dimerizes with an analogous region of a second bZIP protein forming a leucine zipper dimer. The basic region of the paired subunits interacts with a DNA binding site know as CAAT box . During adipogenesis, regulated expression is seen for several C/EBP family members, and recent gain- and loss-of-

function studies indicate that these proteins have a profound impact on fat cell development [69]. In cultured preadipocytic cell lines that have been induced to differentiate, C/EBPβ and δ mRNA and protein levels rise early and transiently. C/EBPα, on the other hand, is induced later in the differentiation process, slightly preceding the induction of most of the end-product genes of fat cells. The proadipogenic role of C/EBPβ and δ was originally made clear in gain-of-function experiments *in vitro* [69, 70]. Ectopic expression of C/EBPβ is sufficient to induce the differentiation of 3T3-L1 cells without the addition of hormonal inducers; similar experiments with C/EBPδ reveal that prodifferentiative agents are still required, but adipogenesis is accelerated. C/EBPβ may also be able to determine cells to the adipocytic lineage as well as promote their differentiation; ectopic expression of C/EBPβ (but not δ) in NIH-3T3 fibroblasts is permissive for adipogenesis in the presence of hormonal inducers [70].

The involvement of C/EBPα in adipogenesis is also strongly supported by *in vitro* data. Overexpression of C/EBPα in 3T3-L1 preadipocytes induces their differentiation into mature fat cells [69], and the expression of C/EBPα antisense RNA in these cells blocks this process. Animals that carry a homozygous deletion of the C/EBPα gene have dramatically reduced fat accumulation in WAT and BAT pads [71]. However, since these mice succumb to hypoglycemia within the first week of life as a result of a failure to activate gluconeogenesis in the liver, their reduced adiposity needs to be considered in light of their severe metabolic derangement. Indeed, the reduction in adiposity appears to be primarily a result of depressed lipogenesis, as markers of fat cell differentiation are still expressed in the fat pads of these animals. These transcription factors are expressed as a cascade in which C/EBPβ and C/EBPδ, expressed during the first stages of the adipocyte differentiation program, induce the expression of C/EBPα and PPARγ2 , the master regulator of adipogenesis [71-73]. PPARγ is a member of the

nuclear hormone receptor superfamily and heterodimerize with another nuclear hormone receptor (the retinoid X receptor, or RXR) to bind DNA and be transcriptionally active. PPARγ exists as two protein isoforms generated by alternative promoter usage and alternative splicing. PPARγ2 is 30 amino acids longer at the amino terminus than PPARγ1, and is the dominant isoform found in fat cells [73]. PPARγ1 is present at lower levels in adipose tissue and in a variety of other cell types, including macrophages, type II pneumocytes, and the epithelia of colon, bladder, breast, and prostate. However, PPARγ2 is more efficient at induce terminal differentiation in *in vitro and in vivo models.* A positive feedback loop mechanism between PPARγ2 and C/EBPα enhances their activities. This transcriptional cascade finishes with the expression of markers of mature adipocytes such as ap2 , adiponectin and adipsin [74-76]. It is possible that FUS-CHOP may interfere in cellular differentiation. In support, various studies suggest that FUS-CHOP functions by inhibiting adipogenesis and maintaining immature adipocytes in a continuous cycle of proliferation without differentiation. Introduction of FUS-CHOP into mice, where expression of the transgene is driven by the ubiquitously expressed elongation factor 1α (EF1α) promoter, results specifically in liposarcomas with inherent induction of adipocyte specific genes such as PPARγ *[77]*. Further evidence of adipogenic differentiation block resulting from FUS-CHOP expression was shown *in vivo* where mice expressing FUS-CHOP under the control of the aP2 promoter, which is a downstream target of PPARγ expressed in immature adipocytes, failed to develop liposarcomas, indicating interference between PPARγ and aP2 activation (figure 13) [78, 79].

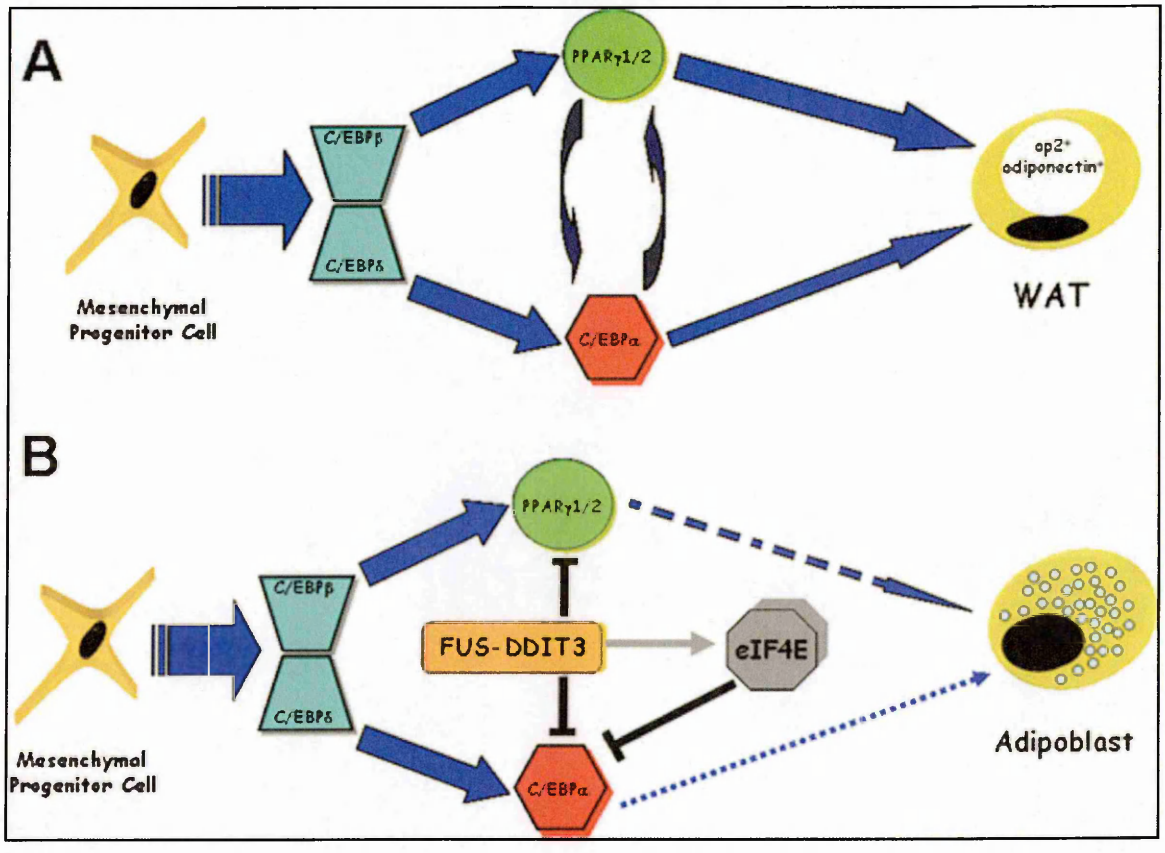

Figure 13 : Adipogenesis pathway: (A) PPARγ and C/EBP family transcription factor are involved in adypocite differentiation. Transcriptions are expressed in cascade in which C/EBPδ and C/EBPβ, expressed during the first stages of the adipocyte differentiation program, induce the expression of C/EBPα and PPARγ, the master regulator of adypogenesis. (B) FUS-DDIT3 blocks the adipocyte differentiation program in mesenchymal cell progenitors by interfering with the PPARγ and C/EBPα activities at the transcriptional level [79].

An emerging clinically relevant targetable pathway in ML involves the receptor tyrosine kinases (RTKs) MET, RET, and the PI3K signaling cascade. RET is overexpressed in ML compared to normal fat [80] and high expression has been correlated with poor metastasis-free survival in ML [81]. RET, IGF1R and IGF2 are highly expressed in ML and promote cell survival through both the PI3K/Akt and Ras-Raf-ERK/MAPK pathways [81, 82]. A panel of tyrosine kinases including PDGFRB, EGFR, MET, RET, and VEGFR2 are activated in both treated (with chemotherapy/radiotherapy or trabectedin) and untreated cases of human ML [83]. In addition to activation of MET in clinical ML specimens, MET and the ligand HGF are potentially regulated by FUS-CHOP. Both MET and HGF are highly expressed in mesenchymal progenitor cells transfected with FUS-CHOP in a disease mimicking allograft mouse model [77]. In a small clinical cohort, specific Akt phosphorylation was observed in the RC variant and 2 treated cases that harbored *PTEN* mutations, implicating RTK pathways signaling through Akt in ML [81].

FLT1 (that encodes the VEGFR1 protein) is expressed as an indirect downstream effect of FUS-CHOP expression in both FUS-CHOP transfected HT1080 (fibrosarcoma) and ML cell lines. However VEGFR tyrosine kinase inhibitors did not have a notable impact on proliferation in MLPS cell lines indicating a separate role in these cells [77, 84, 85].

Akt activation, particularly in the RC variant, suggests a role for phosphoinositide 3-kinases (PI3K). PI3Ks are activated upon phosphorylation of membrane bound receptor tyrosine kinases [82]. PI3K can activate many proteins including the protein serine-threonine kinase Akt, which when phosphorylated causes downstream activation and ultimately cell growth, cell cycle entry, and subsequently survival. The PI3K holoenzyme complex is composed of both a catalytic and regulatory subunit. The catalytic subunit, *PIK3CA*, encodes the p110α isoform and is commonly mutated in

various cancer types including breast, colon, brain and gastric malignancies [86, 87]. A recent study showed 18% of ML patients (n = 71) had *PIK3CA* mutations in either the helical (E542 K and E545K) or kinase (H1047L and H1047R) domain.

The presence of a *PIK3CA* mutation was associated with a shortened disease specific survival. Barrettina et al. showed one tumour with a homozygous *PTEN* mutation [88, 89] . PTEN is a tumour suppressor that dephosphorylates phosphoinositide substrates to negatively regulate the Akt signaling pathway, demonstrating more mechanisms for perturbation of the pathway (figure 14)[88].

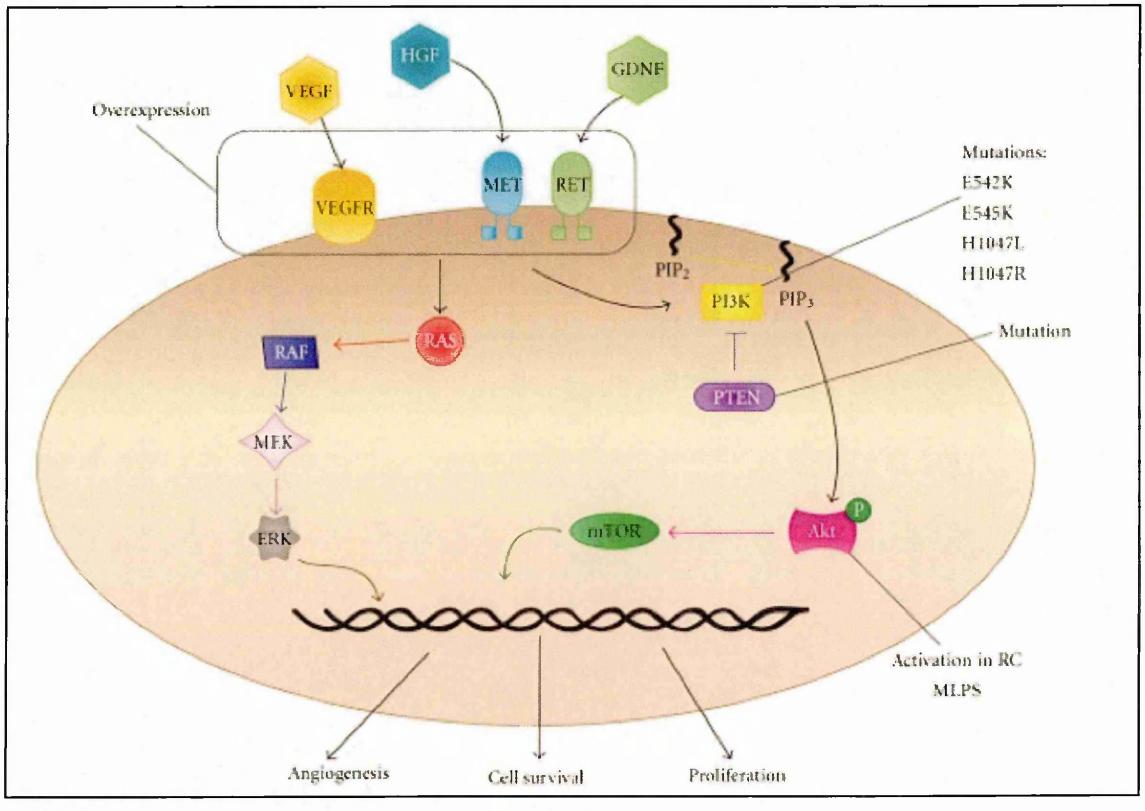

Figure 14: The PI3K pathway is highly active in MLPS, and this is potentiated at least in part by overexpression, and/or activation through RTKs such as MET, RET and VEGFRs. Upon ligand binding, RTKs activate downstream activation of genes involved in multiple cell processes such as cell survival, proliferation, and angiogenesis. These signals are mediated through the PI3K/Akt pathway and also through RAS. PIK3CA and PTEN mutations and Akt activation have also been documented in ML [42].

1.4 Novel Therapeutic Implication in Liposarcomas.

The current modalities available (chemotherapy, surgery and radiotherapy) for the treatment of liposarcoma are limited, creating a need to identify novel therapeutics.

1.4.1 MDM2 antagonist

The activity and level of the tumour suppressor protein p53 is negatively regulated by the E3 ligase MDM2 , which controls both its ability to trans-activate downstream genes and its proteasome mediated degradation. In tumours with wild type p53, its activity may be blocked through amplification and overexpression of the MDM2 locus.2 ,3. Due to the central role of p53 in oncogenesis and therapy response, the p53-MDM2 interaction is an interesting target for small-molecular therapy [90]. The goal is to reactivate p53 and induce downstream effects leading to programmed cell death or increased response to DNA-damaging therapies, as has been pursued by several groups. One of the most promising MDM2 antagonists is Nutlin 3A, which has been shown to activate wild type p53 in cancer cell lines, inducing cell cycle arrest and apoptosis in various cell lines, including osteosarcomas with amplified MDM2 [91, 92]. The amplification of MDM2 is much more frequent in the more common subtype of well-differentiated liposarcoma (WDLS) and dedifferentiated variants, where virtually all tumours contain complex marker chromosomes that always include multiple copies of MDM2 .

Translation from *in vitro* to attractive *in vivo* therapeutic intervention requires that drugs pass Phase I requirements [93]. A small molecule inhibitor was designed, spiro-oxindoles as a new class of inhibitors of the MDM2 -p53 complex. Spiro-oxindoles bind to MDM2 with high affinity and activates the p53 pathway, inhibiting the growth of neoplastic cell lines with wild-type p53 [93, 94] . MI-2 19, the lead compound in this class, demonstrates greater potency along with a superior pharmacokinetic profile

than Nutlin-3a (a MDM2 antagonist, a p53 activator and an apoptosis induce) [91, 93]. MI-2 19 has been shown to stimulate rapid p53 activation in tumour xenograft tissues with resultant inhibition of cell proliferation [91, 93, 95, 96]. Studies using both Nutlin-3a and MI-2 19 show a p53 and p2 1 dependent cell cycle arrest in normal cells, along with p53 dependent cell death specifically in tumour cells [94]. Importantly, Nutlin-3a and MI-2 19 do not cause visible toxicity to animals, as assessed at necropsy [97].

Two others oral MDM2 inhibitors that have been recently entered the clinical setting , JNJ-2 6854165 (Ortho Biotech; Johnson & Johnson) and R7112 (Hoffmann-La Roche). Both agents are being tested in advanced stage or refractory solid tumours Phase I trials [42]. In addition, AT-2 19 (a derivative of MI-2 19) is in preclinical studies with Phase I trials planned. Of relevant interest, an MDM2 antagonist RO5045337 is about to recruit for a Phase I trial in liposarcoma patients [42].

1.4.2 . CDK4 Antagonists

The protein encoded by this gene is a member of the Ser/Thr protein kinase family. This protein is highly similar to the gene products of S. cerevisiae cdc28 and S. pombe cdc2 . It is a catalytic subunit of the protein kinase complex that is important for cell cycle G1 phase progression. The activity of this kinase is restricted to the G1-S phase, which is controlled by the regulatory subunits D-type cyclins and CDK inhibitor p16 (INK4a). This kinase was shown to be responsible for the phosphorylation of retinoblastoma gene product (Rb). Mutations in this gene as well as in its related proteins including D-type cyclins, p16 (INK4a) and Rb were all found to be associated with tumourigenesis of a variety of cancers. Multiple polyadenylation sites of this gene have been reported.

Like p53, the Rb pathway is almost universally deregulated in cancer, although (unlike p53) it has important developmental as well as tumour suppressor roles. The Rb pathway controls the cell cycle at the G1/S checkpoint .

A range of CDK4 antagonists are in clinical development, most in early-phase study, and are fairly nonselective, with effects on several CDKs. Genetic ablation of CDK2 , -4, and -6 in mice seems dispensable in most normal cell cycles, but depends on CDK1 [98, 99].

First generation pan-CDK inhibitors include Flavopiridol and Seleciclib (R-Roscovitine), inhibiting CDK1, CDK2 , CDK4, CDK6, CDK7, and CDK1, CDK2 , CDK7 and CDK9 respectively [99].

Flavopiridol causes arrest in G1 and G2 phases in a range of solid tumour cell lines. Flavopiridol is more potent if tumour cells are in S phase [98, 100-102]. Matranga and Shapiro [102]demonstrated recruitment to S phase using hydroxyurea, gemcitabine and cisplatin, followed by flavopiridol resulting in sequence-dependent cytotoxic synergy [102-104]. Flavopiridol and Seliciclib have been investigated in Phase I/II trials for hematological and solid tumours including sarcomas. Trials include Flavopiridol as a single agent and in combination with taxanes where synergism has been noted [104]. Both Flavopiridol and Seleciclib have shown disappointing results relating to clinical outcome and intolerable side effects [105, 106].

Newer generation CDK inhibitors include PD0332 991, ZK 304709, R 547 and P1446A05. All are available in Phase I and II solid tumour trials [105] . PD0332 991 is one of two more selective CDK inhibitors specific for CDK4 and CDK6. Preclinical data showed inhibition of cell growth through G1 arrest in pRb-positive tumour cell lines and antitumourigenic effects in xenograft models of colon carcinoma [107]. PD0332 991 is available in Phase I and Phase II trials for solid and hematological malignancy. Finally, P1446A05 is the only single CDK4 selective inhibitor available.

No pre-clinical data is publicly available for this compound; however, it has been released as a Phase I drug for refractory solid tumour and hematological malignancies [105].

1.4.3. PPARγ Ligand Agonists

A critical regulator of terminal differentiation for the adipocytic lineage is a nuclear receptor peroxisome proliferator-activated receptor *γ (PPARγ)* [72, 108, 109]. PPARγ is an attractive target in undifferentiated lipomatous tumours such as DDLPS and ML. PPARγ forms a heterodimeric complex with the retinoid X receptor (RXR). This complex regulates transcription of adipocyte-specific genes by binding sites on DNA. Agonist ligands for the PPARγ receptor have been shown to induce terminal differentiation of normal preadipocytes in human liposarcoma cells *in vitro [108]*.

A Dana-Farber Cancer Institute Phase II clinical trial used Troglitazone, a synthetic PPARγ ligand, in patients with high-grade liposarcoma. This trial enrolled three patients. All patients showed histologic and biochemical differentiation *in vivo*, with reduction in immunohistochemical expression of the proliferation marker Ki-67 [108] .

A more recent study with 12 patients with Rosiglitazone, belonging to the same class of drugs (thiazolidinediones) as Troglitazone, was not as promising, with median progression free survival of 5.5 months. Treatment did not produce any convincing adipocytic differentiation with no correlation between the high expression of differentiation genes that was found in two patients, and clinical response [110].

1.4.4 Receptor Tyrosine Kinase Pathway Inhibitors

The high frequency of *PIK3CA mutation* suggests a role for PI3K inhibitors in ML. The non isoform-specific PI3K inhibitors, Wortmannin and LY2 94002, have been widely

used in biological research but are not particularly suited to clinical work due to their lack of specificity, Wortmannin's instability and LY2 94002 's low potency [111]. GDC-0941 and PX-866 are promising PI3K inhibitors curently in clinical trials that have low nanomolar potency against class I isoforms of PI3K [112-114]. In lung cancer cell lines and xenograft models, *PIK3CA* mutants are more sensitive to GDC-0941[115]. Similarly, *PIK3CA* mutant and PTEN-null tumours were sensitive to PX-866 in xenograft models, and phase I clinical trials for solid tumours are currently underway[114]. The Rapamycin derivateve Everolimus inhibits the mTOR complex-1 (mTORC1), which is a downstream effector of PI3K. Both H1047R and E545K PI3K mutant cells are sensitive to Everolimus [116]. PIK3CA mutated ML represents an ideal candidate for PI3K inhibition.

As MET is activated in ML and there are many MET pathway inhibitors currently in development and in clinical trials [117], ML may be a good candidate for MET inhibition. For example, the novel and promising inhibitor Foretinib (XL880) inhibits multiple kinases including both MET and VEGFR2 and exhibits extensive biological activity and clinical efficacy in an early Phase I clinical trial in metastatic or unresectable solid tumours [118].

1.5 Trabectedin

In the continuous search for effective anticancer therapy, nature provides an attractive source of new therapeutic candidate compounds [119-121]. At present, over 60% of the currently approved drugs for the treatment of cancer are derived from natural sources, including plant-derived agents, such as the taxanes, paclitaxel and docetaxel, and microbe-derived agents, such as bleomycin and doxorubicin [121]. Currently, there is a growing interest for potential cytotoxic agents originating from organisms in the sea [120, 122, 123]. Due to advances in diving techniques and deep-sea sample collection, the marine ecosystem became an accessible source for new chemical classes. Furthermore, new technologies in aquacultures provided a means for the production of these potential drugs on a larger scale, which facilitated the development of these agents [124-126]. The first living organisms in the sea appeared about 700 million years ago and, ever since, evolution has provided these organisms with defense mechanisms to survive in the hostile environment [126]. It was suggested that their survival is partly due to the excretion of highly toxic products [126].

*Ecteinascidia turbinate (*figure 15) is a translucent tunicate that grows preferentially on mangrove roots in the Caribbean Sea. The potent cytotoxicity of its extracts was first discovered in the late 1960s; however, the purification of active compounds was not established until 1986 [127]. Trabectedin (Yondelis, ET-743) was one of the isolated compounds and it was selected for further development as an anticancer agent based on its promising cytotoxic activity as well as its abundance in the tunicate. Recently, the features of trabectedin have been briefly reviewed in relation to its potential use in treatment of soft tissue sarcomas [128, 129].

Figure 15: *Ecteinascidia turbina* (modfied from http://sarcomahelp.org/research_center/ET-743.html)

1.5.1 Mechanism of action

1.5.1.1 DNA binding

Trabectedin (figure 16) is formed by a monobridged pentacyclic skeleton composed of two fused tetrahydroisoquinoline rings (A and B), linked to a 10-member lactone bridge through a benzylic sulfide linkage, and attached through a spiroring to an additional ring system made up of a tetrahydroisoquinoline (subunit C).

In contrast to traditional alkylating agents that bind guanine at the N7 or O6 position in the major groove of DNA, trabectedin binds to the exocyclic N2 amino group of guanines in the minor groove of DNA through an iminium intermediate generated in situ by dehydration of the carbinolamine moiety present in the ring A. The carbinolamine moiety is essential for the pharmacological activity of trabectedin, as related compounds without this reactive group (e.g., ET-745) were 100 times less active than trabectedin. The resulting adduct is additionally stabilized through van der Waals interactions and one or more hydrogen bonds between rings A and B, with neighboring nucleotides in the same or opposite strand of the DNA double helix, thus creating the equivalent to a functional interstrand crosslink (figure 16). In fact, hydrogen-bonding rules seem to determine the DNA-binding sequence specificity of trabectedin, with a guanine located in the central position of triplets 5′-purine-GC and 5′-pyrimidine-GG [130]. The binding of the drug in the minor groove induces the formation of DNA adducts and bends DNA toward the major groove in a fashion that seems unique for this compound [127]. The ring C apparently does not participate in DNA binding, and it was proposed to protrude out of the DNA being able to interact with DNA binding proteins, such as transcription factors or DNA repair proteins (figures 16 and 17)

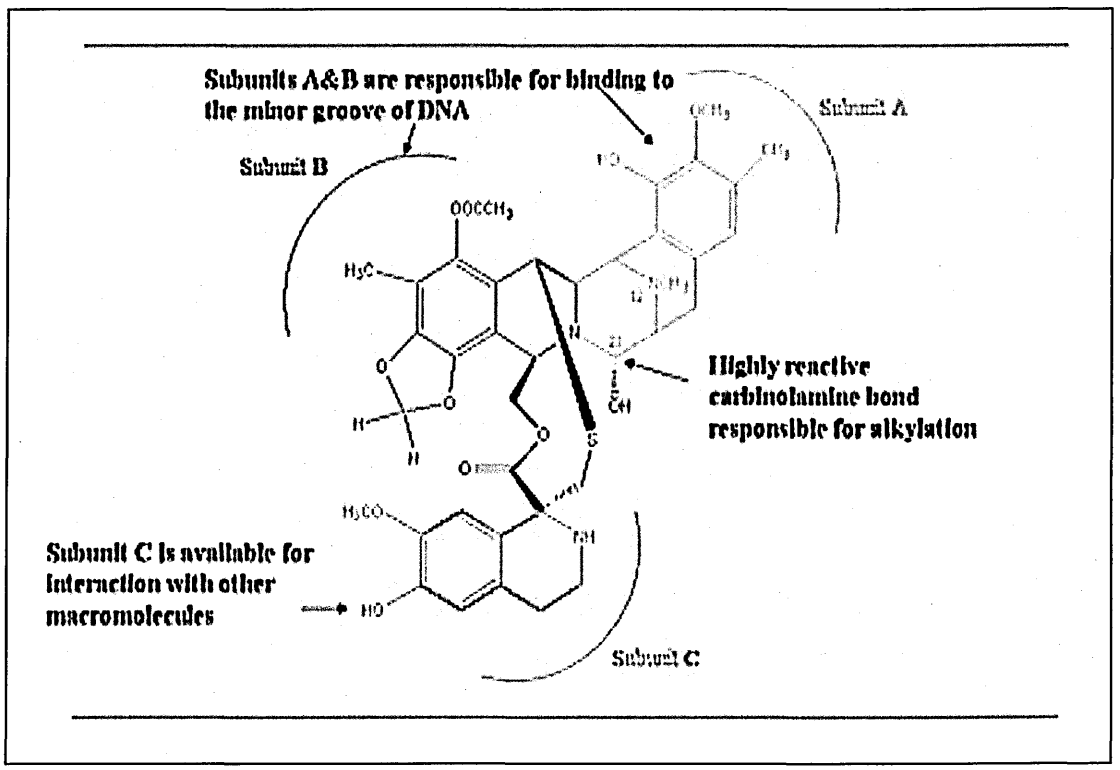

Figure 16: structure of trabectedin. Subunits A and B are responsible for binding to DNA. The binding of trabectedin to DNA changes the normal structure of the molecule, causing it to bend. In addition, the carbinolamine group functions to alkylate the DNA, which is the substitution of one chemical group for an active hydrogen atom in the DNA. When such a substitution occurs, DNA strands are cross-linked and can not replicate, thus causing the cell to die. Subunit C interacts with other molecules, such as transcription factors (modified from http://sarcomahelp.org/research_center/ET-743.html) .

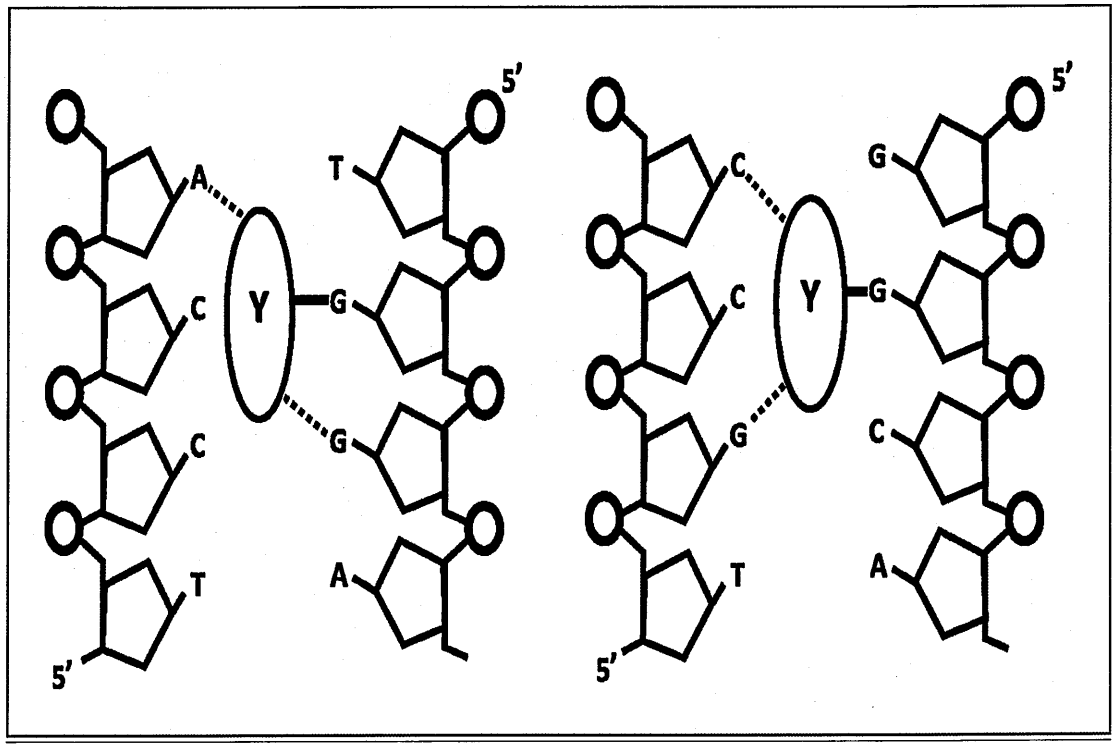

Figure 17 : Schematic of the binding mode of trabectedin to two favored triplets. Drug covalent bonds are represented by solid lines, whereas hydrogen-bonding interactions are represented in dotted lines [131].

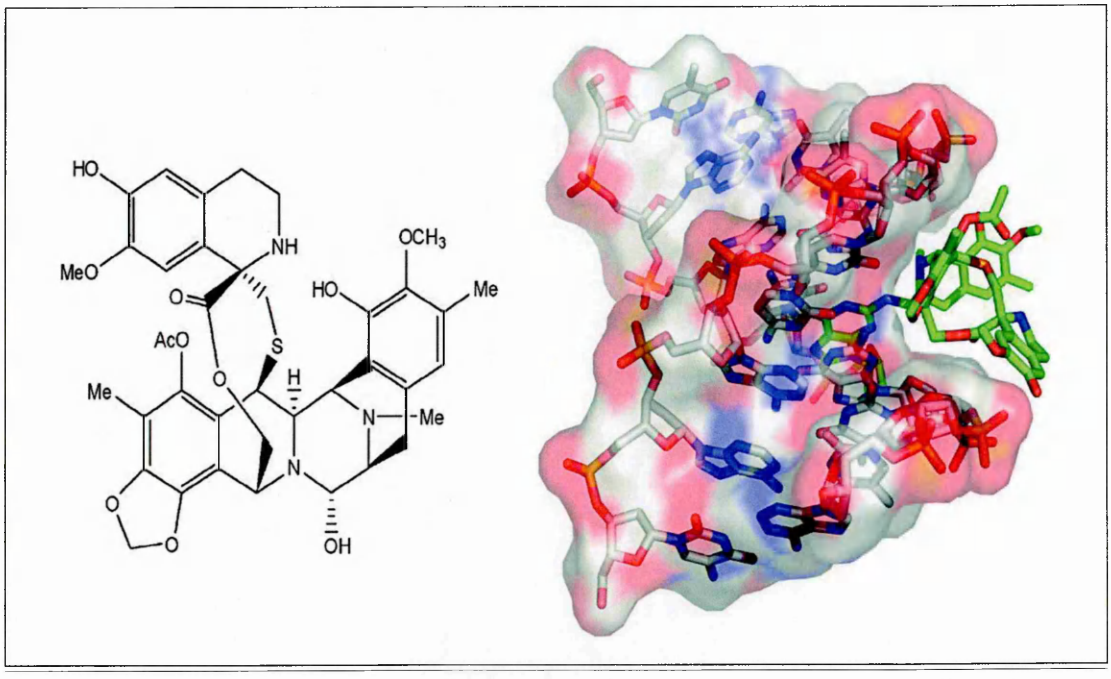

Figure 18: Chemical structure and modeling of DNA-trabectedin complexes [131].

1.5.1.2 DNA repair

The Nucleotide Excision Repair (NER) system is involved in the repair of DNA lesions caused by ultraviolet light or the bulky DNA adducts caused by carcinogens and anticancer agents such as alkylating drugs and cisplatin. Therefore, these cytotoxic drugs are usually more effective in NER-deficient cells as compared to NER-proficient cells. However, when trabectedin binds to DNA, NER recognizes the complex and appears to cause cell death instead of cell repair [132]. This effect was seen at clinically relevant concentrations, i.e. 1–10 nM. Based on the proposed mechanism, trabectedin is expected to be active against cisplatin-resistant cells, which have an enhanced NER system [133]. In vivo experiments have been performed to evaluate the antitumour effect of the combination of trabectedin and cisplatin [134]. This effect was either additive or synergistic in several tumour types, including sarcomas, non-small cell lung cancer, melanoma and ovarian cancer [134]. To gain further insight into this mechanism, a bacterial nuclease system (UvrABC) was used to investigate how the NER system recognizes and repairs DNA adducts caused by trabectedin [135]. Adducts at favored and non-favored binding sites were compared, and it appeared that preferred binding sites are repaired less efficiently than the non-preferred adducts. It was proposed that the inefficient repair is related to the repair-dependent cytotoxicity [135].

Homologous recombination (HR) and nonhomologous end joining (NHEJ) are involved in DNA double strand break (DSB) repair. It was found that HR is particularly important for trabectedin as deficient cells were approximately 100 times more sensitive to the drug. In contrast, these differences were not observed in NHEJ-deficient cells. The lack of HR was associated with the persistence of unrepaired DSBs during the S phase of the cell cycle and apoptosis [136, 137]. The particular sensitivity of cells deficient in HR seems to be confirmed in the clinic, as the tumour expression of BRCA1 or BRCA2 seems inversely related to the response in a series of patients with

sarcomas treated with trabectedin. Although the majority of the DSBs are replication dependent and involve the phosphorylation of H2 AX by ATM, recently it has been proposed that some of them are also replication independent, transcription coupled, and dependent on Mre11-Rad50-Nbs1 [138]. As mentioned above, the DNA monoadducts are stabilized by hydrogen bonds between trabectedin and nucleotides located in the same or in the opposite strand, resulting in a DNA lesion similar to interstrand crosslinks.

Recently, the difference between trabectedin-sensitive and resistant chondrosarcoma cells was investigated, to gain further insight in its mechanism of action. It appeared that the two cell types differed in their migratory ability. The trabectedin resistant cells were found to be less invasive than the sensitive cells possibly due to an inability of the trabectedin resistant cells to digest extracellular matrix [139].

1.5.1.3 transcriptional regulation

The antitumour activity of trabectedin may involve the interaction of trabectedin with DNA. This may result in an impairment of gene regulation, as described for other agents that bind to the minor groove of DNA [140-142].

Three types of factors were studied to elucidate effect of trabectedin on regulation of transcription: A) oncogene products, such as MYC, c-MYB, and MAF; B) transcriptional activators regulated during the cell cycle, such as E2 F and SRF, and C) general transcription factors, such as TATA-binding protein (TBP), and NF-Y. No inhibition of DNA binding was found for MAF, MYB, or MYC; while for TBP, E2 F, and SRF, inhibition was observed at concentrations higher than 50 μM [140]. *In vitro* the inhibition of NF-Y binding was found to occur at trabectedin concentrations in the range of 10-30 μM [140]. Since two subunits of NF-Y have a high analogy with histone 2 B, the effect of trabectedin on nucleosome reconstitution (i.e., a chromatine-like fiber formed *in vitro* by adding histones to DNA) was investigated, and it was found that a complete inhibition occurred at drug concentrations of 3-10 μM. These data suggested that the mode of action correlates with the ability trabectedin to interfere with the binding of regulatory proteins to DNA, thus altering their specific function. NF-Y, one of the factors that was preferentially affected by trabectedin, activates the CCAAT element present in 25% of eukaryotic promoters, including many promoters that regulate genes controlling the cell cycle. Based on this observation, were performed experiments in cell cultures using NIH-3T3 fibroblasts.

NIH-3T3 were transfected with a reporter gene under the control of HSP70 promoter which contains two CCAAT boxes activated by NF-Y. In this system, it was shown that a brief treatment with trabectedin in the nM range inhibited the transcription of HSP70 [143]. It was postulated that physiologically relevant concentrations of trabectedin could

affect the transcription of other NF-Y mediated genes such as MDR1 [144]. It was demonstrated that trabectedin can inhibit activation of the MDR1 promoter by multiple inducers at clinically achievable concentrations. Moreover, constitutive MDR1 transcription is not affected appreciably under these conditions, suggesting that, in the clinic, trabectedin may selectively inhibit activation of MDR1 expression in tumour cells without affecting constitutive expression in normal cells.

Further studies indicated that several genes are either down or up-regulated in HCT116 and MDA-MB-435 cell lines exposed to trabectedin. It should be noted that not all the effected genes were transcriptionally regulated by NF-Y, suggesting that other mechanisms might be involved in the transcriptional effects caused by trabectedin [145].

The orphan nuclear receptor, SXR, coordinately regulates drug metabolism through the induction of transcription of the gene encoding for the cytochrome P450 enzyme, CYP3A4, as well as the transcription of MDR1, a gene encoding Pgp, a glycoprotein that regulates the efflux of several compounds including anticancer drugs. It was shown that many xenobiotics, including drugs such as taxol, activate SXR, thus enhancing both drug metabolism and its Pgp-mediated drug clearance. Trabectedin was found to be able to inhibit SXR and consequently suppressed MDR1 gene. The inhibition of SXR, which appears to have several detoxification genes as targets, might be relevant to the toxicity of trabectedin and of other drugs combined with trabectedin [146]

Others studies proposed topoisomerase I as a putative target of trabectedin . However it should be noted that these experiments were performed by treating tumour cells with 10 μM trabectedin, a concentration 500 to 1,000-fold higher than optimal 50% inhibitory concentration values. In addition, there is evidence suggesting that topoisomerase I may not be the primary target of trabectedin, since the drug was equally active in both wild-

type and DNA topoisomerase I – deleted yeast [132].

It was also demonstrated that trabectedin treatment induces the rapid degradation of transcribing RNA polymerase II (PolI), only in cells with normal TC-NER function, but not in XPD-, XPA-, XPG-, and XPF-deficient cells [147]. However, relatively high and not clinically achievable drug concentrations were required to demonstrate this [131], therefore this finding certainly requires further research. The observation that trabectedin can induce either upregulation or downregulation of the same genes in different cell lines can suggest that cell-specific cofactors may play a role in the ability of the drug to modulate transcription regulation.

1.5.1.4 Cell cycle perturbations and phase specificity

The effects of 1 hour of trabectedin exposure, evaluated by a BrdUrd/DNA biparametric flow-cytometric analysis, showed that cells in the S phase during drug treatment progressed through this phase of the cell cycle more slowly than control cells [148].

In addition, cells that were in the G1 phase progressed through the S phase slowly. At 2 4 hours, a high percentage of trabectedin-treated cells were arrested in the G2 phase, and only 12 0 or 168 hours afterwards, depending on the cell line, did they progress to mitosis and restart a new cell cycle. By synchronizing SW620 colon cancer cells by elutriation, the sensitivity to trabectedin was comparatively evaluated in cells in G1, S, and G2 -M phases. The results showed that the highest sensitivity to the drug occurred when cells were in G1 but the lowest occurred when cells were in G2 -M phase. This finding is of interest, as the majority of available anticancer drugs that interact with DNA are preferentially effective in S-phase cells, thus indicating a biological effect of trabectedin that is distinct from those observed for the other drugs.

Another study showed that trabectedin induced a significant increase in p53 levels, which promoted apoptosis in cell lines expressing wild-type p53 [149]. However, p53 status does not appear to be relevant to the sensitivity to trabectedin, since cytotoxic activity does not correlate with the p53 status of different cell lines [148, 149], and the cytotoxicity is not significantly different in p53 (-/-) or (+/+) mouse embryo fibroblasts or in A2 780 ovarian cancer cells or cells from the A2 780/CX3 subline transfected with a dominant-negative mutant TP53 [148].

1.5.1.4 Effects on Tumour Microenvironment

Different types of cancer take advantage of inflammatory components to improve their survival in organs. A number of growth factors and cytokines (e.g. interleukin (IL)-1, tumour necrosis factor, IL-6, vascular endothelial growth factor) supports malignant cell progression and contribute to the suppression of body's immune defense [150]. Generally two pathways, not mutually exclusive, can be identified as the major affluent to the inflammatory milieu: 1) the intrinsic one (neoplastic cells), where genetic events (e.g. oncogenes, genetic aberrations), inducing neoplastic transformation, activate the production of inflammatory mediators; and 2) the extrinsic pathway (inflammatory leukocytes and soluble mediators) where chronic infections (e.g. viruses, bacteria, and parasites) significantly increase the risk of cancer. Epidemiological studies estimate that about 8%–17% of global cancer burden is linked to chronic infections. Indeed, different common tumours (e.g. bladder, ovarian, gastric, hepatocellular, and colorectal cancer) are associated with unresolved pathogen infections that fuel inflammation [151, 152]. Strategies to modulate the host micro-environment offer new approaches for anti-cancer therapies. For these reasons new molecules with anti-tumour and anti-inflammatory features are looked at with new eyes in the light of the crucial link between

inflammation and cancer.

At sub-cytotoxic concentrations, trabectedin was shown to inhibit *in vitro* production of prion-inflammatory mediators CCL2 and interleukin IL-6 by monocytes, macrophages, and tumour-associated macrophages isolated from ovarian cancer biopsies. These and other mediators of the inflammatory response are frequently expressed in the tumour microenvironment by infiltrating leukocytes, stromal and cancer cells themselves [153].

CCL2 is a major chemokine promoting monocyte recruitment at sites of inflammation and tumours, and its expression significantly correlates with macrophage accumulation [154, 155]. In most studies, CCL2 -mediated attraction of macrophages is associated with the angiogenic switch and poor prognosis [156-159]. The chemokine CXCL8 is a potent mediator of angiogenesis enhancing endothelial cell proliferation, chemotaxis, survival, and protease activation [160, 161]. Moreover, CXCL8 is directly mitogenic for some cancer cells and plays a critical role in tumour growth at metastatic sites [162, 163]. Similar results were recently seen in myxoid liposarcoma (ML) - a tumour particularly sensitive to trabectedin. It was demonstrated that in primary ML cultures, IL-6 and VEGF were also down modulated by trabectedin. VEGF is a key angiogenic factor, which certainly cooperates with the florid vessel network of ML. IL-6 is a growth-promoting and anti-apoptotic inflammatory cytokine [164-166] and a major effector signal of activated nuclear factor $\varkappa$B in the promotion of neoplasia [166].

A collaborative study reported PTX3 as one of the most expressed genes in ML [167]. This study showed that trabectedin caused down-modulation of PTX3 mRNA and protein. PTX3 belongs to the family of acute phase proteins (which also includes CRP and SAP) and plays an important role in innate resistance to pathogens [168]. In addition, PTX3 has been shown to be essential for the construction of the ECM by forming complexes with the TNF-regulated protein TSG6 which, in turn, combines with

hyaluronan [168]. In the tumour microenvironment, the constitution of a dynamic stroma is of overriding importance for the enlarging tumour mass.

Treatment with trabectedin also resulted in a reduction of inflammatory mediators also occurs *in vivo*. Briefly, mice bearing xenograft tumours were treated with three doses of i.v. trabectedin; tumour samples were excised 48 hours after the third dose and stained for CXCL8, CCL2 , PTX3, macrophage infiltration, and vessels. The number of CD68+ infiltrating macrophages significantly decreased after trabectedin from 72 .4 ±8 (mean ± SD, three tumours) to 30.2 ± 6 ($n = 3$; $P < 0.05$). This was associated with significant reduction of tumour vessels. A clear inhibition of CXCL8 and CCL2 staining and a partial reduction of PTX3 were observed after treatment [153].

To further investigate the effect of trabectedin on tumour microenvironment, surgical ML patient samples were resected after several cycles of trabectedin therapy, and compared to the original biopsies. The surgical sample excised after therapy had a marked decrease in CD31+ vessels and CD68+ macrophages; PTX3 positivity was also significantly decreased after therapy. These findings indicate that the reduction of inflammatory mediators observed *in vitro* with trabectedin may have *in vivo* implications [153]. Besides a direct and strong growth-inhibitory effect on cancer cells, trabectedin significantly hampered the production of selected pro-inflammatory cytokines such as IL-6, CCL2 , CXCL8, VEGF, and PTX3. The inhibition of some mediators was confirmed *in vivo* in animals bearing ML xenografts, paralleled by a marked decrease of infiltrating macrophages and tumour vessels. Downregulation of key inflammatory molecules in the tumour microenvironment might be of benefit in light of the increasingly clear relationship between persistent inflammation and cancer progression [131, 153].

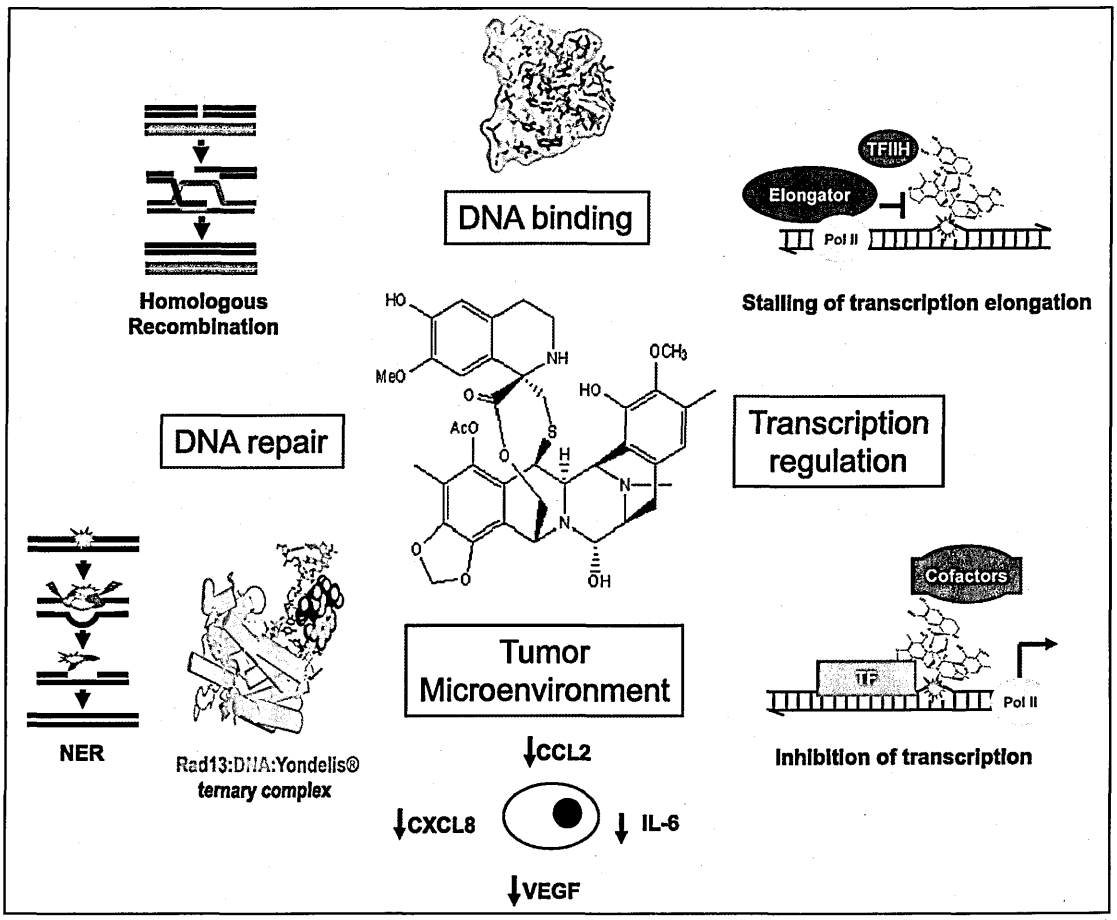

Figure 19: Schematic of the unique and complex mode of action of trabectedin. The antitumour effects of trabectedin are due to multiple mechanisms involving DNA binding in the minor groove, interactions with DNA repair mechanisms, modulation of transcription regulation, and induction of microenvironment changes [131].

1.6 Trabectedin therapy for Adult soft-tissue sarcomas (STS)

Adult soft-tissue sarcomas (STS) have long been viewed as poorly sensitive to most chemotherapeutic agents [169].When trabectedin was approved in the European Union as a further-line of chemotherapy for advanced STS, it was the first drug entering the armamentarium of the sarcoma medical oncologist after doxorubicin in the 1970s and ifosfamide in the 1980s. In the same period, indeed, other drugs were shown to be active in selected histological types of STS, giving rise to the so-called 'histology-driven' medical treatment of this variegated family of rare neoplasms.

Trabectedin contributed to this evolution of thought in STS medical therapy along with gemcitabine in leiomyosarcoma and angiosarcoma, taxanes in angiosarcoma, and then the new molecularly targeted agents, from imatinib in dermatofibrosarcoma to the new agents currently on study. In fact, trabectedin shows selective activity in some STS histologies, even with a variegated mechanism of action depending on the histological type [170].

1.6.1 Pharmacokinetics and phase I studies.

After infusion, trabectedin is rapidly cleared from plasma, undergoing an extensive hepatic metabolism mainly through the cytochrome P450 3A4 [171]. Trabectedin has a high apparent volume of distribution and a half-life of approximately 90 hours [172]. It is mainly excreted in the feces but less than 1% is excreted unchanged in the urine or feces [173].

In phase I studies (Table 3), different schedules were investigated in patients with solid tumours [174]. This schedules range from an intravenous infusion over 1, 3, 2 4, or 72 hours every three weeks to a weekly infusion for three out of a four-week cycle. The dose-limiting toxicities (DLT) were mainly hematological (neutropenia, thrombocytopenia) and fatigue. Grade 3–4 hepatic toxicities were also DLT in some but not all trials [175, 176]. DLT were transient and not cumulative. Nausea and vomiting were managed with 5HT3-antagonists. Fatigue or asthenia grade 3–4 was also frequently described (8% to 50%). Tumours responses were observed in soft tissue sarcoma, osteosarcoma, melanoma, and breast cancer.

Two schedules were recommended for further phase II studies: 1.5 mg/m^2 as a 24-hour continuous infusion given every three weeks and 0.58 mg/m^2 as a three-hour infusion given weekly for three out of four weeks [177].

Reference	Schedule	N	MTD	DLT	Recommended dose for phase II
Ryan Clin Cancer Res. 2001 Feb;7(2):231-42	72 h infusion every 3 weeks	21	1.2 mg/m^2	Transamanitis, rhabdomyolysis, neutropenia	1.05 mg/m^2
Taamma J Clin Oncol. 2001 Mar 1;19(5):1256-65.	24 h infusion every 3 weeks	52	1.8 mg/m^2	Neutropenia, thrombocytopenia	1.5 mg/m^2
Twelves Eur J Cancer. 2003 Sep;39(13):1842-51.	1 h infusion every 3 weeks	40	1.1 mg/m^2	Fatigue, neutropenia, thrombocytopenia	1 mg/m^2
	3 h infusion every 3 weeks	32	1.8 mg/m^2	Fatigue, hyperbilirubinemia, thrombocytopenia.	1.65 mg/m^2
Villalona-Calero Clin Cancer Res. 2002 Jan;8(1):75-85.	Daily for five days every 3 weeks	42	0.325 mg/m^2/d	Neutropenia, thrombocytopenia	0.325 mg/m^2/d
Farouzeh Proc Am Soc Clin Oncol 2001	3 h infusion weekly for three weeks of a four week cycle	31	0.65 mg/m^2	Neutropenia and hyperbilirubinemia	0.58 mg/m^2

Table 3: Dose-limiting toxicity (DLT) and maximum tolerated dose (MTD) in Phase I studies [178]

1.6.2 Phase II studies of trabectedin in pretreated sarcomas

The efficacy of trabectedin was studied in four phase-II studies in pretreated soft tissue sarcoma from US and Europe [179, 180] of which one was a randomized phase II study [181]. Yovine and colleagues [179, 182] investigated trabectedin 1.5 mg/m^2 administered as a 24-hour continuous infusion. Fifty-four patients were enrolled and analyzed in two predefined groups. The first group of 26 patients was pretreated with only one or two single agents or one combination regimen and the second group of 28 patients were heavily pretreated with at least three chemotherapeutic agents or two combinations. The predominant histology was leiomyosarcoma (n = 22, of uterine origin (n = 8), and liposarcoma (n = 6). Two partial responses (3.7% [95% confidence interval (CI): 0.5%–12 .8%]) were reported and both had uterine leiomyosarcoma, four (7.4%) patients had a minor response, and nine (17%) patients had stable disease. Among the six responding patients, five received prior chemotherapy with ifosfamide and doxorubicin. The median progression free survival was 1.9 months after a median follow-up of 26 months. At three and six months, 38.8% and 24.1% of patients were progression-free, respectively. No difference was noted in progression-free survival between the two groups. But the less pre-treated patients had a longer median overall survival of 13.7 months versus 7.9 months. Overall, the median survival was 12.8 months with 30% of patients alive at two years.

Another study reported the results of the phase II trial with trabectedin 1.5 mg/m^2 administered as a 24-hour continuous infusion, conducted in 36 patients pretreated with up to two prior chemotherapy regimens [181].

Gastrointestinal stromal tumours (GIST), mesothelioma, osteosarcoma, carcinosarcoma, Kaposi's sarcoma, or rhabdomyosarcomawere excluded in this study. The main histologies were leiomyosarcomas (n = 13), liposarcomas (n = 10), and synovial

sarcomas (n = 6). One complete response (CR) was obtained in a patient with liposarcoma, and two partial responses (PR) in a patient with leiomyosarcoma and in a patient with liposarcoma, for an overall response rate of 8% (95% CI: 2 %–2 3%). Two other patients had a minor response. The median time to progression was 1.7 months and the median overall survival was 12.1 months with an overall survival rate at one year of 53.1%.

The third study published by Le Cesne and colleagues [180] was conducted in eight European centers by the European Organization for Research and Treatment of Cancer (EORTC) and administered trabectedin at 1.5 mg/m^2 as a 24-hour continuous infusion. One hundred and four patients were accrued with progressive soft tissue sarcomas excluding GIST. Most patients had leiomyosarcomas (n = 43), synovial sarcomas (n = 18), or liposarcomas (n = 10). There were eight partial responses (in leiomyosarcomas [n = 5], synovial sarcoma [n=1], liposarcoma [n=1], and malignant fibrous histiocytoma [n = 1]) and forty-five (40.5%) stable disease. Disease stabilization longer than six months was measured in 2 6% of patients. Of note the tumour control rate (defined as non progressing patients) reached 56% in leiomyosarcomas, 61% in synovial sarcomas, and 40% in liposarcomas. After a median estimated follow-up of 34 months, the median time to progression was 3.4 months. The progression-free rates at 3, 6, and 12 months were respectively 52 %, 2 9%, and 17%. GIST histology has been evaluated separately. Among 28 patients none responded, the best effect was disease stabilization in nine patients. The median time to progression was less than two months suggesting that trabectedin was ineffective in GIST when given alone with this schedule [183]. The results of these three phase II studies involving 183 patients were pooled and analyzed by Le Cesne.

Leiomyosarcoma remained the main histological subtype representing 41% of patients

followed by liposarcoma in 14% and synovial sarcoma in 11%. Most patients (95%) were pretreated with anthacyclines or ifosfamide and 113 patients were resistant to anthracyclines, 81 resistant to ifosfamide, and 63 to both agents. The overall response rate was 7.7%. The clinical benefit, defined as the combination of the rate of objective response and of minor response and of stable disease, was 51.5%. The median overall survival was 10.3 months with an overall survival rate at one year of 47.5% and a progression-free survival rate at six months of 19.8%. The clinical benefit was similar in patients with bulky disease, with multiple pretreatments, with short previous progression-free survival or with early resistance to standard chemotherapy, suggesting the lack of cross-resistance and a specific mechanism of action.

A phase II randomized trial was conducted in patients with liposarcoma or leiomyosarcoma after failure of anthracyclines and ifosfamide (table 4) [182]. Two hundred seventy patients received either trabectedin at 0.58 mg/m^2 as a 3 hour weekly infusion, three out of four weeks or at 1.5 mg/m^2 as a 24 hour continuous infusion every three weeks. A significantly longer time to progression was achieved for the three weekly regimen reaching 3.7 months and 2.3 months for the weekly regimen ($p = 0.0302$, hazard ratio [HR]: 0.734). The median overall survival was 13.8 months for the three weekly and 11.8 for the weekly regimen. The clinical benefit favored the three weekly regimen even if not statistically significant (58% versus 44%). Neutropenia grade 3–4 was described in 47% and 13% on the three weekly and the weekly arm, respectively, but it did not translate to a different rate of febrile neutropenia (0.8%). Similarly grade 3–4 transaminitis (ALAT) was more frequent in the three weekly arm (48% versus 9%), but without clinical consequences.

The results of the compassionate use programs in an unselected population, even though most of them included leiomyosarcomas or liposarcomas, were very similar in term of

efficacy and toxicity [184-187] and in a historical comparison, progression-free survival of trabectedin was better than the other active chemotherapeutic agents.

1.6.3. First line trabectedin in sarcomas

In a phase II trial, 36 patients were evaluated with advanced or metastatic soft tissue sarcomas [59]. The main histological subtypes were leiomyosarcomas (n = 15) and liposarcomas (n = 9). One complete response and five partial responses were observed for an overall response rate of 17.1% (95% CI: 6.6%–33.6%). Responses occurred in three patients with liposarcoma, and one patient each with leiomyosarcoma, synovial sarcoma, and fibrosarcoma. One patient with a uterine leiomyosarcoma had a minor response. The median progression-free survival was 1.6 months and the progression-free rate at 6 months was 24.4%. Median overall survival was 15.8 months and overall survival at one year was 72 %.

Reference	Study type	N	Subtype of Sarcoma	N	Overall response	Disease control	Median TTP (months)	Median OS (months)
Yovine J Clin Oncol. 2004 Mar 1;22(5):890-9	Phase II, second line	28	LMS/Lipo	2	3.7%	24% at six months	1.9	12.8
		22	Other	0				
Garcia-Carbonero J Clin Oncol. 2004 Apr 15;22(8):1480-90	Phase II, second line	23	LMS/Lipo	3	8.3%	ND	1.7	12.1
		13	Other	0				
Le Cesne J Clin Oncol. 2005 Jan 20;23(3):576-84	Phase II, second line	53	LMS/Lipo	6	8.1%	53.6%	3.5	9.3
		51	Other	2				
Le Cesne Onco Targets Ther. 2009; 2: 105–113.	Phase II, second line	183			7.7%	51.4%	ND	10.3
Morgan J Clin Oncol 2007	Phase II, second line	136	3-weekly		5.6	38.9%	3.7	13.8
		134	weekly		1.6	24.3%	2.3	11.8
Garcia-Carbonero J Clin Oncol. 2005 Aug 20;23(24):5484-92.	Phase II, first line	24	LMS/Lipo	4	17.1%	20%	1.6	15.8
		12	Other	2				

Table 4: Efficacy and survival data of trabectedin in phase II trials [178].

Abbreviations: ND, no data; LMS, leiomyosarcoma; Lipo, liposarcoma; TTP, time to progression; OS, overall survival.[i]

1.6.4. Efficacy of trabectedin in advanced pretreated myxoid liposarcomas.

In 2007, Casali group reported their results on patients with myxoid liposarcoma who had been treated on a compassionate basis at five institutions in Europe and the USA [188]. 51 patients (16 women and 35 men) were included in this retrospective analysis.

All patients started treatment with trabectedin between April 4, 2001, and September 18, 2006. ECOG performance status was 0 in 31 patients, 1 in 18 patients, and 2 in two patients. 33 patients were diagnosed with a pure myxoid liposarcoma, the other 18 patients had a round-cell component representing 5–90% of the total tumour. FISH analyses were done in 33 patients, all of whose tumours were found to have the t(12 ;16) chromosomal translocation. In 12 of these 33 patients, the availability of frozen tissue allowed to do RT-PCR experiments. The tissues were sequenced and characterized as: type II fusion transcript in eight patients; type IV and I in one patient; type II and IV in one patient; type III in one patient; and type II and III in one patient. The most common primary tumour site was the thigh. 11 patients presented with metastatic disease at diagnosis. 27 patients had received adjuvant radiotherapy, and ten had received adjuvant chemotherapy (anthracyclines) after complete surgery only. The median number of previous chemotherapy regimens was two (IQR 1–3). Median time from initial diagnosis to start of trabectedin treatment was 46·3 months (31·4–12 0·1), and from relapse to start of trabectedin was 24·3 months (12 ·3–42 ·3). Four patients had locally advanced disease when they started trabectedin treatment, and 47 patients had metastatic disease, with a median of three sites involved (IQR 1–3). All but three patients had been treated with chemotherapy for advanced disease (i.e., metastatic or inoperable disease). 46 received both anthracyclines and ifosfamide (of these, 31 patients received anthracyclines and ifosfamide in combination, and 15 patients

received anthracyclines and ifosfamide in sequence) as first-line chemotherapeutic treatment, which is usual practice in some institutions according to individual patient data; two patients received antrhacyclines.

558 cycles of trabectedin were administered, with a median of ten cycles per patient (IQR 6–14; range 1–2 3). At the time of this analysis, 14 patients were still on treatment with trabectedin. 47 patients were treated with the 24-h continuous intravenous schedule at the following starting doses: 1·5 mg/m^2 in 16 patients, 1·3 mg/m^2 in 28 patients, and 1·2 mg/m^2 in three patients. Four patients were treated with the 3-h schedule at the following starting doses: 1·5 mg/m^2 in two patients, 1·3 mg/m^2 in one patient, and 1·1 mg/m^2 in one patient. Both schedules were repeated every 21 days. No treatment interruption due to toxicity and no unexpected toxic effects or severe adverse events of grade 4 were noted.

In a subgroup of 41 patients, a centralized radiological review was done of available radiographical images from baseline to progression, to best response, and to treatment end; images from study centers in Milan, London, and Boston were used. Only six of the 23 patients in this subgroup with a confirmed CR or PR had achieved these responses by the first response assessment; out of the other 17 patients, eight patients had MR at first assessment, and nine had SD; median time to reach a dimensional decrease of the tumour that configured an objective response was 3·6 months (IQR 2·4–4·6). In these 17 patients who did not have a confirmed CR or PR by the first response assessment, early alterations in tumour appearance detected by CT scan or MRI were noted. The hallmark feature was a decrease in tumour density without substantial changes in tumour dimensions. The same early signs of decrease in tumour density were seen in 11 of the 14 patients with SD as their best response confirmed during central review. Median PFS for the three patients with SD but no radiologically detectable

tissue changes were 2-2 months, 3-4 months, and 5-3 months.

One patient, who had a pericardial metastasis, received nine courses of trabectedin at a very low dose intensity (0.167 mg/m^2) because of bone-marrow toxicity, and achieved a CR that was still maintained after 27 months from treatment initiation. Three patients achieved PR as their best response and continued to respond for up to 19, 20, and 23 cycles, respectively, at which point the patients and the treating clinicians shared the decision to stop treatment in view of the long treatment time. These three patients were then rechallenged with trabectedin on subsequent disease progression, and two of these had a second prolonged disease stabilization, lasting 18 months and 22 months, respectively. One patient, who had a multifocal loco regional relapse of a pure-type myxoid liposarcoma of the thigh, received four preoperative courses of trabectedin. The MRI after four courses of trabectedin showed a marked decrease of contrast enhancement without any tumour shrinkage (figure 20).

When this patient's post-surgery resection specimen was reviewed, both the typical plexiform vascular pattern and the immature spindle cell neoplastic component had disappeared and were replaced by sclerohyaline material in more than 70% of the sample; the remaining areas showed maturation represented by clear adipocytic differentiation (figure 21).

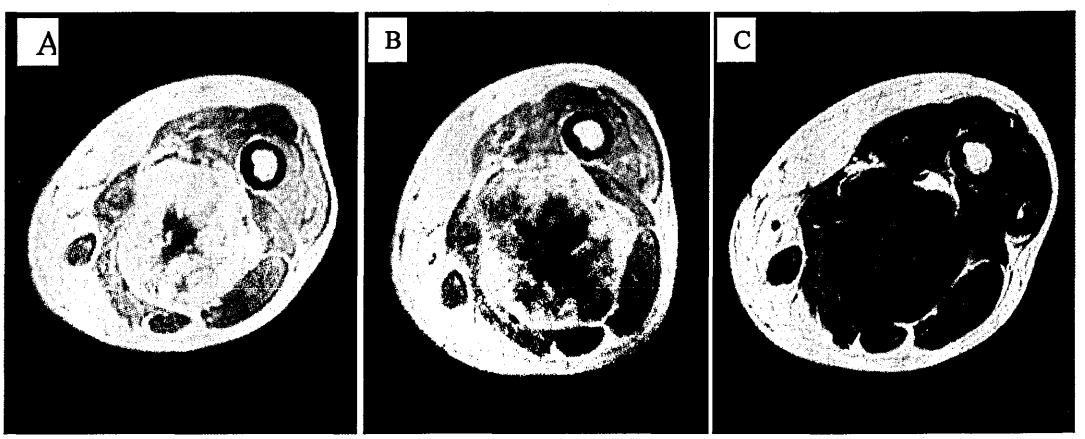

Figure 20: MRI of left thigh showing progressive decrease of contrast enhancement without tumour shrinkage [59].

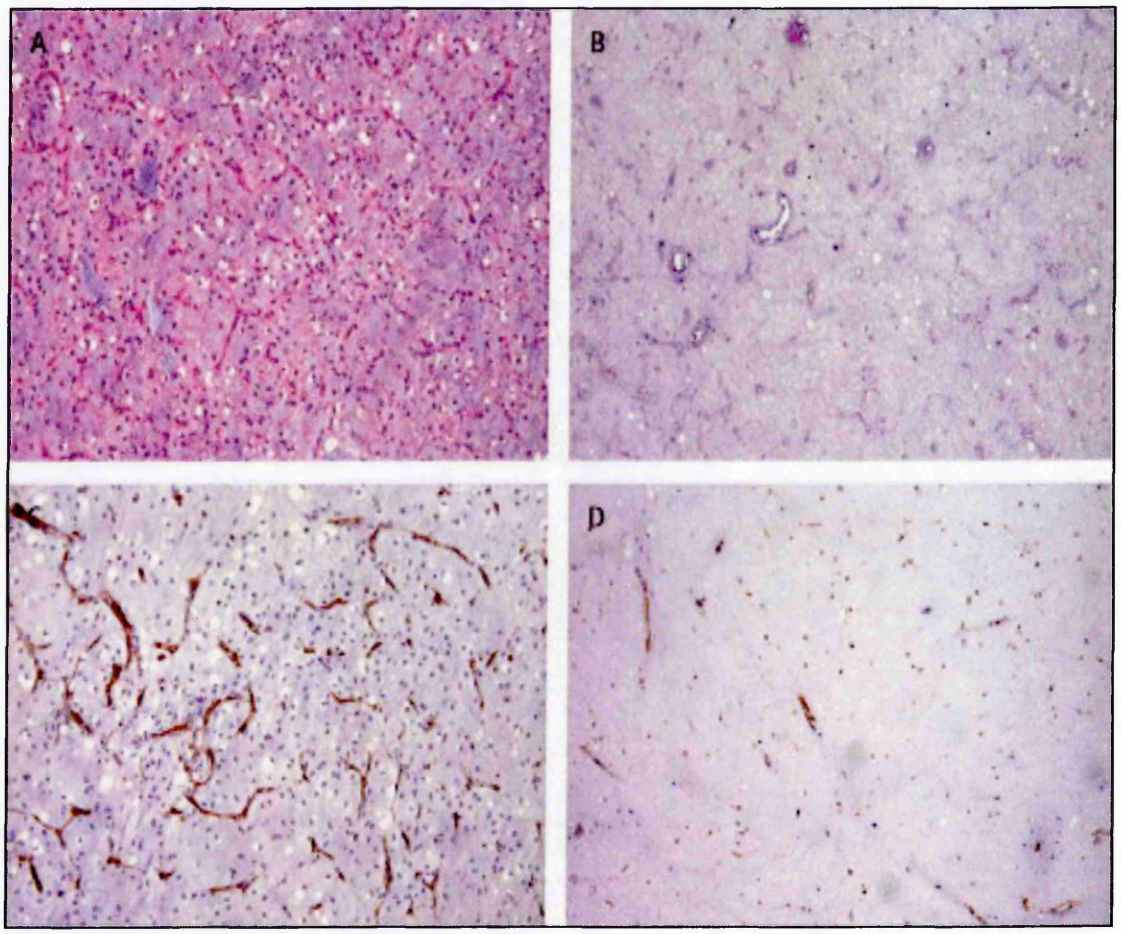

Figure 21: Histological features of tumour tissue from left thigh before and after trabectedin treatment: Pretreatment (A) and post-treatment (B) stained with haematoxylin and eosin; pretreatment (C) and post-treatment (D) with immunostaining with CD31 highlighting the vascular network [59].

A resection specimen from another patient who had a huge abdominal relapse of a myxoid liposarcoma with a cellular component up to 50% at diagnosis, and who was operated on after 17 courses of trabectedin, showed coagulative necrosis in almost half of the sample, sclerohyaline degeneration (20% of the areas), and areas of monovacuolated lipoblasts (figure 22). This patient had achieved an objective PR, which was identified by the early appearance of tumour hypodensity on CT scans (figure 23).

Although the numbers of patients in this study were too small to draw any definite conclusion, no relation between response, trabectedin concentration, infusion modalities, other patient characteristics (ie, patient sex, age, location, and grade of tumour), and previous interventions (ie, surgery, previous chemotherapy or radiotherapy) were apparent. In terms of molecular variants of the CHOP-FUS fusion transcript, of the eight patients who carried the type II transcript, one achieved a CR, three had PR, and four had SD or MR with tissue changes (one of these patients was treated with four cycles of trabectedin and had a major pathological response after surgical excision). One patient carrying both the type II and type IV, and another carrying both type I and type IV transcripts achieved PR. By contrast, the two patients carrying the type III fusion transcript (alone or in combination with another subtype) had disease progression.

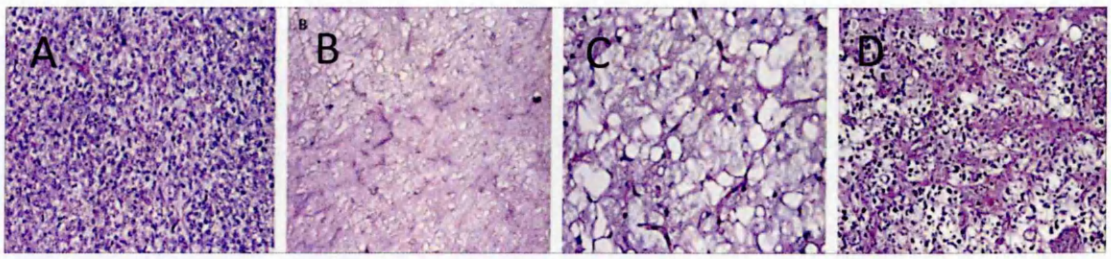

Figure 22 : Histological features of abdominal-tumour tissue before and after trabectedin treatment : Tumour tissue stained with haematoxylin and eosin before treatment (A) and after treatment (B–D): B, deposition of sclerohyaline material and cellular depletion; C, mature lipoblast-featuring cells; D, necrosis [59].

Figure 23: Sequential CT scans of abdominal tumour displaying a decrease in tumour density followed by a decrease in tumour dimensions in patient 2 1Basal CT scan (A); after one course of trabectedin (B); after five courses of trabectedin (C); after eight courses of trabectedin (D); and after 11 courses of trabectedin (E) [59].

Age, years	Sex	Location of myxoid liposarcoma	Myxoid liposarcoma grade	DDIT3-FUS transcript	Metastatic sites	Best response	PFS, months	Trabectedin treatment ongoing*	Status
42	Male	Thigh	High	II	Lung	CR	8·3	Yes	NED
45	Male	Thigh	High	II	Abdominal cavity	PR	16·3	No	NED†
65	Male	Leg	High	II	Mediastinum, pericardium	PR	20·5	No	AWD
34	Female	Thigh	High	II	Bone, liver, pleura, soft tissue	PR	11·1	Yes	AWD
47	Male	Thigh	Low	II	Pelvis, soft tissue	SD	15·2	No	NED†
60	Male	Thigh	High	II	Soft tissue	SD	12·1	Yes	AWD
48	Male	Leg	Low	II	Heart, pericardium	MR	14·5	No	AWD
50	Female	Thigh	High	II	Abdominal cavity	MR	6·7	Yes	AWD
55	Female	Thigh	Low	II and IV	Abdominal cavity	PR	7·3	Yes	AWD
52	Male	Leg	High	I and IV	Bone, pericardium, soft tissue	PR	18·0	No	AWD
58	Male	Groin	High	III	Pelvis, soft tissue	PD	1·3	No	AWD
53	Male	Thigh	High	II and III	Abdominal cavity, soft tissue	PD	1·3	No	DOD

Table 5: Characteristic of 12 patients ML who had molecular analysis [59]

The median PFS on trabectedin of the entire patient group was 14·0 months (95% CI 13·1–2 1·0). PFS of the entire patient group at 3 months was 92 % (85–99), and at 6 months was 88% (79–95). Figure 24 shows the PFS curve of the entire patient group. According to RECIST, the median PFS of patients who attained a PR or CR was 20·3 months (14·0–30·6), and of patients who had SD or MR was 12 ·5 months (8·1–2 1·4), whereas PFS during previous chemotherapy (ie, before starting trabectedin treatment) for 34 patients for whom data were available was 8·4 months (3·1–11·1). This study was a retrospective analysis of patients who were given treatment compassionately. Other limitations of retrospective studies in general include: the use of nonstringent eligibility criteria and absence of a strict follow up protocol, but in this study, the use of a protocol for compassionate use attenuated these limitations. Nonetheless, although this was not a prospective study, this series was collected on a multicentre basis by some of the world's major institutions with extensive experience with trabectedin.

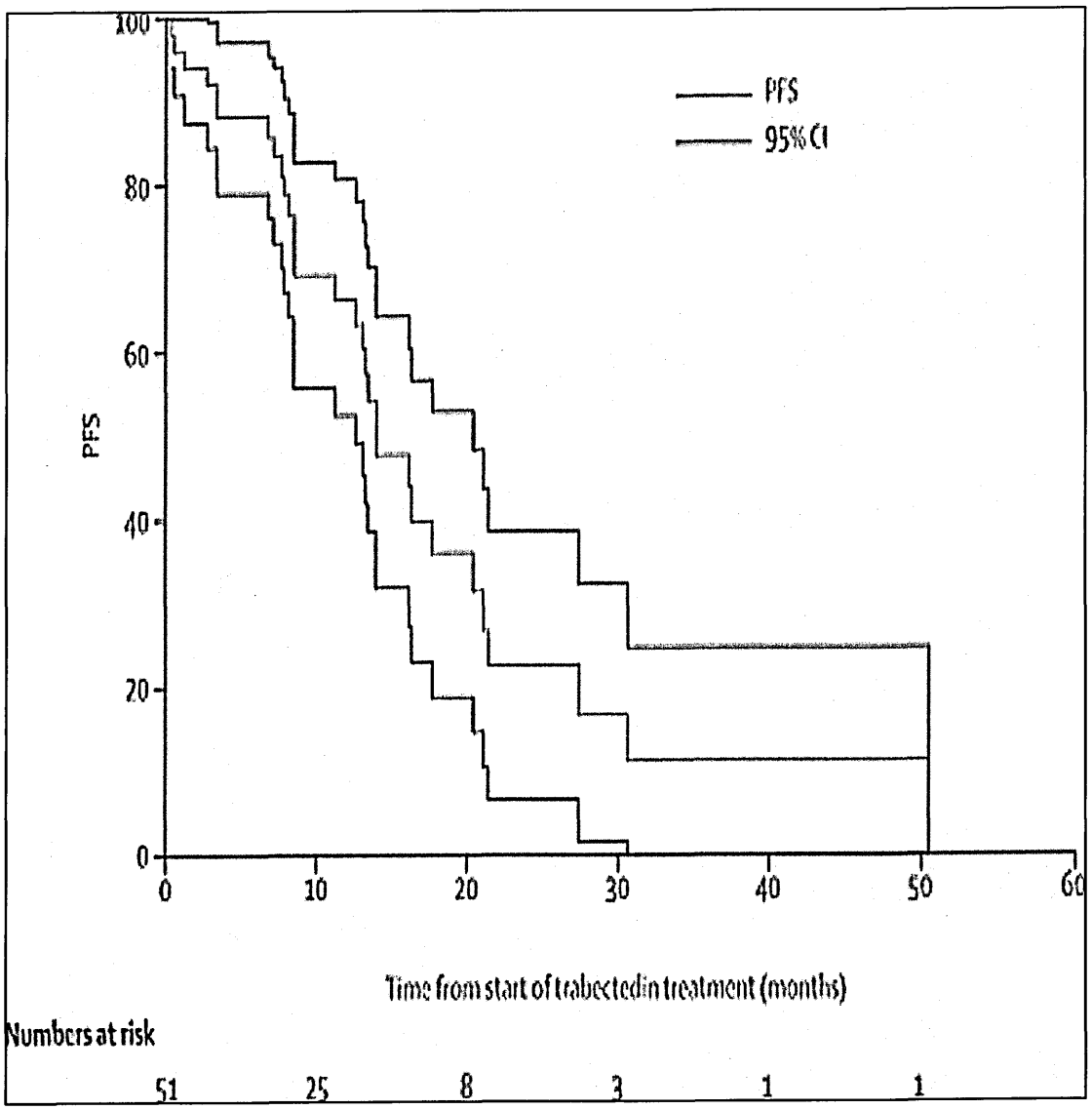

Figure 24: Progression-free survival [59].

In this multicentre, retrospectively studied series of 51 pretreated patients with advanced myxoid liposarcoma, trabectedin showed an objective response as measured by RECIST of 51% (95% CI 36–65), with an additional 20 patients achieving MR or SD. The PFS was 88% at 6 months. Only five patients exhibited progressive disease. In the subgroup of 38 patients who did not have evidence of progression and with available radiographical images, 29 showed signs of a tissue response, with substantial radiological changes in the density of tumours, often before tumour shrinkage became evident.

Indeed, of the 29 patients with radiographical density changes at first tumour assessment, an objective response was documented in 17 patients after additional trabectedin treatment, and in the others an MR or a prolonged stabilization of disease was noted. Moreover, in two patients of this series whose disease was resected after preoperative trabectedin, the seradiological findings were consistent with a major pathological response, marked by cellular depletion, disappearance of the plexiform vascular structure, deposition of sclerohyaline material and increase of monovacuolated lipoblasts.

All these observations suggest that trabectedin induced hypodensity in tumours might be a biologically and clinically relevant tumour response to the drug. Indeed, such patterns of tumour response have been reported with molecularly targeted treatments, in patients with gastrointestinal stromal tumours who receive KIT-kinase inhibition with imatinib or sunitinib, and in those with other solid tumours (eg, chordoma) who are undergoing molecular targeted treatments [188-191]. Trabectedin might target a molecular mechanism with crucial transforming activity in myxoid liposarcoma, therefore, accounting for the unexpectedly high response rates in this subtype. CHOP fusion oncogenes are found in virtually all myxoid liposarcomas, and preclinical studies

have shown that trabectedin has transcriptional regulatory functions [60]. In this study, in 12 patients with the type of fusion transcript characterized, the two who had early progression had the much less common type III transcript, thus further suggesting a molecular specificity of action, preliminary and scant though these observations might be. These fusion transcript types contain a variable number of exons of fusion (involved in t(12 ;16) in malignant liposarcoma [FUS]) and CHOP. Type III is the longest fusion transcript, containing the first eight exons of FUS fused to exons 2 to 4 of CHOP. Compared with type III, in type II and I, FUS contributes less to the fusion protein (exons 1–5 and 1–7 respectively), while type IV is the shortest transcript, comprising exons 1–5 of FUS and exons 3–4 of CHOP.

Preclinical studies performed in a myxoid liposarcoma cell line indicate that trabectedin modulates transcription, presumably interfering with the fusion oncoprotein FUS-CHOP [60]. In the presence of trabectedin, it is transcribed normally, but is not able to activate the transcription of target genes. In this sense, the mechanism of action of trabectedin could be highly selective in myxoid liposarcoma, with the depression of the expression of genes that are crucial for the late phase of adipocytic differentiation. The findings observed in myxoid liposarcoma could also be extrapolated to other sarcomas in which the translocation results in an altered regulation of the expression of transcription factors. For example, some responses observed in patients with Ewing's sarcomas could be explained by this mechanism. This disease is characterized by a translocation, most frequently resulting in the creation of an aberrant transcription factor (EWS-Fli1 fusion protein), known to regulate more than 70 genes required for the survival of Ewing's cells. It was recently shown that trabectedin has a direct inhibitory effect on EWS-Fli1 transcriptional activity [192].

1.6.4.1 Phase II clinical trial of neoadjuvant trabectedin in patients with advanced localized myxoid liposarcoma.

Surgery and radio-chemotherapy are the standard therapy for ML, but few data are accessible on neoadjuvant treatment . In Grosso study, the results of preoperative trabectedin in a cohort of advanced MLs, in two patients with multifocal and huge tumour masses, respectively, showed regression of 50%–70% of their tumours, with adipocyte differentiation observed in one of them [59], motivated the conduction of the present clinical trial.

The aim of this investigative phase II clinical trial was to examine the efficacy and safety of neoadjuvant trabectedin in patients with locally advanced ML previously untreated with chemotherapy or radiation.

Twenty-nine patients were included and treated with neoadjuvant trabectedin between 16 April 2007 and 12 January 2010. Their demographic and baseline characteristics are summarized in Table 7. One patient had a non-ML as per centralized review. Metastatic disease at baseline was disclosed in three patients after their enrollment in the trial. Two additional patients did not complete neoadjuvant treatment and discontinued therapy due to adverse events after one and two cycles, respectively. These six patients were excluded from the primary analysis: pathological response. 3 of 23 ML patients treated with neoadjuvant trabectedin, achieved a pCR according to centralized pathological review (13%; 95% CI, 3% to 34%). In addition, very good and moderate responses were observed in 2 and 10 patients, respectively. In one of the very good responders, the presence of residual tumour component was confirmed only trough FISH analysis [59], which showed the FUS–CHOP translocation in few remaining tumoural cells. In all the regressed cases, the decrease of cellular components paralleled the replacement with an acellular stromal component. These observations closely mirror results obtained in xenografts of ML treated with trabectedin [48]. The decrease in arborizing vascularity

was also in agreement with the known capability of trabectedin to inhibit proinflammatory cytokines release by human ML .

The rate of objective response rate per RECIST was 24% (95% CI, 10% to 44%), with no disease progression. This objective response rate is higher than the 17% previously reported in chemotherapy-naive STS patients according to World Health Organization criteria (Garcia-Carbonero R, Supko JG, Maki RG et al. Ecteinascidin-743 (ET-743) for chemotherapy-naive patients with advanced soft tissue sarcomas: multicenter phase II and pharmacokinetic study. J Clin Oncol 2005; 23: 5484–5492)

Apart from the different criteria used to evaluate tumour size, this difference in response could be explained by the STS subtypes analyzed. In the present study, all patients had ML, which appears to be extremely sensitive to trabectedin, while only 25% of patients had this sarcoma subtype in the study reported by GarcıaCarbonero et al. [193]. Consistently, three of six responses observed in this latter study occurred in patients with ML.

A higher response rate by RECIST (50%–51%) has been reported in a retrospective series of ML patients treated with trabectedin [59, 194]. Differences in objective response per RECIST could be partially explained by difference in treatment duration between the neoadjuvant and the advanced setting. Neoadjuvant treatment was limited here to a maximum of six cycles previous to surgery, while in the study by Grosso et al. [194] patients received a median number of 10 cycles in the advanced setting. Late responses are often observed with trabectedin [170], and this fact could account for the differences in response rate. In the present study, 16 of 21 patients with stable disease had tumour shrinkage of 7%–25% (data not shown). Some of these patients could have achieved response if treated for a longer period of time. Tumour shrinkage is usually preceded by a change in tumour density, which is not picked up by RECIST criteria. Patients in this series were not prospectively evaluated by functional imaging or CHOI

criteria, but based on the few available data it is very likely that these tools would have better described the activity of this drug in this disease. Future studies will have to incorporate these procedures to properly assess response, especially in these tumour types [195].

Trabectedin was generally well tolerated and showed manageable toxicity when administered to ML patients as neoadjuvant chemotherapy. Common adverse reactions (nausea/vomiting, fatigue, neutropenia and transient transaminases increases) were those usually associated to trabectedin in patients with STS [170, 196-198] or other tumour types [193],[199]. In general, these events were transient, decreased in frequency over cycles, were not cumulative, had no relevant clinical consequences in most patients and were manageable by appropriate dose modifications or administration delays. These findings support that trabectedin 1.5 mg/m^2 given as a 24-h i.v. infusion every 3 weeks is a therapeutic option with significant efficacy and minimal toxicity in the neoadjuvant setting of patients with ML.

Demographic and baseline characteristics ($n = 29$).

Characteristic	*n*	%
Gender		
Male	16	55
Female	13	45
Age (years)		
Median	47	
Range	23–75	
ECOG PS		
0	23	79
1	6	21
Tumour variant[a]		
Myxoid	16	55
Myxoid/round cell	12	41
Primary tumour site		
Upper extremity	2	7
Lower extremity	23	79
Trunk/abdominal wall	3	10
Other	1[b]	3
Tumour stage		
I	2	7
II	1	3
III	25	86
Unknown	1	3
Size of the largest tumour		
<5 cm	1	3
5–10 cm	10	35
>10 cm	17	59
Unknown	1	3
No. of sites		
Median	1	
Range	1–2[c]	
More frequent sites of disease at baseline[d]		
Thigh	14	48
Gluteus	3	1

		0
Leg	3	10
Popliteal fossa	3	10
Previous anticancer therapy		
Surgery		
All types	2 9	100
Surgery other than diagnostic/exploratory		
Marginal excision	2	7
Wide excision	3	10
Compartment resection	2	7
Other	1[e]	3
Radiotherapy		
External radiotherapy	1[f]	3

TABLE 7: Data shown are no. of patients (%) except for 'age' and 'no. of sites' (median and range). The median time from initial diagnosis to trabectedin treatment was 1.1 months (range, 0.3–2 31.5mg/m2 mg/m2 months) and the median time from histological analysis to trabectedin treatment was 1.1 months (range, 0.3–31.1 months).

[a] One patient with non-myxoid liposarcoma (not included in the analysis of efficacy).

[b] Corpus cavernosum bulb.

[c] Three patients had metastatic disease at baseline (hepatic, pelvic and lymph nodes metastases) not reported at study entry. These cases were declared protocol deviations and, therefore, they were not included in the primary analysis of efficacy. Upon evaluation for the secondary efficacy end point, all three had stable disease according to RECIST.

[d] Other less frequent sites included arm, pelvis and trunk ($n = 2$ patients each), and mesenterium, liver and lymph node ($n = 1$ patient each).

[e] Right leg amputation.

[f] 60 Gy in the right thigh after surgery (compartment resection).

ECOG PS, Eastern Cooperative Oncology Group performance status. [200]

	n	95% Binomial exact estimator (CI)
pCR per central pathology (primary efficacy end point)	3	13% (3-34%)
Tumor regression by central pathology review		
Very Good	2	9% (1-28%)
Good	10	44% (23-66%)
Low	7	30% (13-53%)
Objective response per RECIST (secondary efficacy end point)	7	4% (10-44%)
	n	**%**
PR	7	24
SD	21	72
NE	1	3

TABLE 7: Pathological response according to RECIST after trabectedin neoadjuvant therapy [200]

1.6.5 Tolerability.

The toxicity profile encountered in the phase II trials was similar to the results observed in the phase I studies evaluating the 2 4-hour continuous infusion of trabectedin at the recommended dose. Myelosuppression and hepatic toxicity were the most frequently observed adverse events (Table 8). Despite neutropenia grade 3–4 in 33%–61% of patients, there was a low incidence of febrile neutropenia (6%–7%), quite different from other agents as doxorubicin (up to 19%) [201]or ifosfamide regimens (up to 39%). [201, 202]. Thrombocytopenia and anemia grade 3–4 was seen in 9%–22 % of pretreated patients, but not in first line therapy.

Liver toxicity was frequent, but not cumulative and rapidly reversible. Transaminase elevation at more than five times the normal range was described in 20% to 57% of pretreated and 30% of the nonpretreated patients. This toxicity could be improved by dexamethasone premedication. In xenografts models, the hepatotoxicity induced by trabectedin was markedly reduced or avoided after administration of metabolism modulators such as dexamethasone or beta-naphtoflavone 24 h before trabectedin [203]. The authors reported no difference in antitumour efficacy and hypothesized a decreased hepatic exposure to trabectedin, perhaps by regulation of hepatic metabolism [204]. In the clinic dexamethasone premedication was retrospectively analyzed by Grosso and colleagues[184]. Twenty-three patients treated with trabectedin 1.0 to 1.65 as a three-hour or 2 4-hour continuous infusion every 21 days did not receive premedication whereas 31 patients received dexamethasone 4 mg per os bid 24 hours before therapy. The incidence of grade 3–4 transaminitis was reduced from 70% to 3% of patients by the dexamethasone premedication. The incidence of neutropenia and thrombocytopenia was also less important at 10% and 0% instead of 39% and 35%, respectively. The antitumour activity was similar between the two groups and comparable to the ones

reported in other phase II trials. The overall response rate was 9% and the median progression-free survival was 2.6 months.

The analysis of four treatment-related deaths in the European phase II study [180] revealed a statistical correlation between these severe toxicities and liver dysfunction. The influence of patient characteristics and pathophysiological variables was analyzed in 69 patients treated in phase II studies [205]. The incidence of severe toxicity was significantly ($p = 0.02$) greater for patients with any baseline liver function test exceeding the upper limit of the normal range. Thus the administration of the full dose of trabectedin at 1.5 mg/m^2 requires normal alkaline phosphatase and transaminase levels, checked before each cycle, and the dose should be reduced to 1.2 in case of abnormal bilirubin level, and more than 2.5 increase of transaminase or alkalin phosphatase above the normal range.

Other frequent toxicities included nausea, vomiting and fatigue that could be grade 3–4 in up to 9% of patients. Elevation of creatine phosphokinase (CK) has been reported in 2 6% of patients and a few cases of severe and fatal rhabdomyolysis have been observed in the phase I–II studies [175, 179, 206]. Trabectedin induced necrosis of skeletal muscle resulting in subsequent release of intracellular contents leading to electrolyte imbalance, renal failure and death. Caution should be taken when used with other medications known to cause muscle injury as statins. CK is the most sensitive indicator of muscle injury and should be $\leq 2.5\times$ upper limit of normal before each treatment and closely monitored during therapy.

Reference		N	Neutropenia	Febrile neutropenia	Thrombocytopenia	Transaminitis	Nausea	Asthenia/fatigue
Yovine J Clin Oncol. 2004 Mar 1;22(5):890-	Phase II, second line	54	33 (61%)	4 (7%)	10 (19%)	26 (48%) ASAT 31 (57 %) ALAT	4 (7%)	8 (15%)
Garcia-CarbJ Clin Oncol. 2004 Apr 15;22(8):148	Phase II, second line	36	12 (34%)	2 (6%)	6 (17%)	9 (26%) ASAT 7 (20%) ALAT	2 (6%)	0
Le Cesne J Clin Oncol. 2005 Jan 20;23(3):576-	Phase II, second line	104	52 (52.5%)	9 (9.1%)	18 (18.2%)	35 (35.3%) ASAT 44 (44.5%) ALAT	7 (7.1%)	0
Garcia-Carbonero J Clin Oncol. 2005 Aug	Phase II, first line	36	12 (33%)	0	0	12 (34%) ASAT 13 (36%) ALAT	5 (14%)	4 (11%)
Abbreviations: ALAT, alanine aminotransferase; ASAT, aspartate aminotransferase.								

Table 8: incidence, of grade ¾ toxicities in phase II trial [178]

1.6.6 Combinations

Combination treatments with doxorubicin [207] rinotecan, [208] and paclitaxel [209] were evaluated in preclinical studies showing synergistic effects against sarcomas. Trabectedin was combined with doxorubicin, egylated liposomal [210] doxorubicin, paclitaxel, and capecitabine in phase I studies involving patients with solid tumours. The DLT were essentially myelosuppression and hepatotoxicity.

In sarcomas a phase I study combining doxorubicin and trabectedin reported that the maximum tolerated dose was 60 and 1.1 respectively. Preliminary pharmacokinetics of both agents were not significantly modified by the combination. Because of severe neutropenia at the first dose level, granulocyte colony-stimulating factor had to be added subsequently. The dose limiting toxicities were neutropenia and thrombopenia. Dose reduction was required in 51% of patients for trabectedin and 27% for doxorubicin. Among the 41 treated patients, five achieved a partial remission and 34 had a disease stabilization that lasted more than six months in 15 patients.

1.6.7 Resistance to Trabectedin

Only a few cell lines have been described that show specific resistance to trabectedin. The resistance to trabectedin of the colorectal carcinoma ER5 cell line (derived from the HCT116 cells) is associated with a loss of heterozygosity at 13q33, where the gene encoding for XPG is located. Sequential analysis of the XPG gene showed an insertion of adenine at codon 240, which resulted in a stop codon at position 243 [148,211] . Another mechanism associated with trabectedin's resistance has been described in human surgically resected chondrosarcoma cells (CS-1; [212]). Alteration in the cytoskeleton architecture, mainly related to modified types I and IV collagen expression, has been shown in this cell line model [139]. In a different study, continuous exposure for 10 months to increasing doses of trabectedin (up to 800 nmol/L) generated highly resistant, overexpressing P-gp ovarian cancer cells [213].

1.7 Summary

A sarcoma is a type of cancer that develops from certain tissues, like bone or muscle. There are 2 main types of sarcoma: bone sarcomas and soft tissue sarcomas. Soft tissue sarcomas can develop from soft tissues like fat, muscle, nerves, fibrous tissues, blood vessels, or deep skin tissues. They can be found in any part of the body. There are about 50 different types of soft tissue sarcomas and most of them develop in the arms or legs. They can also be found in the trunk, head and neck area, internal organs, and the area in back of the abdominal cavity (known as the *retroperitoneum*). Liposarcomas are malignant tumors of fat tissue. They can develop anywhere in the body, but they most often develop in the thigh, behind the knee, and inside the back of the abdomen. They occur mostly in adults between 50 and 65 years old.

After a sarcoma is found and staged, the cancer care team will recommend one or several treatment options. In choosing a treatment plan, factors to consider include the type, location, and stage of the cancer, as well as your overall physical health. The main types of treatment for soft tissue sarcoma are: Surgery, Radiation, Chemotherapy, Targeted therapy.

Interest in marine natural products has allowed the discovery of new drugs and trabectedin (ET-743, Yondelis), derived from the marine tunicate Ecteinascidia turbinata, was approved for clinical use in 2007. It binds to the DNA minor groove leading to interferences with the intracellular transcription pathways and DNA-repair proteins. In vitro antitumor activity was demonstrated against various cancer cell lines and soft tissue sarcoma cell lines. In phase I studies tumor responses were observed also in different soft tissue sarcoma subtypes.

The most common toxicities were myelosuppression and transient elevation of liver function tests, which could be reduced by dexamethasone premedication. The

efficacy of trabectedin was established in three phase II studies where it was administered at 1.5 mg/m^2 as a 24 h intravenous infusion repeated every three weeks, in previously treated patients. The objective response rate was 3.7%–8.3% and the tumor control rate (which included complete response, partial response and stable disease) was obtained in half of patients for a median overall survival reaching 12 months. In non-pretreated patients the overall response rate was 17%. Twenty-four percent of patients were without progression at six months. The median overall survival was almost 16 months with 72% surviving at one year. Predictive factors of response are being explored to identify patients who are most likely to respond to trabectedin.

Trabectedin was associated with antitumour activity in a series of patients with myxoid liposarcoma. The noted patterns of tumour response were such that tissue density changes occurred before tumour shrinkage in several patients. In some patients, tissue-density changes only were seen. Long-lasting tumour control was noted in responsive patients. The surprising finding on the sensitivity of liposarcoma tumors carrying a specific translocation involving a negative regulator of adipogenesis prompted us to investigate the mechanism of action of trabectedin related to this differentiation pathway.

Chapter 2:

MATERIALS AND METHODS

2 .1 Animals

Female athymic NCr-*nu/nu* mice, seven weeks old, were obtained from Harlan Laboratories (Udine, Italy). They were maintained under specific pathogen-free conditions, housed in individually ventilated cages and handled using aseptic procedures. Procedures involving animals and their care were conducted in conformity with the institutional guidelines that are in compliance with national (Legislative Decree 116 of Jan. 27, 1992 Authorisation n.169/94-A issued Dec. 19, 1994 by Ministry of Health) and international laws and policies (EEC Council Directive 86/609, OJ L 358. 1, December 12, 1987; Standards for the Care and Use of Laboratory Animals, United States National Research Council, Statement of Compliance A502 3-01, November 6, 1998).

2.2 *In vivo* studies

For the antitumour activity studies, female athymic nude mice were engrafted s.c. with ML014, ML015 (with type II fusion transcript) or ML004, ML006 (with type III fusion transcript) myxoid liposarcoma fragments as previously described by Roberta Frapolli [48]. The growing tumour masses were measured with a Vernier caliper, and the tumour weights ($1mm^3$ = 1mg) were calculated with the formula: length x $(width)^2/2$. When tumour weight reached about 400 mg, mice were randomized and treatment started. Trabectedin (generously provided by PharmaMar, Madrid, Spain) was given i.v. at the dose of 0.15 mg/kg, every seven days for three times (q7dx3). Each group comprised at least seven mice. Drug efficacy was calculated as T/C%, where T and C are the mean tumour weights of treated and control groups, respectively. The treatment was considered active when T/C<42 %.

For the molecular analysis mice bearing type II (ML015, ML014) or type III (ML006 or ML004) xenografts were treated with trabectedin starting when tumour weight reached about 600 mg. Mice where sacrificed at different time points after the first and the third dose of trabectedin. Tumours were immediately collected and snap-frozen on dry-ice or processed for chromatin immunoprecipitation as described later.

2.3 Chromatin Immunoprecipitation

Tumours and cells were washed in phosphate-buffered saline and incubated for 10 min with 1% formaldehyde (VWR International PBI srl, Milan, Italy). After quenching the reaction with glycine 0.1 M, the cross-linked material was sonicated into chromatin fragments of an average length of 500/800 bp. Chromatin was kept at -80°C. Immunoprecipitations were performed with ProtG Sepharose (KPL, Milan, Italy).
Italy and 5µg of the indicated antibodies: CHOP (F-168, Santa Cruz, California, USA), FUS (Bethyl, Milan, Italy) and anti-Flag antibody (F742 5, Sigma Aldrich, St Louis, USA). The chromatin solution was precleared by adding ProtG-Sepharose for 2 hours at 4 °C and was aliquoted and incubated with the antibodies overnight at 4°C on a rotating wheel. ProtG-Sepharose was blocked with 1 µg/l salmon sperm (Sigma Aldrich) and 10 µg/l bovine serum albumin overnight at 4 °C and then incubated with chromatin and antibody for 2 hours. Immunoprecipitated material was washed 9 times with wash buffer. Cross-links were reversed by incubating samples for 5 h at 65 °C in 200mM NaCl and 10µg of RNase A to eliminate RNA. Recovered material was treated with proteinase K, extracted with phenol/chloroform/isoamyl alcohol (25:24:1), and precipitated. The immunoprecipitated DNAs were resusepended in 50µl of H2O and analyzed by quantitative Real Time PCR. Values are reported as fold enrichment over the control antibody–Flag (Sigma Aldrich). Satellite sequences repeated at multiple

positions in the genome were used as a control for unspecific precipitation and as a loading control.

2.4 Western Blot analysis

Western blot analysis ensures separation of proteins according to size using sodium dodecyl sulphate polyacrylamide gel electrophoresis (SDS/PAGE), transferring them to membrane electrophoretically and then using specific antibodies to detect the protein of interest.

2.4.1 Protein extraction preparation.

Total proteins were extracted from cultured cells by a lysis method. Basically cell cultures were washed twice with ice-cold PBS and then detached with a disposable scraper. The suspension was then centrifuged at 1500 rpm for 5 minutes and, after centrifugation, the pellet was resuspended in an amount of lysis buffer dependent on the size of cell pellet.

Lysis buffer composition: 50 mM Tris-HCl pH=8 , 150 mM NaCl, 10% glycerol, 1 mM $MgCl_2$, 1 mM EGTA, 100mM NaF, 1% Triton X-100 in the presence of 1X protease cocktail inhibitor (Sigma) and 5mM Na_3VO_4 as phosphatase inhibitor.

Lysates were incubated on ice for 30 minutes. Insoluble cellular debris were pelleted at 13000 x g for 10 min at 4°C and the total protein present in the supernatant was recovered and placed in a fresh Eppendorf tube (1.5 ml). An aliquot (2 ul) was used to determine protein concentration.

To evaluate xenograft proteins, explanted tumours were immediately snap-frozen. Frozen specimens were diluted into a volume of ice-cold lysis buffer in a fixed ratio (1 ml / 10 mg) and homogenized with a ultra-turrax homogenizer. Lysates were incubated on ice for 30 minutes and then centrifuged at 13000 rpm (17000 x g) for 10 min at 4°C

at least two times to pellet insoluble cellular debris. 2 ul of clear lysates were used to measure protein concentration.

2.4.2 Calibration Curve Preparation.

For the calibration curve, a solution of bovine serum albumin (BSA) (1 mg/ml) was prepared dissolving powdered BSA (Sigma) in water. For each calibration point, 800 ul of distilled water were mixed with 200 ul of BioRad Protein Assay (BioRad) and transferred into disposable cuvettes (PBI International). Calibration points of the standard curve were generated by adding 2 ,4,6, 8 and 10 ul of BSA solution to 1 ml of Biorad diluted solution. The absorbance at 595 nm was measured in the spectrophotometer. The absorbance value corresponding to the blank sample was subtracted from the values obtained from the BSA-containing samples. The calibration curve obtained in such a way allows extrapolation of the exact absorbance value corresponding to 1 ug of proteins present in the solution.

2.4.3 Determination of protein concentration

The concentration of proteins in the samples was determined by mixing 2 ul of protein cellular extract to the Biorad diluted solution as done for the calibration curve points. Protein sample concentration was found by interpolating the registered absorbance with the standard curve.

2.4.4 SDS-PAGE

Depending on the protein under evaluation, 30 ug to 100ug of protein total extract were mixed with a corresponding volume of 5X SDS loading buffer (50 mM tris-HCl pH=6.8; 2 % SDS, 0.1% Bromophenol Blue, 10% Glycerol, 5% β-Mercapto Ethanol) and the mixture was boiled for 5 min. Samples were loaded onto a 5% stacking gel and a range of 6-15% separating gel:

Stacking and running gel were prepared shortly before pouring. Ammonium persulphate catalyses polymerization and TEMED accelerates the reaction and so these two reagents were added last.

Proteins were resolved on a minigel apparatus (BioRad) and run for approximately 2 h at 100V in 1X TGE running buffer (2 5 mM *Tris base, 2 50mM glycine, 0.1% SDS*):

Electrophoresis progress was followed using pre-stained molecular weight markers (11-170 Kda, Page Ruler Prestained Protein Ladder, FERMENTAS)

2 .4.5 Protein Transfer and Detection.

The separated proteins were transferred onto nitro-cellulose (Whatman Protran, Milan, Italy) or PVDF membrane (Millipore, Billerica, MA, USA), depending from the protein under evaluation, using BioRad Mini transfer blot equipment in 1X Transfer Buffer (50mM *Tris base, 100mM glycine, 0.01% SDS, 2 0% methanol*). A constant power of 60V was applied for 2 hours.

Filters were stained with Ponceau red solution (Sigma) to check for sample loading and transfer. Nitrocellulose Membrane was saturated with 5% non-fat dried milk dissolved in TBS-T (Tris-HCl pH=8 10mM, NaCl 150mM, Tween 200.05%) for 1 hour to block

non-specific binding. Identical effect was obtained by air-drying PVDF membrane for 1 hour after washing it in pure methanol.

All the following procedures were carried out on a shaker. Blots were exposed for 2 h at room temperature or O/N at 4°C to the desired primary antibodies diluted at the appropriate concentration in 5% non-fat dry milk in TBS-T or in TBS-T 5% BSA.
After incubation, blots were washed twice for 15 minutes with TBS-T 0.1% and incubated with the appropriate horseradish-peroxidase linked anti-mouse, anti-goat or anti-rabbit IgG secondary antibody (SantaCruz) for 2 h using 1:3000 dilutions in 5% non-fat dry milk in TBS-T to reveal primary antibody binding. Blots were washed for at least 1 hour in TBS-T, and detection was performed with an enhanced chemiluminescent detection system (ECL, Amersham-Life Science). Immunoblotting was carried out with the following antibodies: CHOP (F-168, Santa Cruz Biotechnology), PTX3 (kindly gave by Lavena P), PPARγ1,2 (E-100, Santa Cruz Biotechnology), C/EBPα (C-18, Santa Cruz Biotechnology), β-Actin (C-4 Santa Cruz Biotechnology). Binding was detected using peroxidise labelled secondary antibodies and visualised using a chemiluminescence kit (Amersham, Milan, Italy).

2 .4.6 Isolation of Nuclear Proteins

At least $10x10^6$ 402 -91 cells were scraped from the culture plates into ice-cold PBS and harvested by centrifugation at 1500 rpm for 5 min; the pellet was resuspended in 400 uL of ice-cold buffer A (250 mM sucrose; 20 mM Hepes-KOH pH 7.5; 10 mM KCl; 150mM MgCl2 ; 1 mM Na-EDTA; 1 mM Na-EGTA; 1 mM DTT; 0.1 mM PMSF) and homogenized 40 times on ice with a Teflon potter to break open the cell membranes. The homogenate was centrifuged twice at 750 x g for 10 minutes at 4°C to precipitate nuclei. The supernatants was centrifuged at 10,000 x g for 15 min at 4°C to discard the

pellet (residual nuclei and mitochondria-containing fraction), and supernatant (cytosolic fraction) was collected. Protein expression in nuclei and soluble fraction was determined as previously described.

2 .5 Transcripts analysis

2 .5.1 RNA extraction and purification

The SV total RNA isolation kit (Promega, Madison, Wi, USA) was used for isolating total RNA. With this method is possible to isolate pure RNA from relatively few cells (10^6) in a limited time (1-2 hours). The cells are lysed in a guanidine thiocyanate containing solution which maintains the integrity of RNA while disrupting cells and dissolving cell components. RNA was then prepared following manufacture's instructions. The purified RNA is then eluted with a small volume of water (generally 50 microliters). 2 ul of this solution were used to determine RNA concentration by using NANO-DROP technology. Samples were stored at –20°C until required for use. Alternatively an aliquot (2 ul) of this solution was diluted in sterile water to a final volume of 100 ul, and the RNA concentration was measured spectrophotometrically following the formula RNA (mg/ml) = $OD_{2\ 60\ nm}$ x 40 x dilution factor. The amount of RNA is calculated considering that a solution of 40 ug of RNA in one ml would give an absorbance reading of 1.0 at 260 nm. The 260/280 assorbance ratio must be between 1.8 and 2 .0 for a sample of reasonable purity. RNA was eluted by adding 100 ul of pre-heated nuclease-free water on the filter followed by centrifugation at maximum speed for 30 sec. Total RNA's concentration was measured as previously indicated.

2 .5.2 Semi-quantitative RT-PCR

cDNA Archive KIT (Applied Biosystems, Monze, Italy) was used to perform retrotranscription reaction: A range from 200 ng to 1 ug of total RNA is retrotranscribed to cDNA using random hexamers.

Optimal primer pairs spanning splice junctions were chosen, using PRIMER-3 software (http://frodo.wi.mit.edu/cgi-bin/primer3/primer3_www.cgi) and their specificity was verified by the generation of single amplicon bands of in the PCR products and melting curves. Primers pairs to detect specific FUS-CHOP isoforms were as previously described (CCR VOL7, pg 3977-3987 December 2001).

The reaction protocol was: 16°C for 30 min - 42 °C for 30 min – 85° for 5 min and final hold at 4°. cDNA reaction products were stored at -20°C until the PCR steps.

Primers used to detect FUS-CHOP

FUS-CHOP forward TGGCTATGAACCCAGAGGTC
FUS-CHOP reverse TCCCGAAGGAGAAAGGCAAT

2 .5.3 Real Time PCR Procedures

PCR reaction master mix was made in a final volume of 20 ul following the manufacturer's instructions.

Regarding SYBR green technology, all couples of primers were designed on the basis of the sequence reported in the Ensembl database. "Primer3" software freely available online was used to design the best set of primers to be used for each gene. Synthesis of oligonucleotides used as primers was performed by Sigma.

5 to 10 ng of cDNA were used for each reaction of Real-time PCR. GoTaq qPCR Master Mix (Promega) was used with the following primers to perform reactions on 7900HT Sequence Detection System (Applied Biosystems).

Differences in gene expression were determined by real time RT-PCR (ABI-7900, Applied Biosystems) using Syber Green (Applied Biosystems). The reactions were subjected to initial incubation at 95°C for 10min followed by 45 cycles of 95°C for 15sec and 60°C for 1min'. Raw data were generated with SDS Relative Quantification Software (Applied Biosystems). To calculate the relative expression of each mRNA, we used the 2^{-DDCT} method to average the threshold cycle (CT) values for three replicates.

ChIp analysis was determined by RT-PCR (ABI-7900, Applied Biosystems) using Syber Green (Applied Biosystem). The reactions were subjected to initial incubation at 95°C for 10 min followed by 40 cycles of 95°C for 30sec, 66°C for 30 sec and 72 ^{0}C for 30 sec. Raw data were generated with SDS Relative Quantification Software (Applied Biosystems). Values are reported as fold enrichment calculated with the following formula:2 ^ΔCtx - 2 ^ΔCtb, where ΔCtx = Ct input – Ct sample and ΔCtb = Ct input - Ct control Ab (Flag).

Primers used for gene expression analysis

PTX3 forward CCCACCAAATTCAGGGGAACT
PTX3 reverse CCACTACCCCTTCCAGGACT
FN-1 forward CTTCGCTTCACACAAGTCCA
FN-1 reverse GCAGCGAACAAAAGAGATGC
.C/EBP beta forward GAGGAGGCGGAGGTTTCAG
C/EBP beta reverse GTGGGAGTTTACGGGAGGAA
.C/EBP alfa forward GCCTGCCGGGTATAAAAGCTC
C/EBP alfa reverse GACTCCATGGGGGAGTTAGAG

Primers used for ChIP analysis

PTX3 forward CCCACCAAATTCAGGGGAACT
PTX3 reverse GCATTGCTGGAGAGACGCAAA
FN-1 forward CTTCGCTTCACACAAGTCCA
FN-1 reverse GCAGCGAACAAAAGAGATGC
CHOP forward CCTAGCGAGAGGGAGCGACG
CHOP reverse GTCTCTGACCTCGGGAGCGCC
IL-8 forward AGGTTTGCCCTGAGGGGATG
IL-8 reverse GCTTGTG TGCTCTGCTGTCTC
SAT11 (Control satellite sequences were amplified using) forward CAATTATCCCTTCGGGGAATCGG
SAT11 reverse GGCGACCAATAGCCAAAAAAGTGAG
TSP-1 forward CCCAACAAATTCAGGGGAATT
TSP-1 reverse GCATTGCTAGAGAGACGCAAA

2 .6 Acquisition of tumour biopsies

The biopsy was obtained from a 43 year-old patient with recurrent myxoid liposarcoma started as round cell in a lower extremity and eventually with metastasis to soft tissue, pleura, mediastinum, heart. Trabectedin was used as front-line therapy at a dose of 1.1 mg/kg via portable infusion device (pump baxter) infusion for 24 h.

The biopsy was obtained before and 24 h after the first cycle.The patient has continued for 11 cycles of infusions in total, resulting in a response both in size and density of the tissue already after 3 cycles of treatment.

2 .7 Cells and culture conditions

The myxoid liposarcoma cell line 402 -91 was kindly supplied by Aman P. (36). 402 - 91 cell were grown in adhesion in RPMI-1640 medium (Biowest S.A.S., Nuaillé, France) supplemented with 10% fetal bovine serum (Sigma Aldrich, St.Louis, USA), 1% L-glutamine 2 mmol/L, Biowest) and 1% penicillin-streptomycin 10.000µg/ml, (Biowest). Cells were maintained at 37°C in a humidified 5% carbon dioxide atmosphere in T2 5 and T75 cm^2 tissue flasks (IWAKI, Bibby Sterilin, Staffordshire, UK).

2 .8 ELISA assay

Enzyme linked immunosorbent assay (ELISA) is a quantitative technique to evaluate the presence of a specific antigen into a solution. From a standard curve, made from a series of known concentrations of our target, is possible to find the unknown concentration of the specific antigen present in the sample of interest. Human TSP-1 in the plasma of tumor-bearing mice was detected with Quantikine Immunoassay (R&D System). Sensitivity of the assay was 0.355 ng/mL. Each sample was analyzed in duplicate. This analysis was routinely performed in the " Thrombosis Unit" at the Mario Negri Bergamo. Proteins from treated and untreated samples were given to be analyzed.

Chapter 3

AIM

Previously, It was identified the effects of trabectedin on the promoters of several cancer related genes and has shown that this compound affects transcription factor regulation [143, 214]. Based on our data, we hypothesize that the selective anti-tumour activity of trabectedin against ML is due to its ability to counteract the oncogenic activity of the FUS-CHOP fusion protein generated by the tumour specific translocation [60].

During my PhD, I wanted to build up on discoveries made in previous studies and to characterize the mechanism of the selective activity of trabectedin in ML. The aim of my project was to study the effect of trabectedin on ML at the molecular level *in vitro* and at the cellular level *in vivo*. My project will involve:

1) Molecular characterization of the interference of trabectedin with transcription alteration caused by the expression of the FUS-CHOP fusion gene.
2) Determination of differential sensitivity of FUS-CHOP variants to trabectedin and its clinical significance.
3) Identification of the effect of trabectedin on angiogenesis pathway *in vivo* and *in vitro*.

My goal was to gain further insight into the mechanism of action of trabectedin at the molecular level, particularly focusing on the effect of trabectedin treatment on the expression of genes induced by FUS-CHOP fusion.

Chapter 4:

RESULTS

4.1 Detection of FUS-CHOP fusion transcripts in 402 -91cell line.

Previous studies have demonstrated that trabectedin has a selective antitumour activity against ML with the translocation t (12;16) (q13; p11) with a FUS-CHOP fusion gene of type 1 and 2 [59]. According to this, as cell line model, I have chosen the 402-91 cell line carrying type 1 FUS-CHOP fusion. To determine the presence of the chimera type 1, I have done RT-PCR using primers able to discriminate between the different FUS-CHOP isoforms.

RT-PCR analysis with FUS-CHOP Type I isoform specific primers identified a single band at 526 bp confirming the presence of the expected fusion transcript in 402-91 cells (Figure 25).

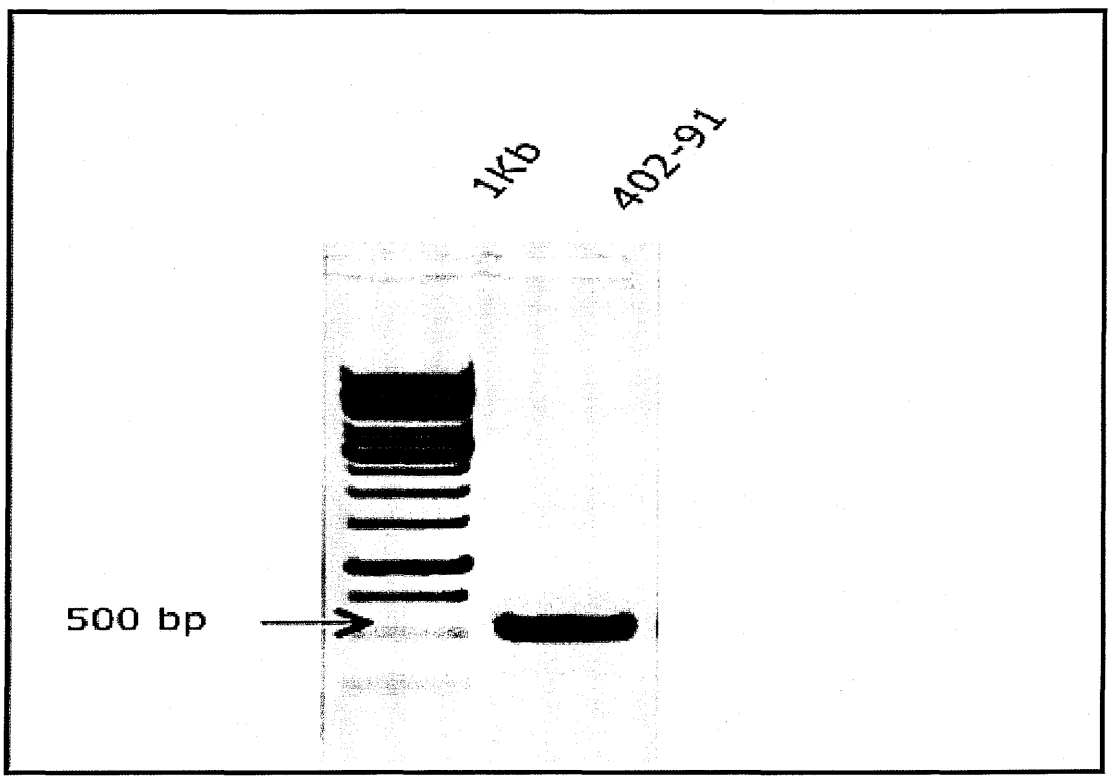

Figure 25: RT-PCR analysis of FUS-CHOP fusion mRNA. Lane 1- 1Kb DNA Ladder, Lane 2 - RT-PCR analysis of FUS-CHOP mRNA in 402 -91 cells. Note the presence of a single band at 526 bp identifying the presence of type I isoform in 402 -91 cell line.

4.1.1 Effect of trabectedin treatment on transcription regulation of FUS-CHOP

To delineate the mechanistic basis of how trabectedin treatment could affect the expression of genes, such as PTX3 and FN-1, already known to be specifically regulated by FUS-CHOP, I have performed RT-PCR analysis on 402 -91 cells.

402 -91 cells were treated with trabectedin at 5nM, corresponding to the IC50 value or with 10nM (=2 xIC50) trabectedin. After trabectedin was washed out, cells were incubated in drug free medium and were allowed to recover for 6 or 24 hours. mRNA levels of PTX3 and FN-1 extracted from cells treated with 1 hour of trabectedin and a recovery of 6 hours were decreased significantly when compared to untreated cells. The mRNA levels of PTX3 and FN-1 were further reduced in cells treated and recovered for 24 hours compared to untreated controls (figure 26).

The expression of PTX3 and FN-1 were significantly altered even with the low dose of trabectedin. Thus, the decrease in expression of FUS-CHOP targets is likely due to the trabectedin effect on the transcription factor activity of the fusion protein indicating that the chimera could be directly affected by the compound.

To determine whether trabectedin could cause a decrease in the protein level of FUS-CHOP, I have analyzed the expression of the chimera by western blot before and after the treatment. To detect FUS-CHOP protein I have used an antibody against CHOP because there is no antibody specifically against the chimera. However, it is possible to discriminate the oncogenic fusion from the endogenous CHOP protein by difference in their molecular weights.

First, I have confirmed that the chimera protein was present exclusively in the nuclear fraction as previously shown (Figure 27). This corroborates the fact that FUS-CHOP protein could be acting as a transcription factor.

By western blot analysis I found that the protein levels of FUS-CHOP fusion in the nucleus were the same treated and untreated 402 -91 cells. There was no change in the

cellular localization of the chimera with trabectedin treatment. These results showed that trabectedin affects were not due to a decrease of the protein level or localization of FUS-CHOP fusion.

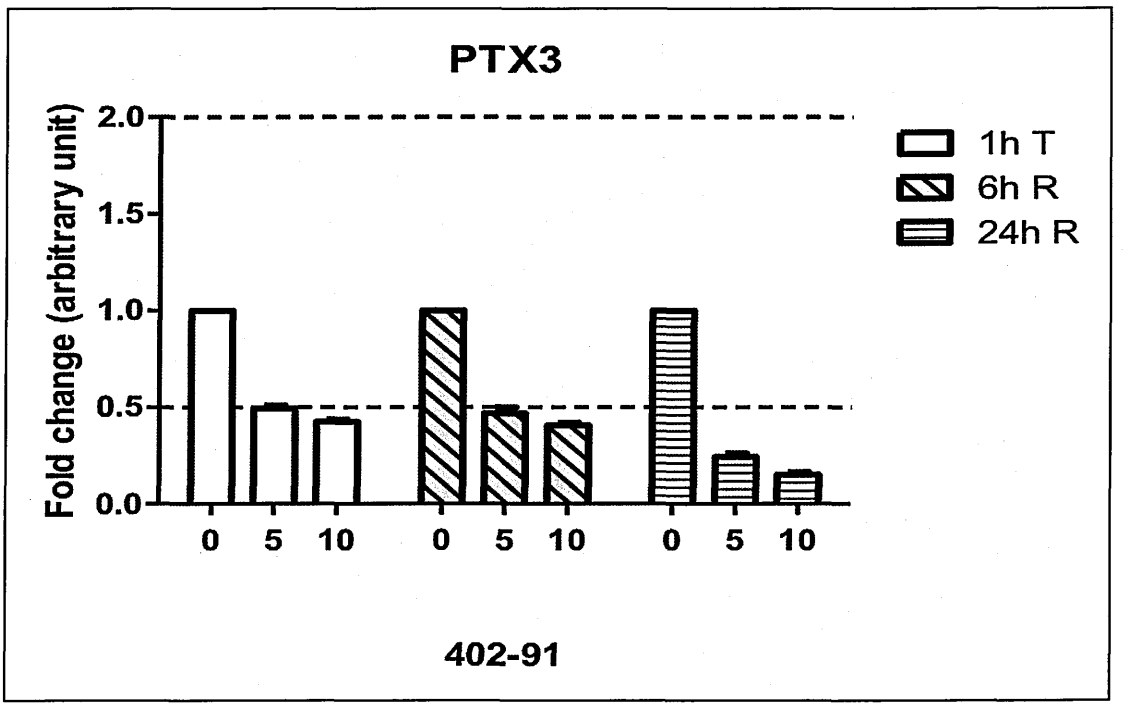

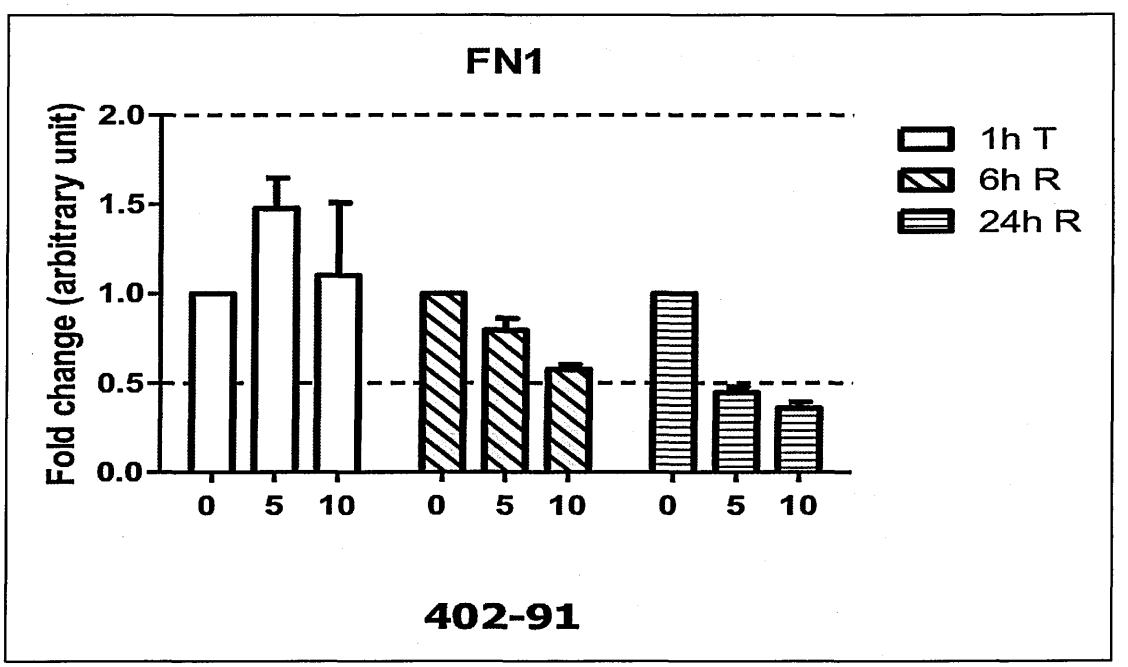

Figure 26: Real time RT-PCR analysis performed in 402 -91 at different times of recovery in drug free medium after 1h of treatment with different doses trabectedin (0, 5 and 10 nM). Data were analysed by the ΔΔCT method and expressed as fold changes (arbitrary unit) compared to their untreated control set as 1. Data are the mean of three independent experiments performed in triplicates. Bars, +/- SD.

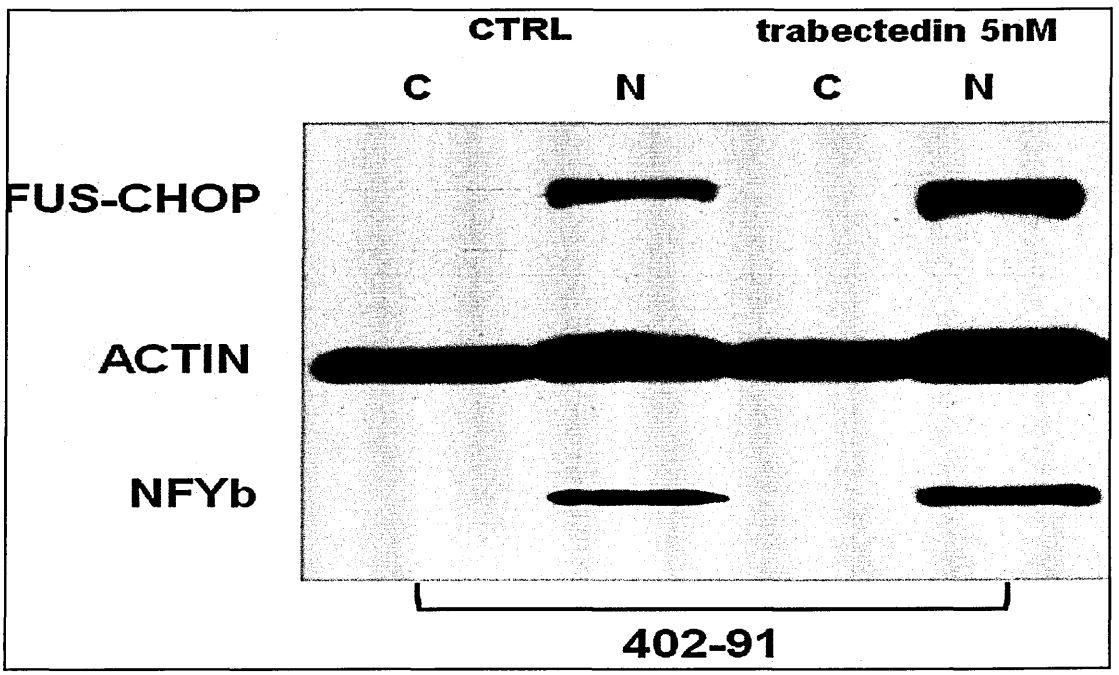

Figure 27: Western blot analysis of 402 -91 cell lines carrying the translocation t(12 ; 16) (q13; p11), using anti-CHOP antibodies (GAD153). The cells were harvested after 1 hour after treatment with the indicated concentrations of trabectedin. Yb was used as nuclear loading marker for data normalization.

4.1.2 Trabectedin's effect is related to changes in the transcription modulation mediated by FUS-CHOP.

Despite the significant effect of trabectedin on the transcription of FUS-CHOP target genes, we have not seen a significant change in the FUS-CHOP protein levels with treatment, suggesting that trabectedin might be affecting the DNA binding activity of FUS-CHOP. In order to verify this hypothesis, I have looked closely at the DNA binding activity of FUS-CHOP.

To determine whether the transcriptional changes were primary events, I monitored binding of FUS-CHOP to promoters of PTX3 and FN-1 by ChIP. For this purpose, I have established ChIP protocol and optimized the conditions to obtain reliable and consistent results with selected antibodies. Since, no antibody was available to recognize the specific chimera, FUS-CHOP was precipitated by the anti-FUS and anti-CHOP antibodies separately. It was therefore essential to monitor both CHOP and FUS in the same ChIP. A satellite 11 (Sat11) sequence that is repeated multiple times in the genome was used as a control for non-specific precipitation along with an irrelevant anti-Flag as a negative control. To test if FUS-CHOP was binding to the PTX3 and FN-1 promoters, I initially performed ChIP assays using untreated 402-91 cell line. I have evaluated both promoters in quantitative RT-PCR. Values were reported as a fold enrichment over a Flag antibody as a negative control.

I next checked whether the trabectedin treatment affected the chimera fate. I've performed three independent experiments in triplicates each time. 402 -91 cells were treated with 2 nM of trabectedin for 1 hour and recovered in drug free medium for 6 hours and 24 hours. I saw that the enrichments were significantly reduced in the treated cells already after 1 hour of treatment (figure 28). With respect to the anti-Flag control

antibody, binding was significantly affected on all the promoters tested even after 6 hours and 24 hours of recovery (figure 29, figure 30).

Most importantly, I observed that trabectedin caused detachment of the chimera from PTX3 and FN-1 promoters already after 1h of treatment confirming that trabectedin removes FUS-CHOP from its target promoters at low dose. I concluded that trabectedin induces the removal of the chimera from promoters, which in turn alters their expression and their functionality.

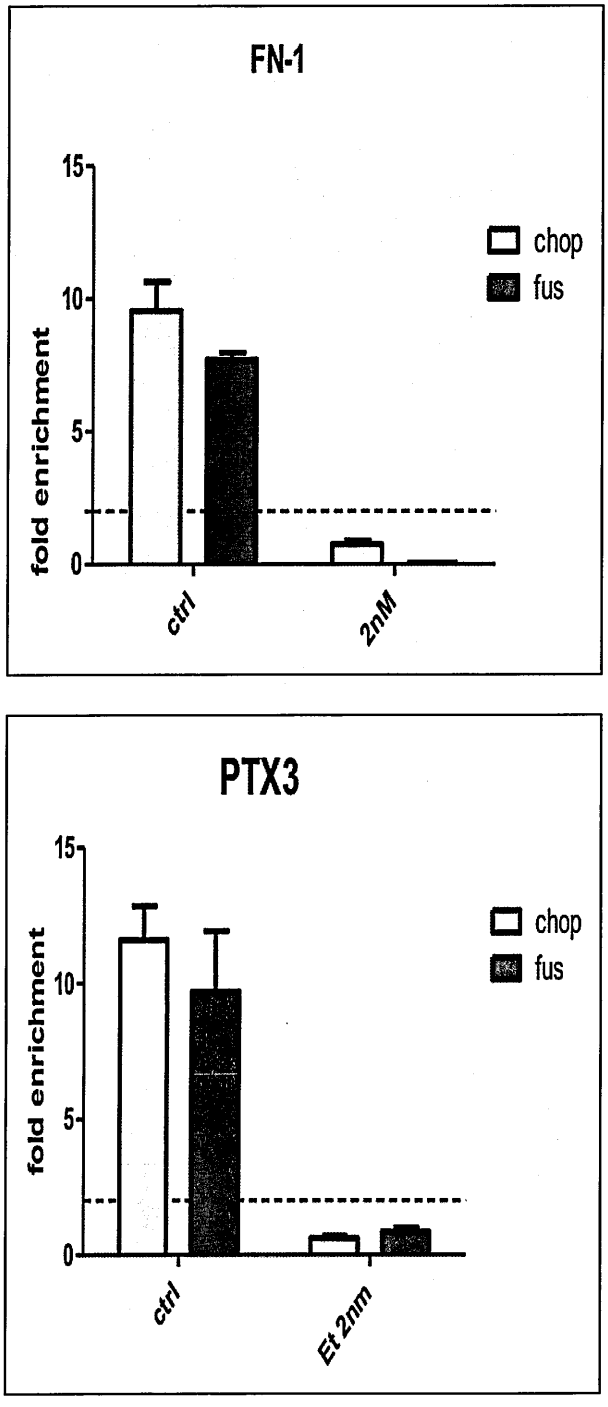

Figure 28: ChIP from untreated cells and treated with 2 nM of trabectedin for 1 hour with, α-CHOP, α-FUS, α-Flag (Ctl) antibodies. Two promoters were evaluated in quantitative Real Time PCR analysis. Values are reported as fold enrichment over anti-Flag antibody.

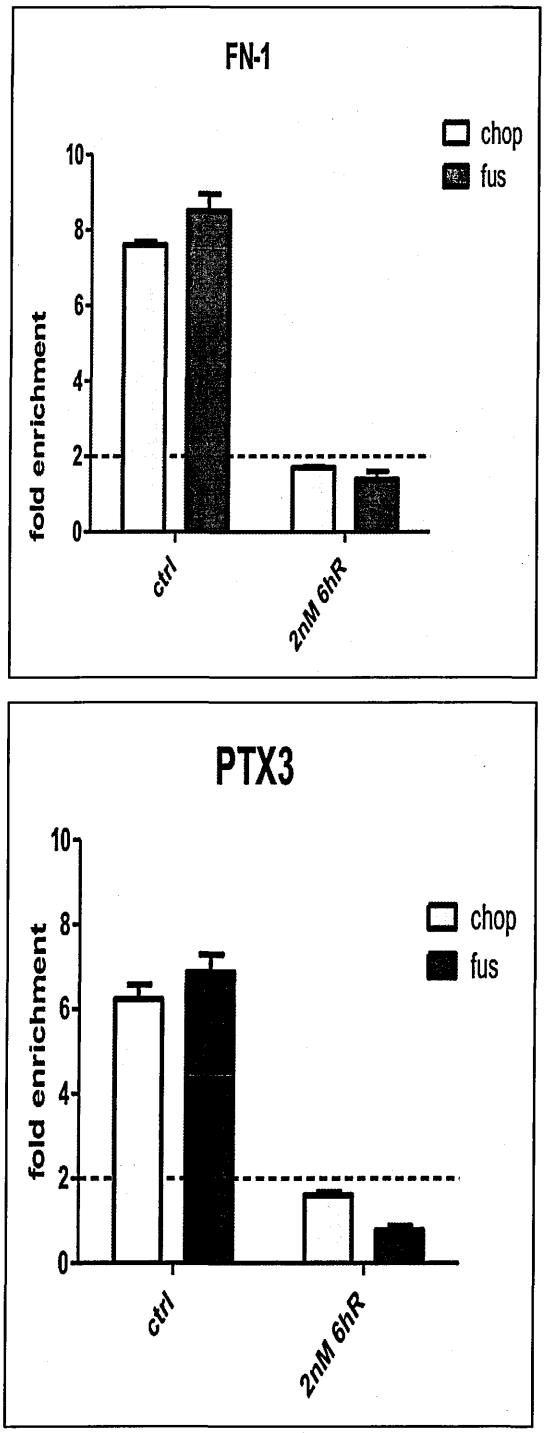

Figure 29: ChIPs analysis of 402 -91 cells untreated and treated with 2 nM of trabectedin at 6 hours of recovery in a drug free medium after 1 hour of treatment. The promoters region of PTX3 and FN-1 were amplified. Values were measured as fold enrichment over a Flag control antibody in quantitative RT-PCR analysis.

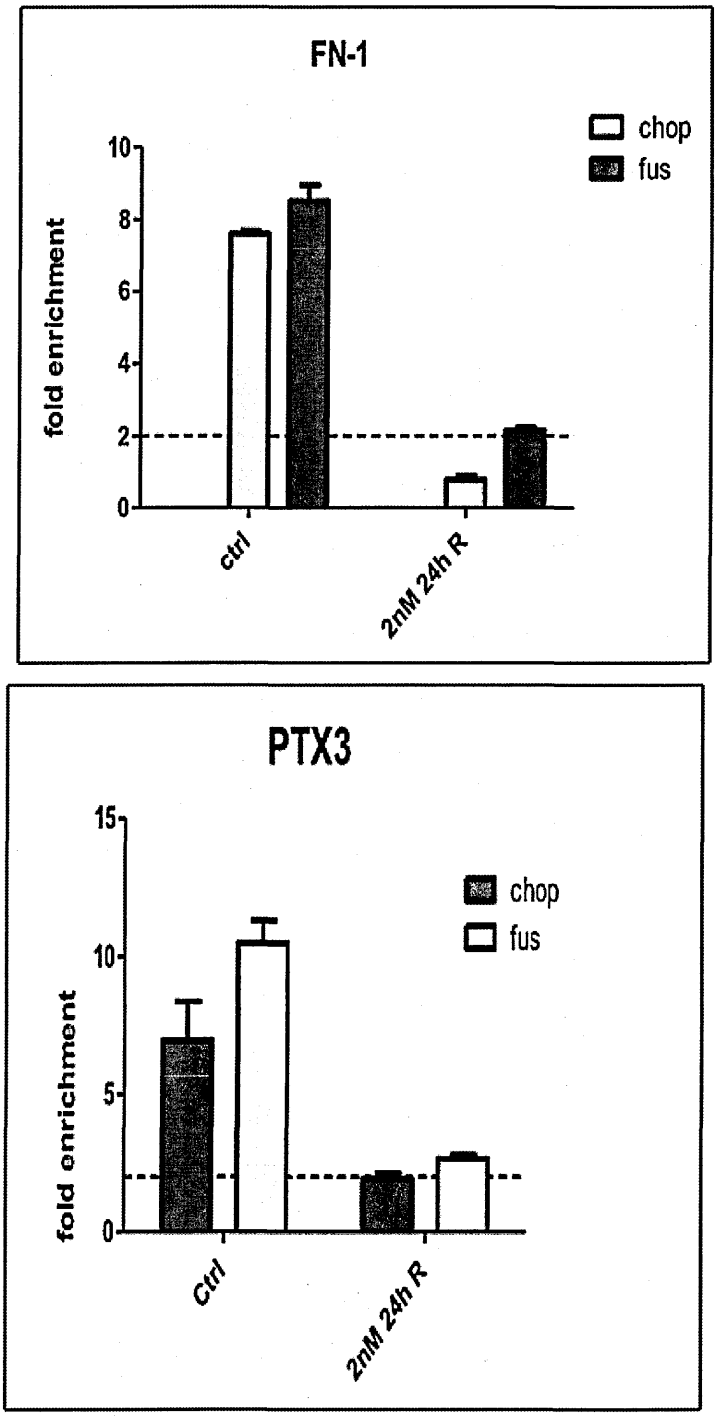

Figure 30: 402 -91 cells were treated with 2 nM of trabectedin and recovered for 24 hours in drug free medium and chromatin analyzed by ChIP with the indicated antibodies. PTX3 and FN-1 promoters bound by FUS-CHOP, were evaluated in quantitative RTPCR analysis. Values are reported as fold enrichment over the control Flag antibody.

4.1.3 Trabectedin rescues the adipocyte differentiation block *in vitro*.

Previous studies have identified a number of transcription factors involved in adipocyte differentiation. These include PPARγ and members of the C/EBP family of transcription factors. These transcription factors are expressed as a cascade in which C/EBPβ and C/EBPδ, during the first stages of the adipocyte differentiation program, induce the expression of C/EBPα and PPARγ, the master regulator of adipogenesis [69, 70, 79].

Based on ChIP results, I have performed RT-PCR with mRNA extracted from 402 -91 cells untreated or treated with trabectedin. I have found that C/EBPβ was present in untreated cells and increased after the treatment with trabectedin (figure 31). On the other hand, C/EBPα was not present in untreated cells and was rapidly induced at the mRNA level by trabectedin (figure 31). Taken together these data indicate that trabectedin could be involved in the induction of adipocyte differentation in 402 -91 cells, by removing the chimera from its own target genes.

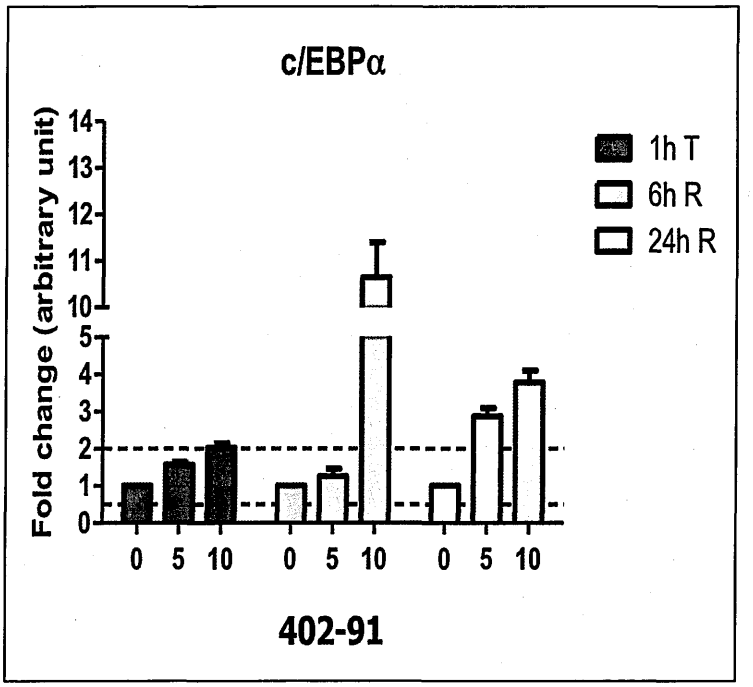

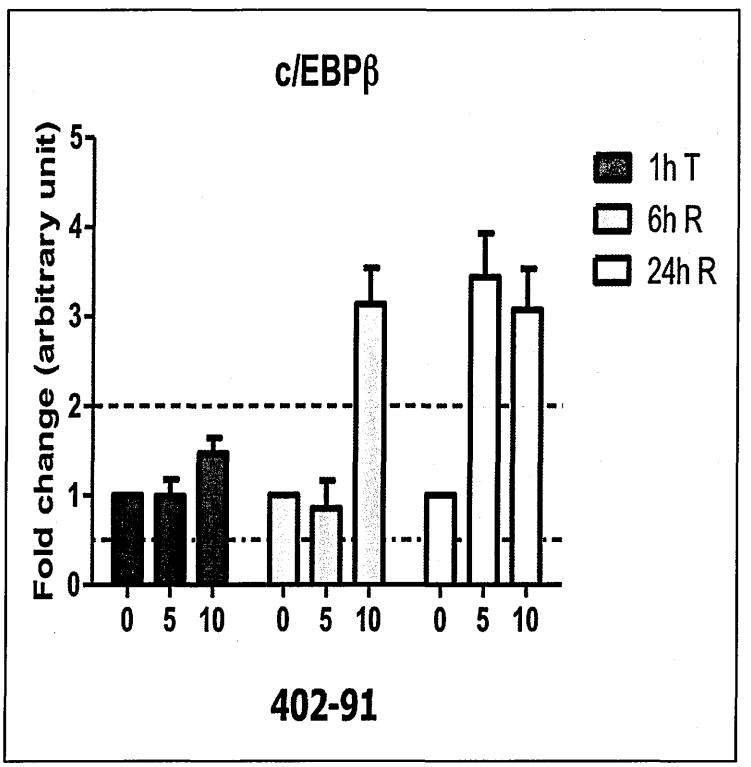

Figure 31: ML 402 -91 cells were treated with 5 and 10 nM of trabectedin. Cells were washed after 1 hour of treatment and allowed to recover for 6 and 24 hours. Data are the mean +/- SD (Bars) of three replicates for real time RT-PCR and 1. Only fold changes <0.5 or >2 were considered to be statistically significant.

4.2 Trabectedin blocks FUS-CHOP binding *in vivo*.

In parallel, I planned to set up the methodology to perform the ChIP assay in samples from xenografts in mice, to see how trabectedin treatment affects the tumour composition in an *in vivo* xenograft model. The technical challenge was to optimize the ChIP protocol for its application in ex vivo ML tissue, which was not done before.

Microscopically ML is made of uniform round-oval primitive non-lipogenic cells and variable numbers of uni-multivacuolated lipoblasts intermixed with a well-developed plexiform capillary network and embedded in a myxoid matrix composed of hyaluronic acid. Depending on the proportion of the cellular component to the stroma and the prevalence of immature and mature cellular features ML is divided into a usual or pure subtype, and a round cell or cellular (RC) subtype. Usual ML is the most differentiated form and shows low cellularity, evidence of lipoblast differentiation and a conspicuous vascular network while the RC subtype presents the opposite extreme of the differentiation gamut, and shows high cellularity made up of primitive non-lipogenic cells, little or no intervening myxoid stroma and a capillary vascular pattern that is not easy to visualize. Diagnosis of the RC subtype requires >5% hypercellular area [48].

For these particular features that characterize ML, the main problem for performing ChIP on xenografts was to obtain sufficient number of cells necessary for immunoprecipition -5 millions cells at least. I discovered that incubation of ML xenografts with collagenase enzyme allowed efficient dissociation of the tumour single cells. From 100mg of ML xenografts I obtained 50 millions cells after collagenase digestion, the protocol that I have set up is described in more details in paragraph 4.4 (Methodological design for Chromatin Immunoprecipitation to increase the fold enrichment).

These cells were used for Chip assay. I monitored the binding of FUS-CHOP to its promoters by ChIP with anti-CHOP, anti-FUS, and control antibody: an irrelevant anti-Flag.

The xenografts used after were previously established and characterized by Roberta Frapolli [48], ML004 and ML006 carrying FUS-CHOP type III. Both of the xenografts were treated with trabectedin at 0.15 mg/kg every 7 days for 3 times. Samples were collected 24 hours after the first dose, 24 hours after the third dose and 15 days without trabectedin. I have evaluated promoters of well-known FUS-CHOP chimera target genes (PTX3, FN-1, IL-8, CHOP) in quantitative RT-PCR. Values were reported as fold enrichment over a Flag antibody as a negative control.

ML004

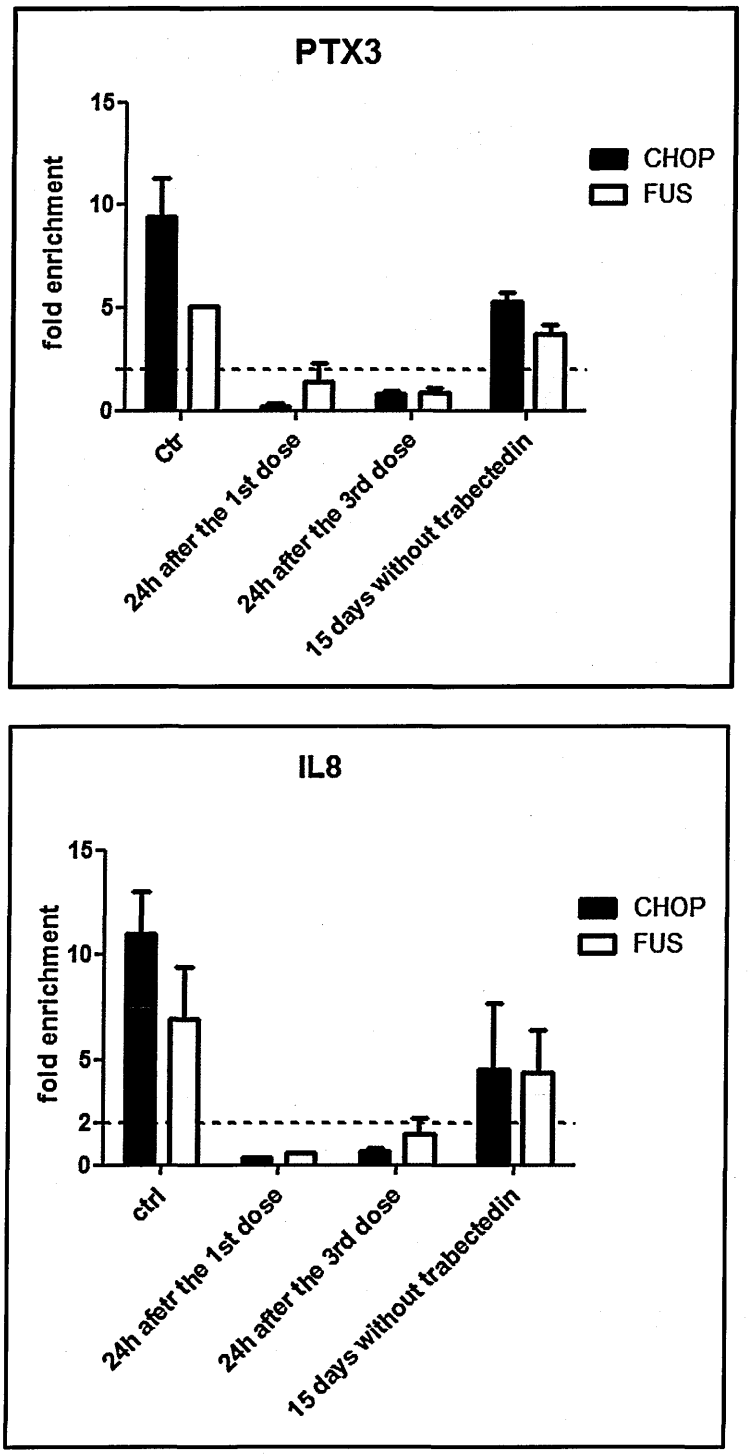

Figure 32 : ChIPs were performed on xenograft model ML004 with the indicated antibodies and analyzed by RT-PCR with the appropiate primers. Values are reported as fold enrichment calculated with the following formula:2 ^ΔCtx - 2 ^ΔCtb, where ΔCtx = Ct input – Ct sample and ΔCtb = Ct input - Ct control Ab (Flag). Samples were collected 24 hours after the first dose, 24 hours after the third dose and 15 days without trabectedin. I have evaluated selected promoters such as PTX3, FN-1, IL-8, CHOP in quantitative RT-PCR. Values were reported as fold enrichment over a Flag antibody as a negative control.

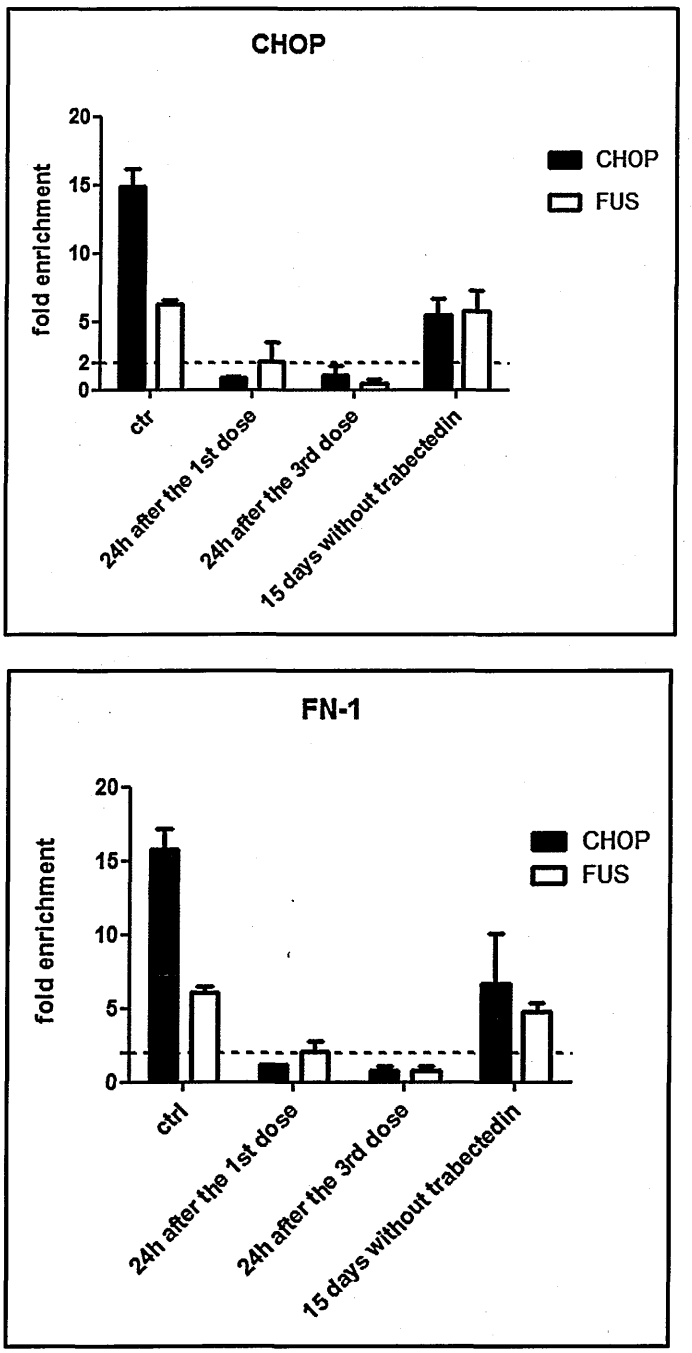

Figure 32 (continued): ChIPs were performed with the indicated antibodies and analyzed by RT-PCR with the appropiate primers. Values are reported as fold enrichment calculated with the following formula:2 ^ΔCtx - 2 ^ΔCtb, where ΔCtx = Ct input – Ct sample and ΔCtb = Ct input - Ct control Ab (Flag).

ML006

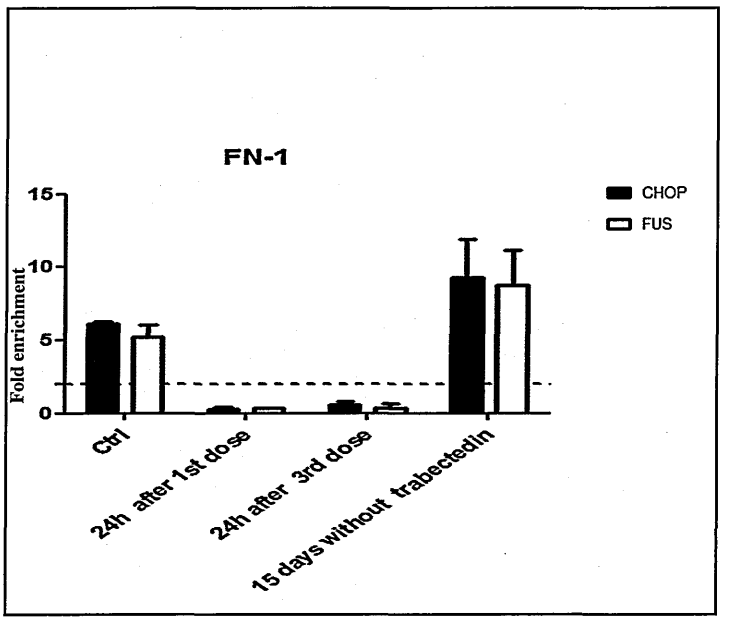

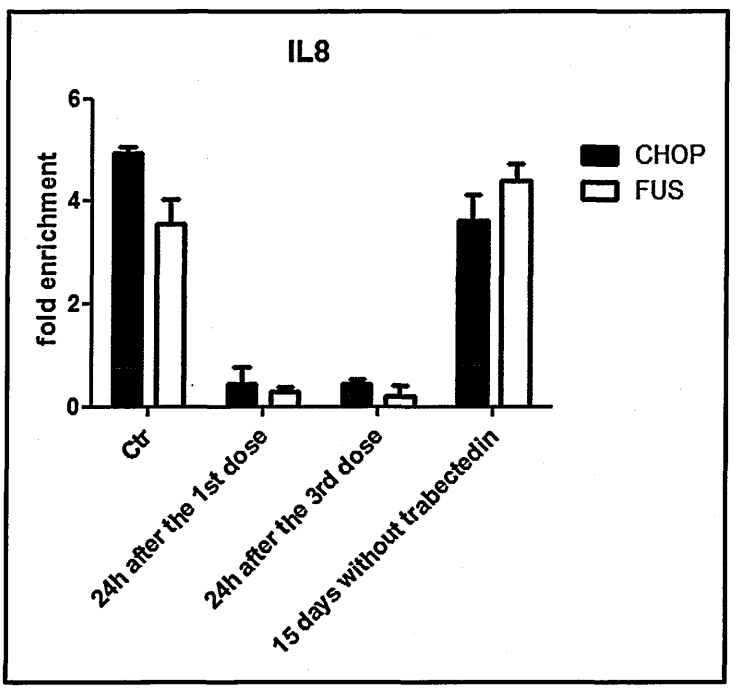

Figure 33: ChIPs were performed on xenograft model ML006 with the indicated antibodies and analyzed by RT-PCR with the appropiate primers. Values are reported as fold enrichment calculated with the following formula:2 ^ΔCtx - 2 ^ΔCtb, where ΔCtx = Ct input – Ct sample and ΔCtb = Ct input - Ct control Ab (Flag). The xenografts were treated with trabectedin at 0.15 mg/kg every 7 days for 3 times.

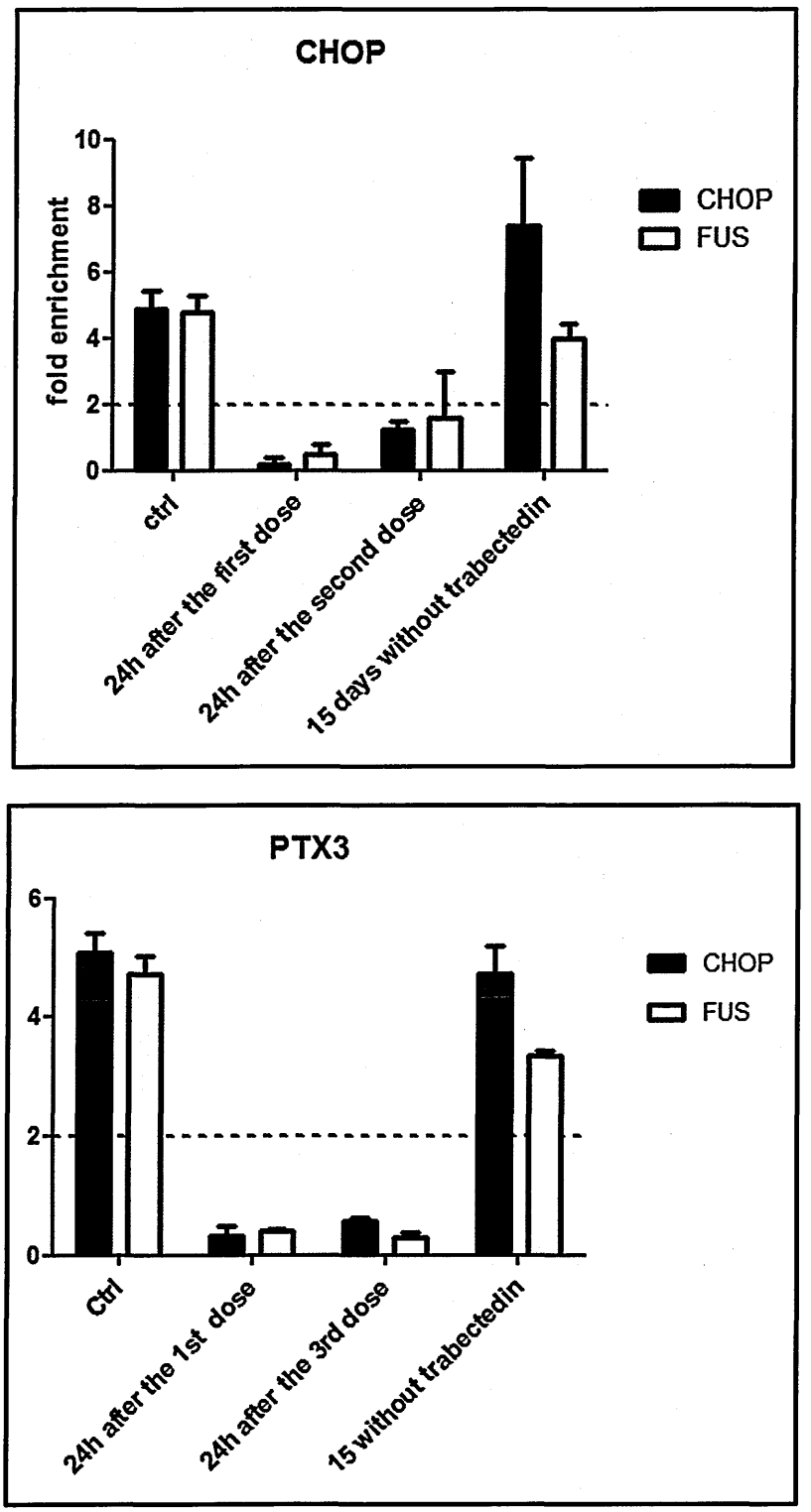

Figure 33 (continued) : ChIPs were performed with the indicated antibodies and analyzed by RT-PCR with the appropiate primers. Values are reported as fold enrichment calculated with the following formula:2 ^ΔCtx - 2 ^ΔCtb, where ΔCtx = Ct input – Ct sample and ΔCtb = Ct input - Ct control Ab (Flag).

I saw that the enrichments were significantly reduced in the trabectedin treated xenografts already 24 hours after the first dose (figure 32 , figure 33). With respect to the anti-Flag control antibody, binding was significantly affected on all the promoters tested even after 24 hours after the third dose.

Even at 24h after the first dose of Trabectedin, detachment of the chimera from all the promoters was seen confirming that it removes FUS-CHOP from its target promoters in xenograft ex vivo ML tissue, like previously observed in ML cell line.

15 days after treatment, FUS-CHOP was again bound to its own target genes, like before treatment. These data indicate that trabectedin induces the removal of the chimera from promoters which in turn alters their expression and their functionality even on xenografts samples, suggesting that this is the mechanism of action of trabectedin *in vivo* as well as *in vitro*.

4.2 .1 Expansion of previous findings on the effects of trabectedin on FUS-CHOP target in new ML xenografts carrying FUS-CHOP type II.

Previously I described that Trabectedin caused detachment of the chimera from the promoters of target genes selected already 24 hours after the first dose of treatment confirming that it removes FUS-CHOP from its target promoters in xenograft in vivo ML tissue carrying FUS-CHOP TYPE III, as previously observed in ML cell line.

To further investigate if this mechanism was present in others ML, ChIP assay was performed in xenografts carrying FUS-CHOP type II; ML014, Ml015 established and characterized by Roberta Frapolli [48]. Both xenografts were treated with trabectedin at 0.15 mg/kg every 7 days for 3 times. Samples were collected 24 hours after the first dose, 24 hours after the third dose and 15 days without trabectedin. All FUS-CHOP gene targets promoters selected were evaluated in quantitative RT-PCR. Values were reported as fold enrichment over anti-flag antibody as a negative control.

In both xenografts ML014 and ML015 (figure 34, figure 35), the enrichments were significantly reduced in the trabectedin treated xenografts already 24 hours after the first dose. With respect to the anti-Flag control antibody, binding was significantly affected on all the promoters tested even after 24 hours after the third dose.

Trabectedin caused the detachment of FUS-CHOP from PTX3, FN-1, IL-8, CHOP, promoters already 24h after the first dose of treatment and 15 days after treatment, FUS-CHOP was again bound to its own target genes, like previously observed in xenograft ML carrying type III. These data indicate that trabectedin induces the removal of the chimera from promoters which in turn alters their expression and their functionality even on xenograft samples characterized by FUS-CHOP type II, suggesting that this could be the mechanism of action of trabectedin *in vivo* in all the types of chimera.

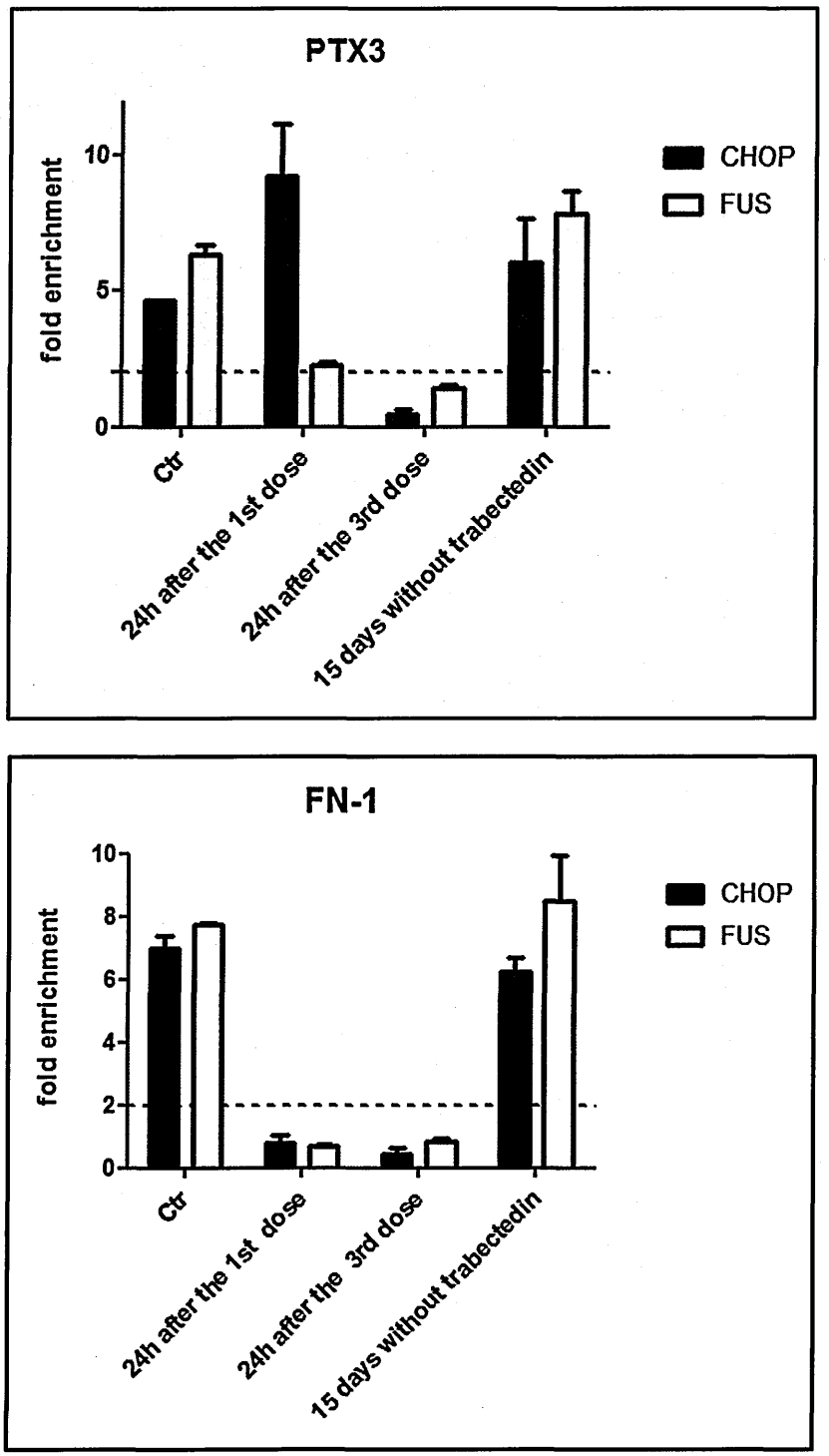

Figure 34 : ChIPs were performed on xenograft model ML014 with the indicated antibodies and analyzed by RT-PCR with the appropiate primers. Samples were collected 24 hours after the first dose, 24 hours after the third dose and 15 days without trabectedin. All FUS-CHOP gene targets promoters selected were evaluated in quantitative RT-PCR. Values were reported as fold enrichment over anti-flag antibody as a negative control.

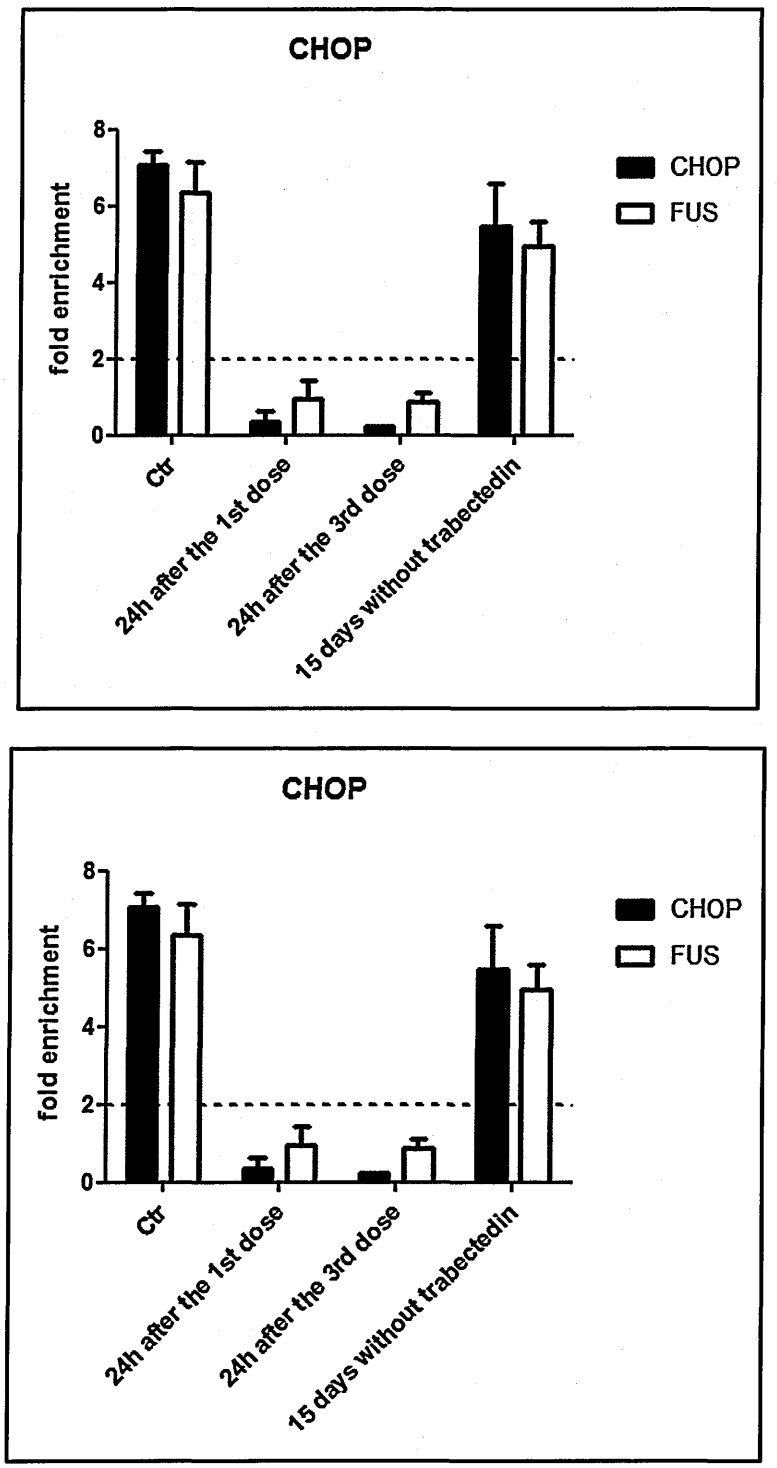

Figure 34 (continued) : ChIPs were performed with the indicated antibodies and analyzed by RT-PCR with the appropiate primers. Values are reported as fold enrichment calculated with the following formula:2 ^ΔCtx - 2 ^ΔCtb, where ΔCtx = Ct input – Ct sample and ΔCtb = Ct input - Ct control Ab (Flag).

ML015

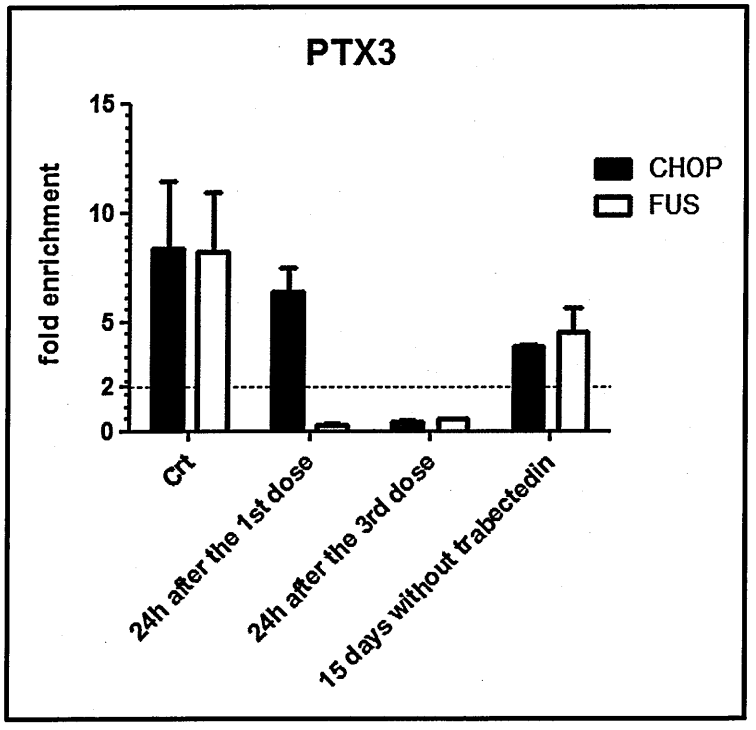

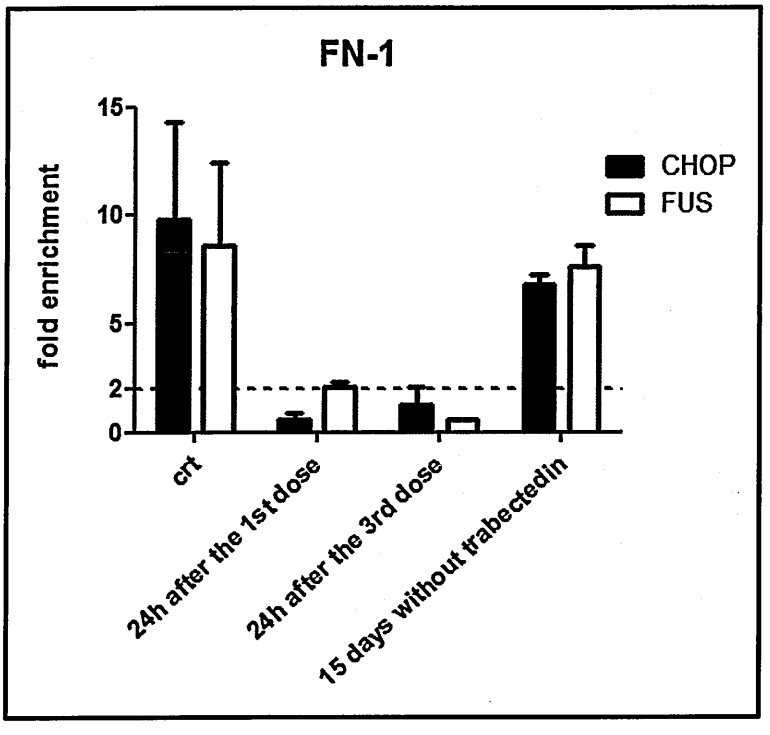

Figure 35: ChIPs were performed on xenograft model ML015 with the indicated antibodies and analyzed by RT-PCR with the appropiate primers. Values are reported as fold enrichment calculated with the following formula:2 ^ΔCtx - 2 ^ΔCtb, where ΔCtx = Ct input – Ct sample and ΔCtb = Ct input - Ct control Ab (Flag). Samples were collected 24 hours after the first dose, 24 hours after the third dose and 15 days without trabectedin.

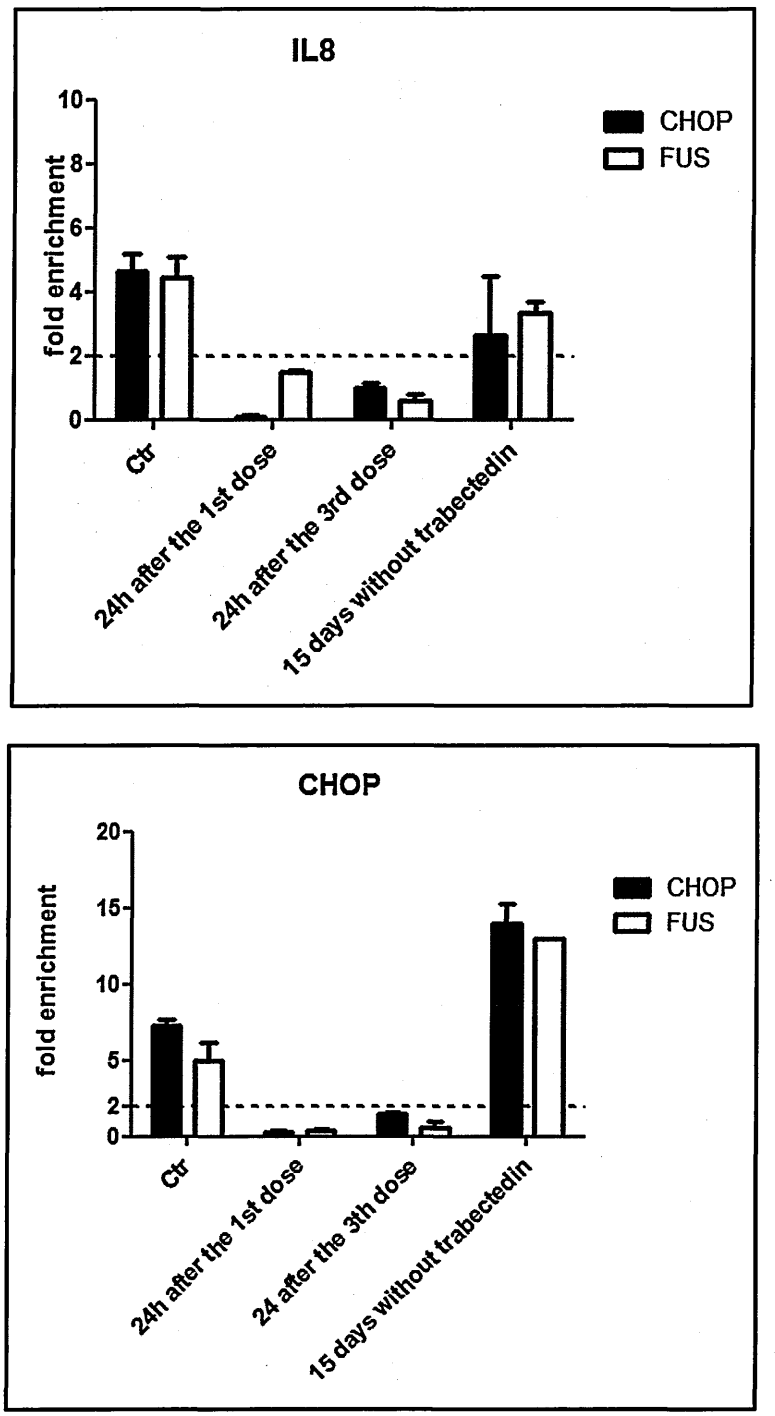

Figure 35 (continued) : ChIPs were performed on xenograft model ML0015 with the indicated antibodies and analyzed by RT-PCR with the appropiate primers. Values are reported as fold enrichment calculated with the following formula:2 ^ΔCtx - 2 ^ΔCtb, where ΔCtx = Ct input – Ct sample and ΔCtb = Ct input - Ct control Ab (Flag).

4.2.2 Doxorubicin does not cause the detachment of FUS-CHOP from on its own target genes.

To verify the specificity of the drug for FUS-CHOP, we treated ML004 with doxorubicin 8mg/kg and samples were collected 24 hours after the first dose (figure 36). After doxorubicin treatment FUS-CHOP was still attached to PTX3 promoter confirming that the detachment of the chimera is only caused by trabectedin but not by other drugs.

ML004

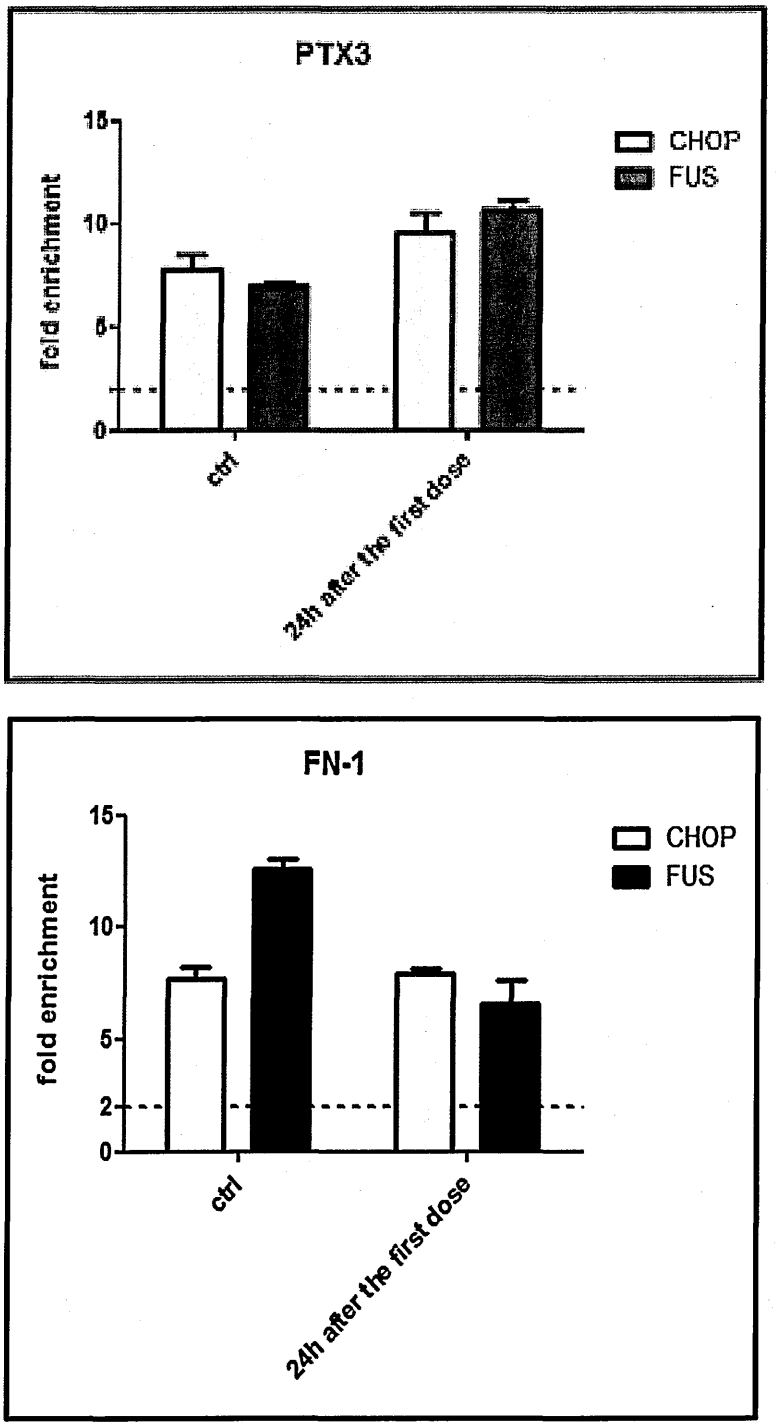

Figure 36: The promoter region of PTX3 and FN-1 were amplified. Values were measured as fold enrichment over a Flag control antibody in quantitative RT-PCR analysis. ML004 was treated with doxorubicin 8mg/kg and samples were collected 24 hours after the first dose.

4.2 .3 Anti-tumour activity of trabectedin in xenograft models.

The antitumour activity of trabectedin was evaluated in ML004, ML015 xenografts after i.v. administration of 0.15 mg/kg, every seven days for three times. Treatments started when tumour burden reached 400-500 mg (late stage tumours) giving us the possibility to observe both tumour growth or tumour regression. As shown in figure 37, trabectedin was only marginally active in ML004 xenograft being able to slightly reduce tumour growth rate but without reaching a significant value of T/C (52 .2 % on day 156).

On the contrary ML015 was very sensitive to the treatment (T/C 17.4% on day 175): in this xenograft model trabectedin was able to induce a 50% tumour regression, followed by a long lasting tumour growth arrest (figure 37). Histological analyses were performed before and 15 days after the end of treatment. H&E sections of the xenograft ML004 before and after treatment did not show any morphologic change (figure 38) whereas H&E sections of the ML015 xenograft showed a partial response in post-treatment samples characterized by a consistent cellular depletion (figure 39).

ML004

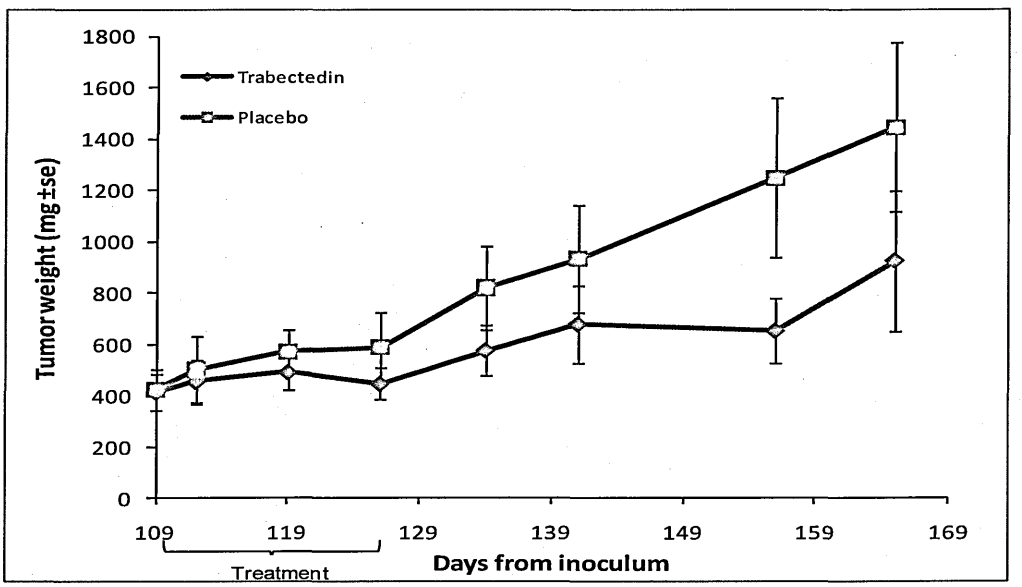

ML015

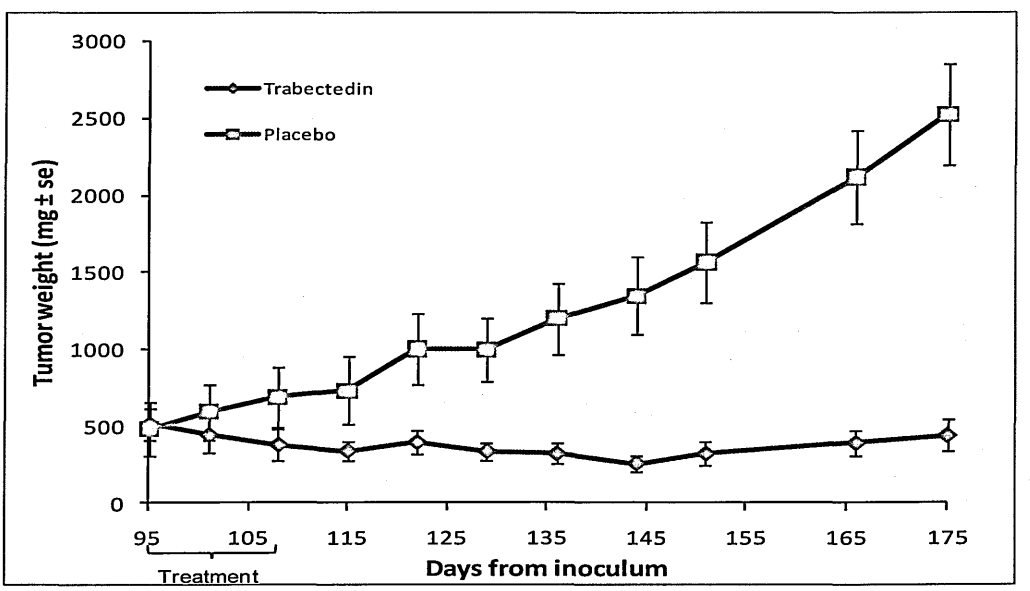

Figure 37: Antitumour activity of trabectedin in ML004 xenograft and ML015 (B): tumour bearing mice were treated with trabectedin 0.15 mg/kg i.v., q7dx3. Treatment started when the mean tumour weight was about 500 mg. Bars, ±SEM.

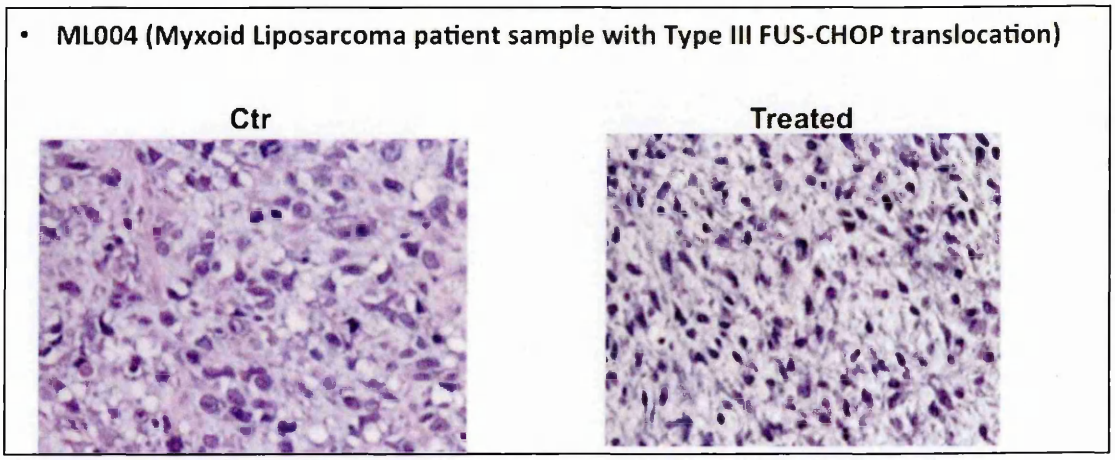

Figure 38: Bars, ±SEM. Hematoxylin/eosin sections of or ML004 xenografts were performed before and 15 days after the end of treatment.

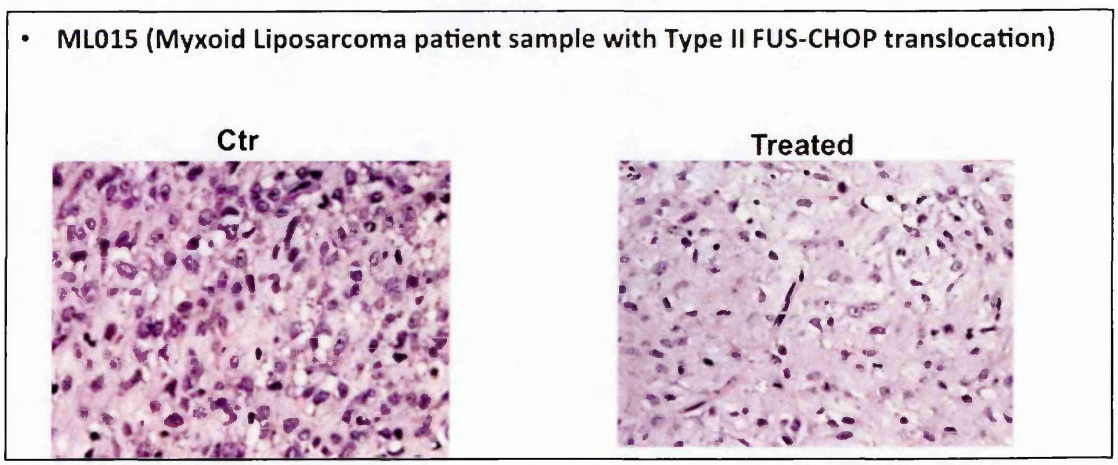

Figure 39: Bars, ±SEM. Hematoxylin/eosin sections of ML015 xenografts were performed before and 15 days after the end of treatment.

4.2 .4 Trabectedin induces adipocytic differentiation in ML type II but not in ML type III.

Histological analysis revealed that trabectedin causes a consistent cellular depletion, and a progression toward a differentiated lipoblast phenotype in type II ML, while it induced a minor effect in type III ML (figure 38, 39). Previously, it was shown that trabectedin induced a transcription program of adipogenesis, specifically in 402 -91 cells, by inducing the master genes of this process such as C/EBPβ and C/EBPα. In order to confirm that trabectedin treatment induced the adipogenesis in vivo, we examined the expression levels of the proteins responsible for normal adipogenesis such as C/EBPα and PPARγ2 using *in vivo* xenograft before and after the treatment. As shown in figure 40 and 41, before the treatment only PPARγ1 was expressed in both ML015 (type II) and ML004 (type III). Before treatment, none of the tumours expressed C/EBPα or PPARγ2 . After trabectedin treatment, PPARγ2 and C/EBPα expression was induced only in ML015 (type II) but not in ML004 (type III). Interestingly, we found that in ML004 (type III), after treatment there was no increase in the protein expression compared to the control (figure 41). Taken together, these results suggest that trabectedin induces maturation /adipocyte differentiation in ML carrying FUS-CHOP type II but not in ML carrying FUS-CHOP type III.

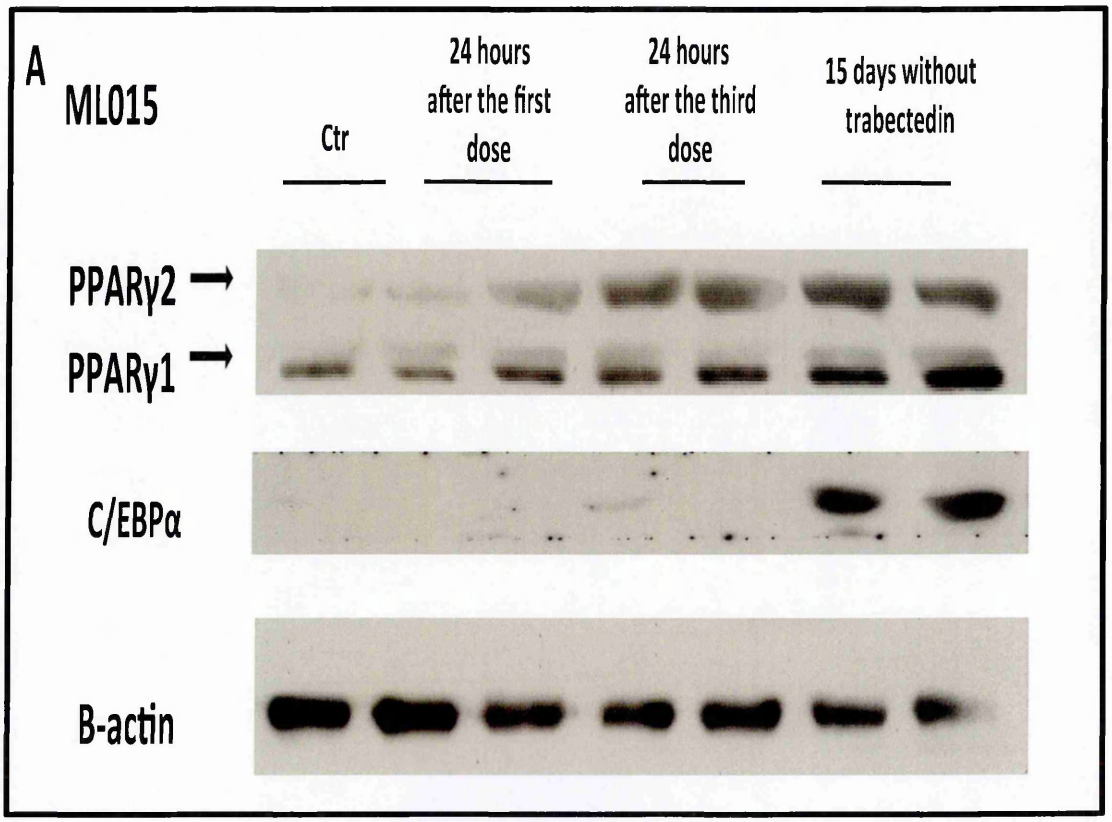

Figure 40: Analysis of adipocytic markers in xenograft model ML015: Trabectedin was administered i.v. at the dose of 0.15 mg/kg every seven days for three times (q7dx3). Western blot analysis was done on samples 24 hours after the first and the third dose and 15 days without trabectedin with antibodies against PPARγ1,2 (A) and C/EBPα (B).

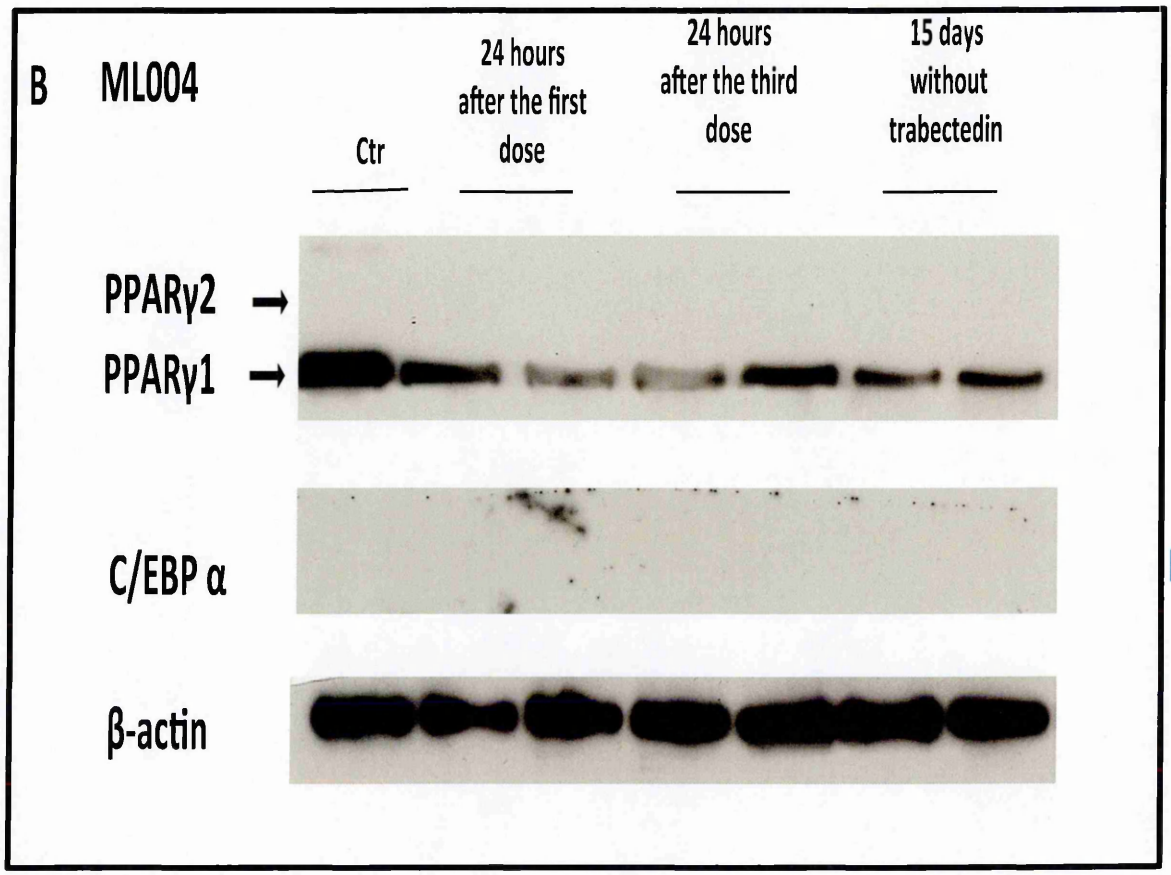

Figura 41: Analysis of adipocytic markers in xenograft model ML004: Trabectedin was administered i.v. at the dose of 0.15 mg/kg every seven days for three times (q7dx3). Western Blot analysis of PPARγ (A) and C/EBPα (B).

4.2 .5 Trabectedin decrease the expression of CHOP and PTX3 in ML015 (type II) but not in ML004 (type III) xenograft tumours.

To determine if trabectedin could cause a decrease in the protein levels of PTX3 and CHOP which are FUS-CHOP target genes, I have analyzed the expression of both proteins by westernblot in ML004 and ML015 xenograft models.

Tumours were collected 24 hours after the first dose, 24 hours after the third dose, and 15 days without trabectedin. As shown in figures 42 and 43, before trabectedin treatment CHOP and PTX3 were expressed in both tumours. 15 days after trabectedin CHOP and PTX3 protein levels were dramatically decreased compared to the control in the ML015, but not ML004 xenograft tumour. This is consistent with the histological analysis. However these data were in contrast to the ChIP data showing that trabectedin had the same ability to display FUS-CHOP types from the selected gene targets in both ML004 and ML015.

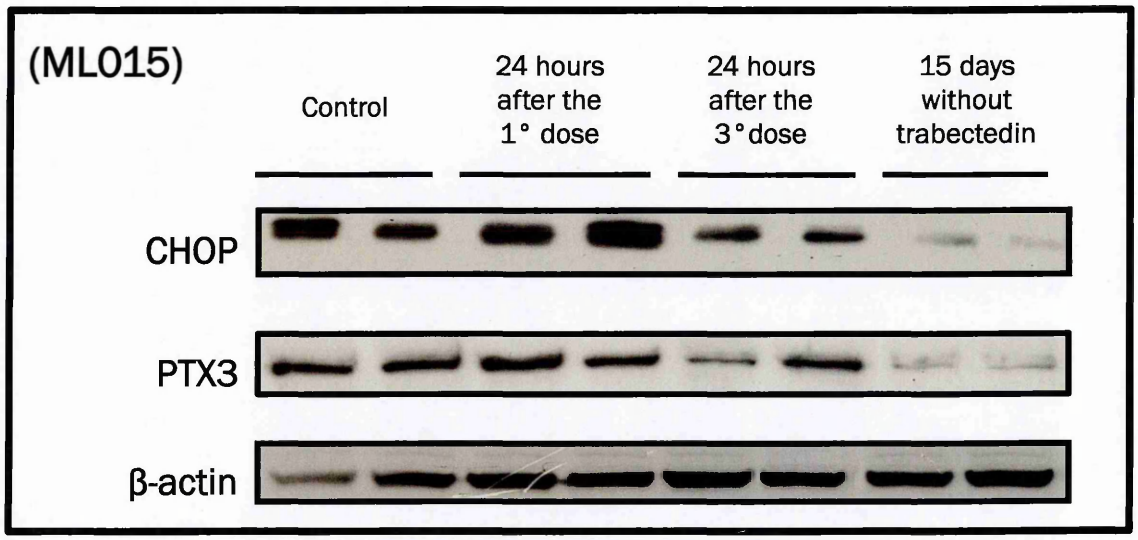

Figure 42 : Analysis of FUS-CHOP target after trabectedin treatment in Xenograft models ML015. Xenografts were treated with trabectedin at 0.15 mg/kg every 7 days for 3 times. Samples were collected 24 hours after the first dose, 2 4 hours after the third dose and 15 days without trabectedin. Total extracts were subjected to Western Blot with CHOP and PTX3. Antibody against actin was used as a loading control.

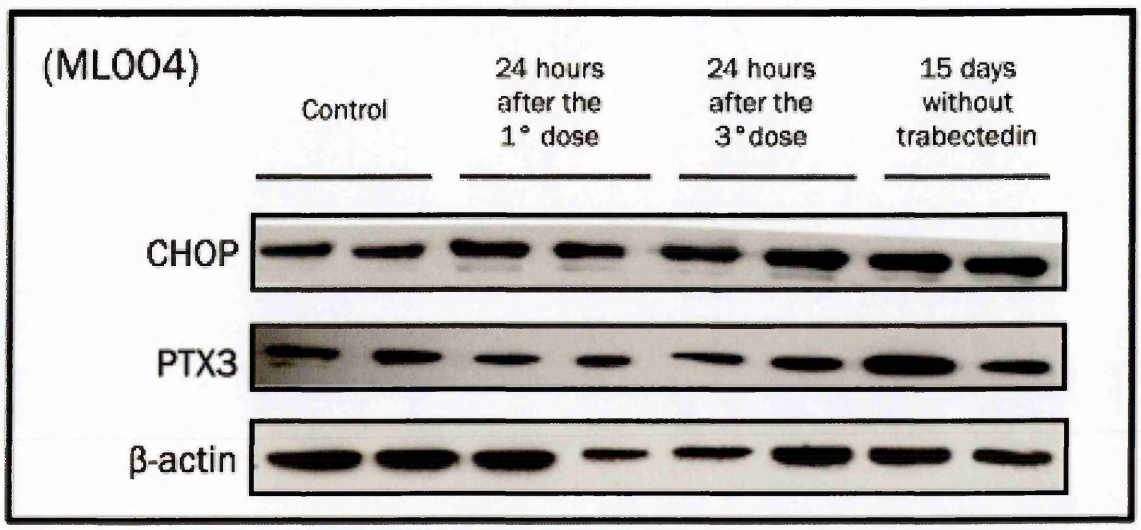

Figure 43: Analysis of FUS-CHOP target after trabectedin treatment in Xenograft models ML004. Xenografts were treated with trabectedin 0.15 mg/kg every 7 days for 3 times. Samples were collected 24 hours after the first dose, 2 4 hours after the third dose and 15 days without trabectedin. Total extracts were subjected to Western Blot with CHOP and PTX3. Antibody against actin was used as a loading contro

4.2 .6 Trabectedin inhibition is more prolonged in tumours with FUS-CHOP type II than FUS-CHOP type III.

Trabectedin showed a minimal activity against ML004 xenograft (best T/C 52 %, day 156) as confirmed by the histological analysis that showed no regression. Nevertheless, trabectedin showed a very good antitumour activity against ML015 xenograft (best T/C 17%, day 175) and the histological analysis showed a partial regression with reduction of cell number and vasculature. To further investigate the difference response we performed ChIP to assess if there was a difference in the kinetics of rebinding of FUS-CHOP between ML type II and type III. Xenografts were treated with trabectedin at 0.15mg/kg every 7 days for three times. Samples were collected 72 hours after the first dose, 72 hours after the third dose, 12 0 hours after the third dose and after 7 days without trabectedin. PTX3 and FN-1 promoters were evaluated in RT-PCR as fold enrichment over anti-flag antibody. ChIP analysis performed on ML004 revealed that 72 hours after treatment, FUS-CHOP Type III was attached to selected targets whereas FUS-CHOP Type II remained unbound but was rebound to the promoters 120 hours after the third dose (figure 44, 45). These results suggest that the greater sensitivity of type II than of type III myxoid liposarcoma xenografts could be related to a more prolonged drug-induced detachment of the chimera FUS-CHOP from its target genes.

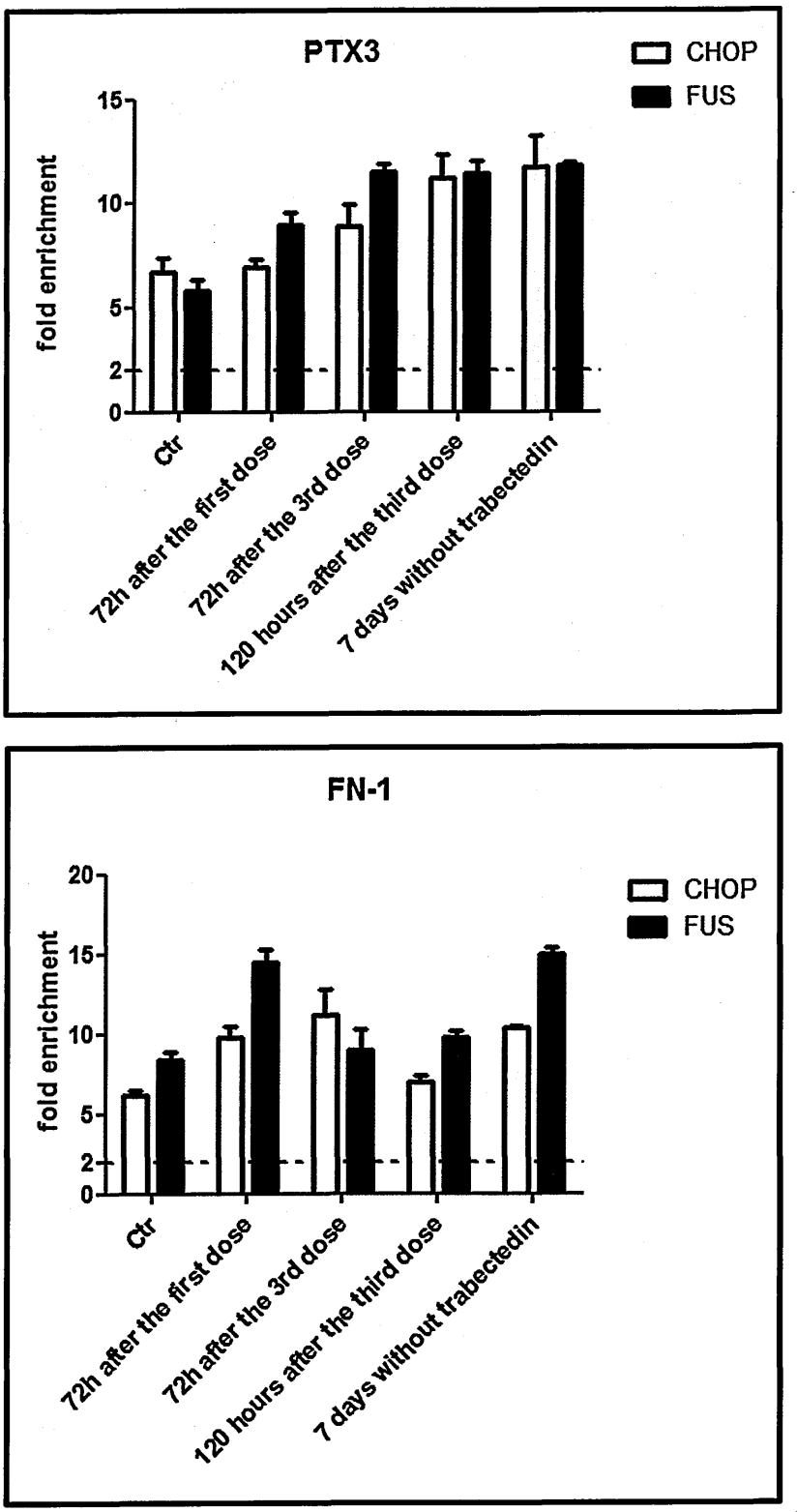

Figure 44: In ML004 xenograft model, samples were collected 72 hours after the first dose, 72 hours after the third dose, 120 hours after the third dose and after 7 days without trabectedin. FUS-CHOP type III is binding its own target genes 72 hours after the 1st and the 3rd dose of trabectedin.

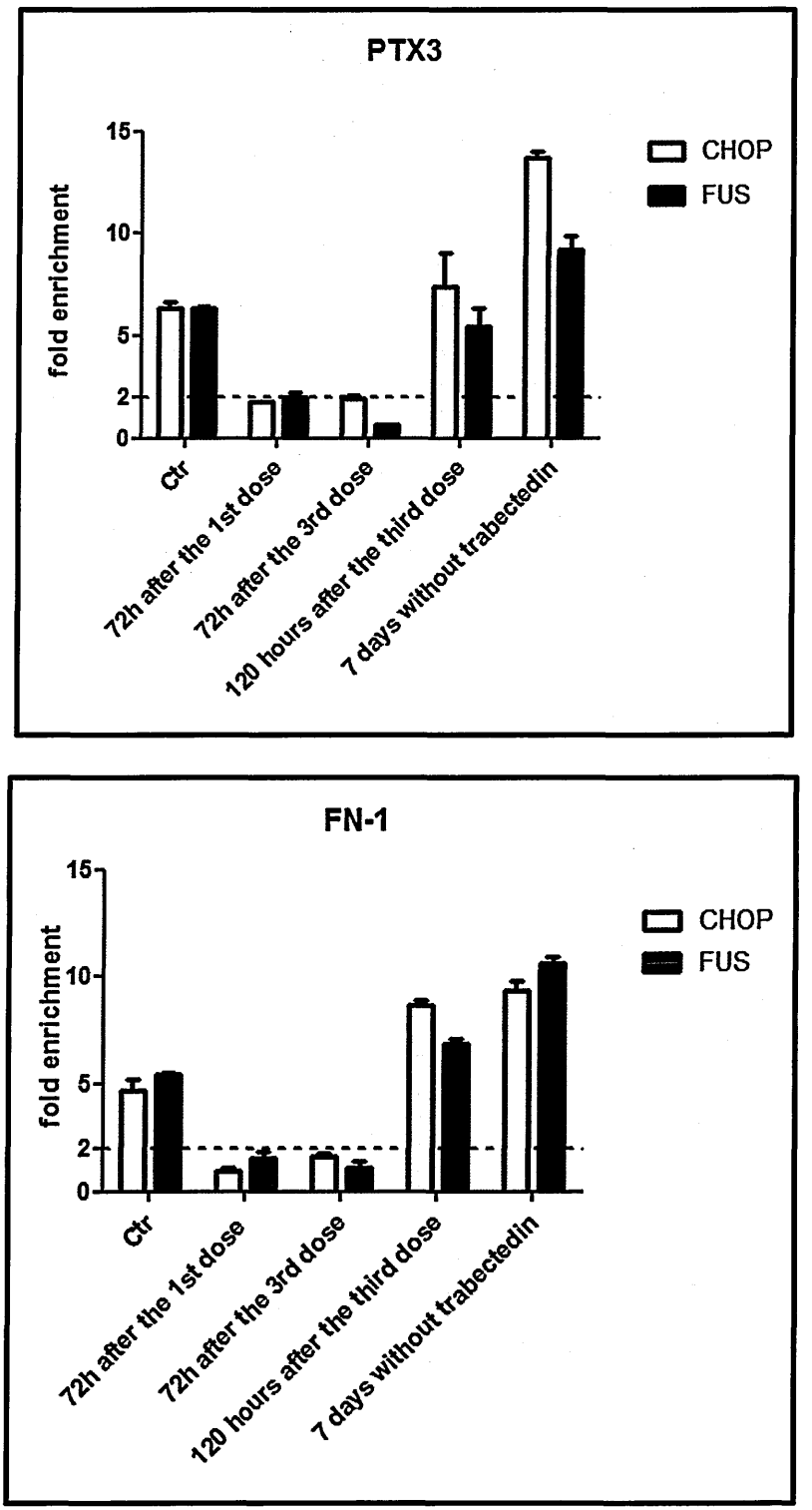

Figure 45: In ML015 xenograft model samples were collected 72 hours after the first dose, 72 hours after the third dose, 12 0 hours after the third dose and after 7 days without trabectedin. FUS-CHOP type II is detached from its own target genes, 72 hours after the 1st and the 3rd dose of trabectedin .

4.2 .7 Biopsies of metastatic lesions of Myxoid Liposarcoma.

In one case of ML we obtained tumour biopsies both before and after trabectedin treatment. Figure 46 shows that after trabectedin the enrichment of CHOP in clearly decreased. When we received the samples we were not informed that the tumour did not express the most frequent FUS-CHOP chimera, but instead the least frequent EWS-CHOP chimera. Therefore we have used the antibodies against FUS and CHOP like the experiments conducted in xenograft biopsies. The decrease in CHOP enrichment indicates that trabectedin was able to remove the oncoprotein from DNA in clinical tumour biopsy taken 24h after treatment with trabectedin at the dose of 1.1.

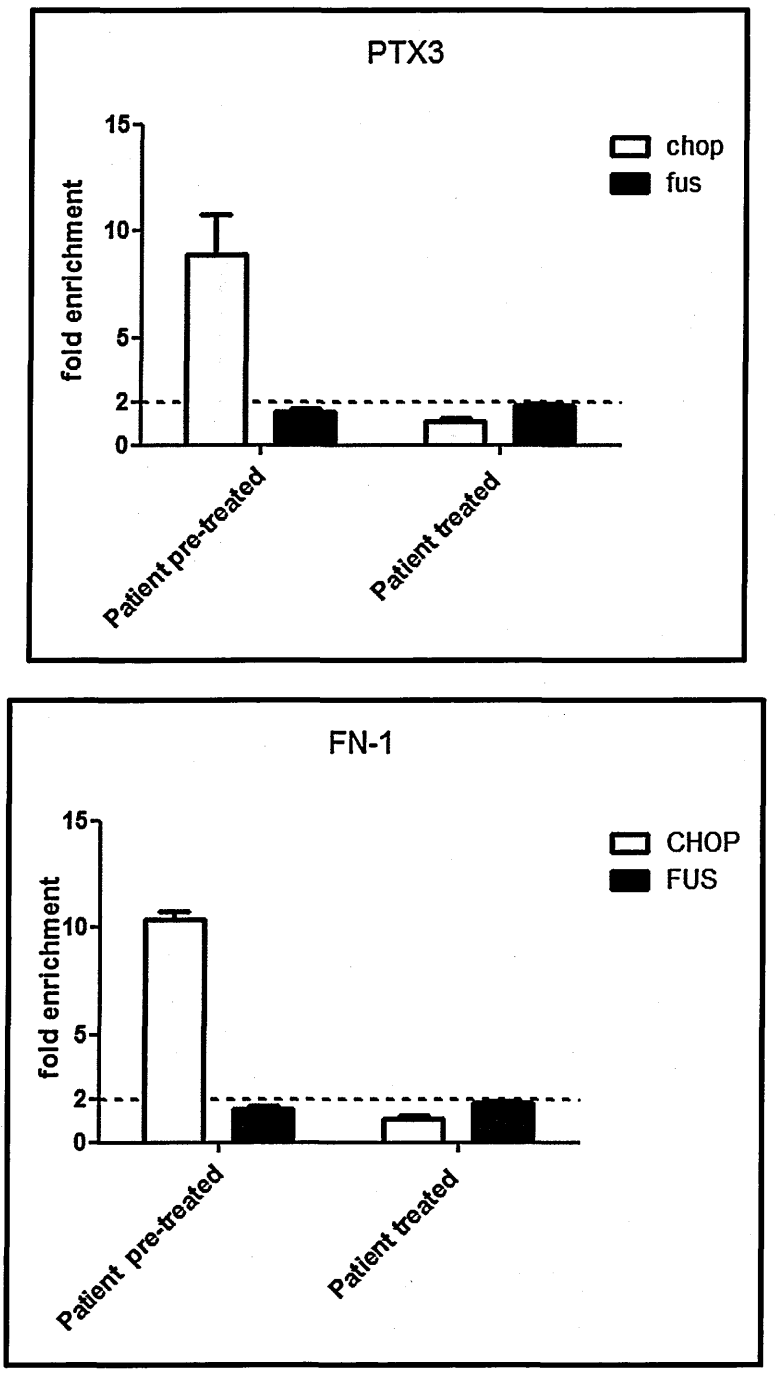

Figure 46: ChIP analysis from human biospies. PTX3 and FN-1 promoters were evaluated in RT-PCR as a fold enrichment over anti-flag antibody.

4.3 To investigate the effects of trabectedin on factors that modulate angiogenesis response of myxoid liposarcoma.

As already outlined in the background section, the formation of the tumour vasculature is critical for the growth of ML. An experimental study has recently demonstrated that dormancy of liposarcomas is associated with impaired angiogenesis, whereas the acquisition of the angiogenic ability ("angiogenic switch") triggers the passage from dormant, poorly vascularized lesions to rapidly growing malignant liposarcomas [215, 216]. Preliminary observations indicate that following treatment with trabectedin tumours appear less vascularized. It is therefore plausible that inhibition of angiogenesis might contribute to the antineoplastic activity of trabectedin on ML. The aim of the current task is to investigate whether the changes in gene expression caused by trabectedin might modify the host / tumour interaction by inhibiting the angiogenic potential of tumour cells.

To verify whether trabectedin is an indirect inhibitor of angiogenesis, the effect of trabectedin on the production of angiogenesis regulatory factors was investigated *in vitro* [217, 218].

402 -91 cells were exposed to trabectedin and the production of angiogenic factors and endogenous inhibitors of angiogenesis, were measured by real time PCR and ELISA analysis of supernatant.

Initially we checked the expression of mRNA levels of VEGF using the 402 -91 cell line. Previously, the IC50 concentrations for trabectedin on 402 -91 cells were calculated as 5nM. 402 -91 cells were treated with 1nM, 5nM (=IC50) and 10nM (=2 xIC50) of trabectedin. mRNA levels of VEGF extracted from cells treated with 1 hour of trabectedin were increased significantly when compared to untreated cells (figure

47). However, ELISA analysis showed that VEGF protein levels in untreated cells, at detection limit, were not changed by trabectedin (figure 47).

Based on previous studies showing that thrombospondin-1 (TSP-1) is a critical regulator of angiogenesis in sarcoma [131], we wanted to investigate if the production of TSP-1 was affected by trabectedin treatment in 402 -91cell line. 402 -91 cells were treated with 1nM, 5nM and 10nM of trabectedin for 1 hour. Trabectedin caused a significant increase in the production of TSP-1, as increase in mRNA and protein secreted in the supernatant and measured by ELISA (figure 48). Taken together these data show that trabectedin does affect the expression of specific angiogenesesis regulatory genes, hence potentially impairing tumour cells' ability to stimulate angiogenesis.

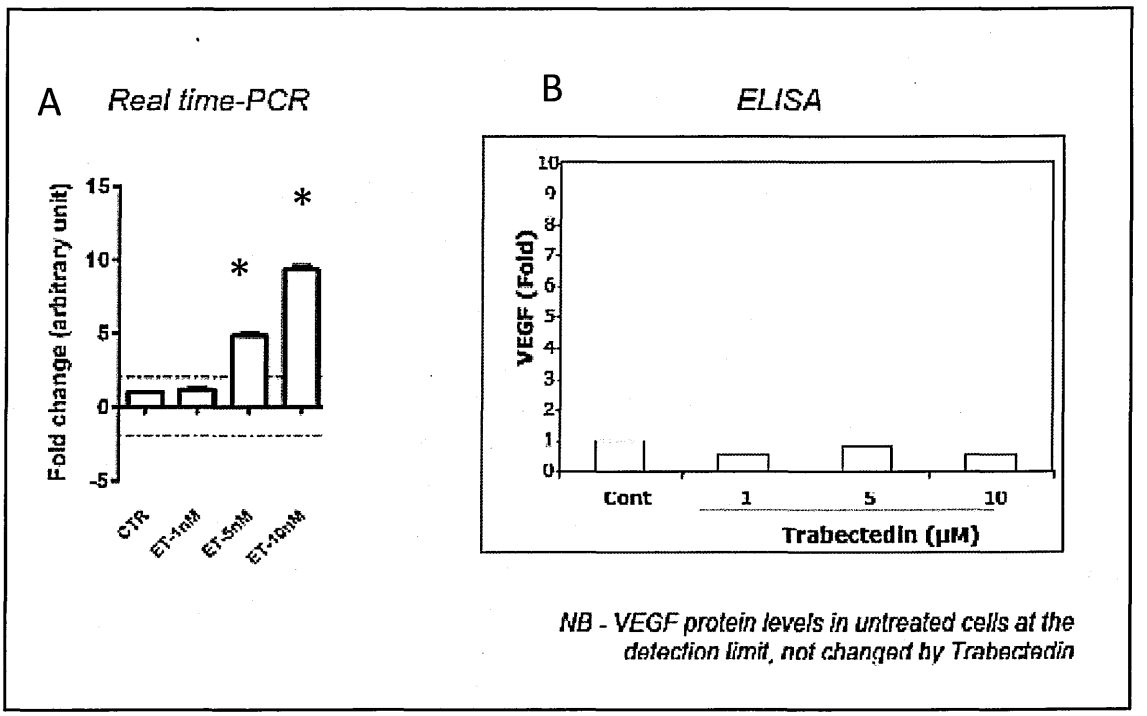

Figure 47: Effect of trabectedin of VEGF by 402-91 cells, in vitro. Production of VEGF in 402-91 cells exposed to the indicated concentration of trabectedin was analyzed by real time PCR (**A**) or ELISA assay of the conditioned media (**B**). Data, expressed as fold increase, are the mean and SE of values from 3 independent assays. *p <0.05 compared to controls (ANOVA followed by Dunnett's multiple comparison test).

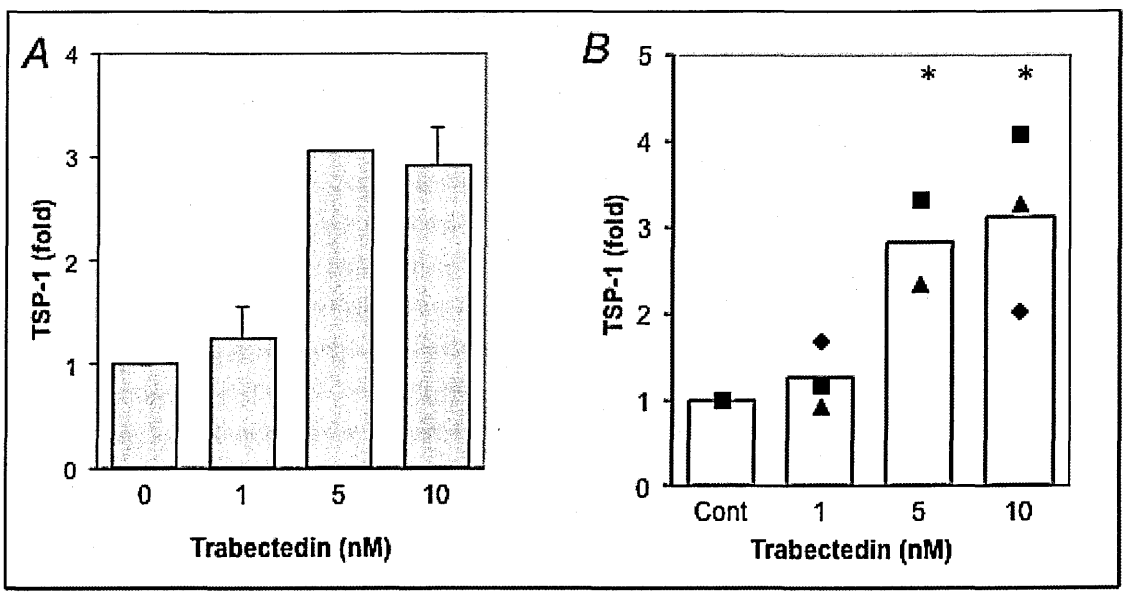

Figure 48: Effect of trabectedin of TSP-1 by 402-91 cells, in vitro. Production of TSP-1 in 402-91 cells exposed to the indicated concentration of trabectedin was analyzed by real time PCR (**A**) or ELISA assay of the conditioned media (**B**). Data, expressed as fold increase, are the mean and SE of values from 3 independent assays. *p <0.05 compared to controls (ANOVA followed by Dunnett's multiple comparison test).

To better understand the effects of trabectedin we wanted to investigate if TSP-1 protein levels were affected by trabectedin also *in vivo*.

ML004 Xenograft (carrying FUS-CHOP TYPE III) and ML015 (carrying type II) were characterized by R. Frapolli and treated with 0.15mg/kg of trabectedin.

TSP-1 plasma levels were detected by an ELISA that recognizes only human (hence tumour-derived) TSP-1. Plasma was collected 24 hours after the first dose (T1) and 24 hours after the third dose (T2) and 15 days without trabectedin (recovery). In trabectedin-sensitive ML015, TSP-1 protein levels were increased already 24 hours after the first dose; in the ML004 model, less responsive to trabectedin, TSP-1 protein levels were induced after the third dose of trabectedin (figure 49).

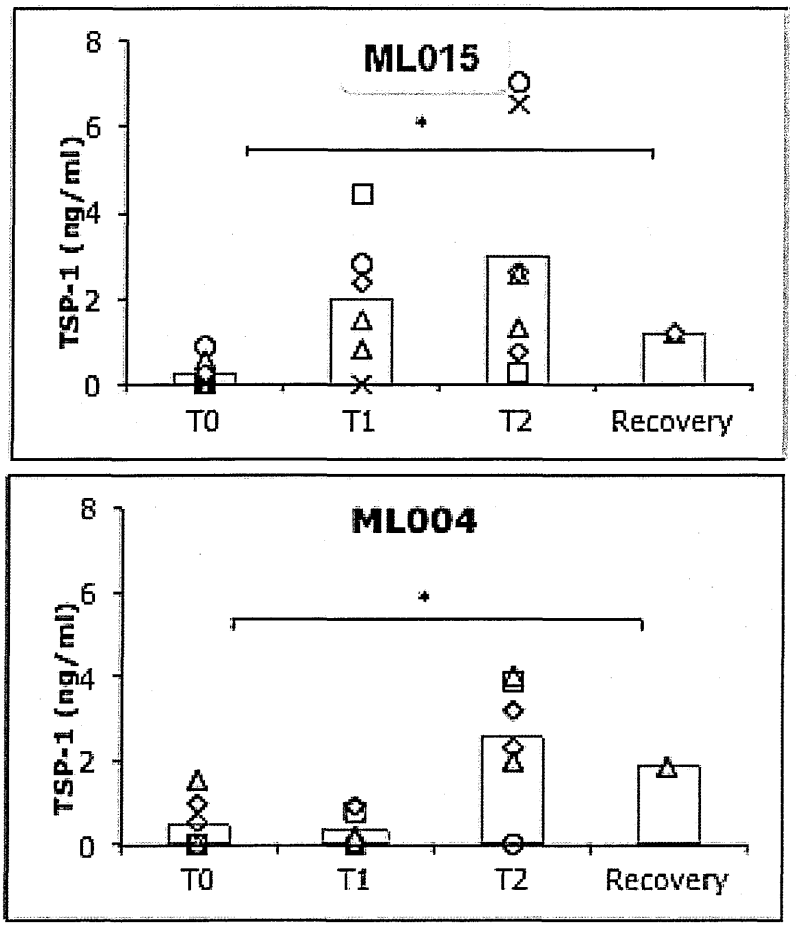

Figure 49: In vivo stimulation of TSP-1 production by trabectedin in ML xenografts. Mice bearing the responsive ML015 or the poorly responsive ML004 tumors, were treated with trabectedin (0.15 mg/kg, every 7 days for 3 times) and for each mouse, plasma samples were collected before, 24h after the first or 24h after the third administration of trabectedin. Human TSP-1 protein was measured by ELISA. Symbols refer to each mouse. *$p<0.05$ compared to control, vehicle-treated mice (ANOVA followed by Dunnett's multiple comparison test).

4.3.1 C/EBP β but not FUS-CHOP binds to the TSP-1 promoter in xenograft model ML015 and ML004.

Previous studies have shown that TSP-1 can be upregulated by C/EPB β which binds to a TGGCGCAAG consensus site at the TSP-1 promoter [219]. C/EPB β, which is the preferred dimerization partner of CHOP, and also binds to FUS-CHOP, has been reported as an important regulator of IL6 expression. It was shown, by RNA interference experiments, the presence of C/EPB β is essential for expression of IL6 in FUS-CHOP carrying cells. By ChIP analysis, it was demonstrated that C/EBP β binds the IL6 promoter in FUS-CHOP carrying cells but found no direct binding of FUS-CHOP to this promoter. Thus, the effect of FUS-CHOP on IL6 expression must be indirect, possibly by interaction with C/EPB β [220].

Based on this study, I used ChIP to investigate if FUS-CHOP or C/EBPβ bound directly to the TSP-1 promoter in ML xenograft model. ML0015 xenograft tumour was treated with trabectedin at 0.15 mg/kg and samples were collected 24 hours after the first dose. RNA polymerase II was used as control to validate if the regulation of TSP-1 was affected by trabectedin treatment. I have analyzed the selected promoters PTX3 and TSP-1 and values were reported as fold enrichment over a Flag antibody as a negative control.

Interestingly, the results showed that FUS-CHOP type II did not bind to TSP-1 promoters where as C/EBP β did in the control, but after trabectedin treatment C/EBP β was detached from the promoter (figure 50).

To further investigate if the effect of trabectedin on TSP-1 was similar to the effect observed on FUS-CHOP target genes, I performed ChIP on ML015 and ML004 xenograft models. Both of the xenografts were treated with trabectedin at 0.15 mg/kg every 7 days for 3 times. Samples were collected 24 hours after the first dose, 24 hours

after the third dose and 15 days without trabectedin. TSP-1 promoter was evaluated in quantitative RT-PCR. Values were reported as fold enrichment over a Flag antibody as a negative control.

I found that trabectedin displaces C/EBP β from TSP-1 promoter in both ML xenografts but after 15 days without trabectedin, C/EBP β was partially rebinding just on TSP-1 promoter in ML004 (51, 52). Taken together, these data not only highlight roles of trabectedin in the transcription regulatory pathway but also underline that in this context C/EBP β could interact with FUS-CHOP repressing the expression of TSP-1.

ML015

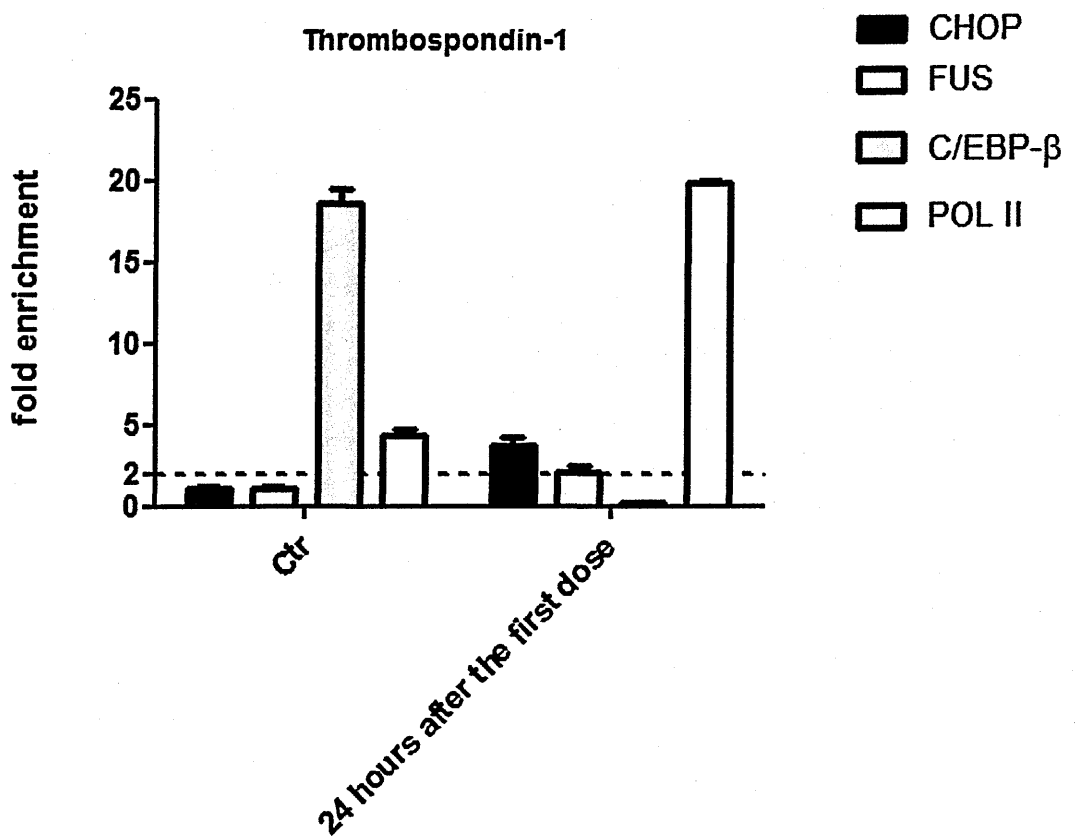

Figura 50: ChIPs were performed on xenograft model ML015 with the indicated antibodies and analyzed by RT-PCR with the appropiate primers. Values are reported as fold enrichment calculated with the following formula:2 ^ΔCtx - 2 ^ΔCtb, where ΔCtx = Ct input – Ct sample and ΔCtb = Ct input - Ct control Ab (Flag).

ML015

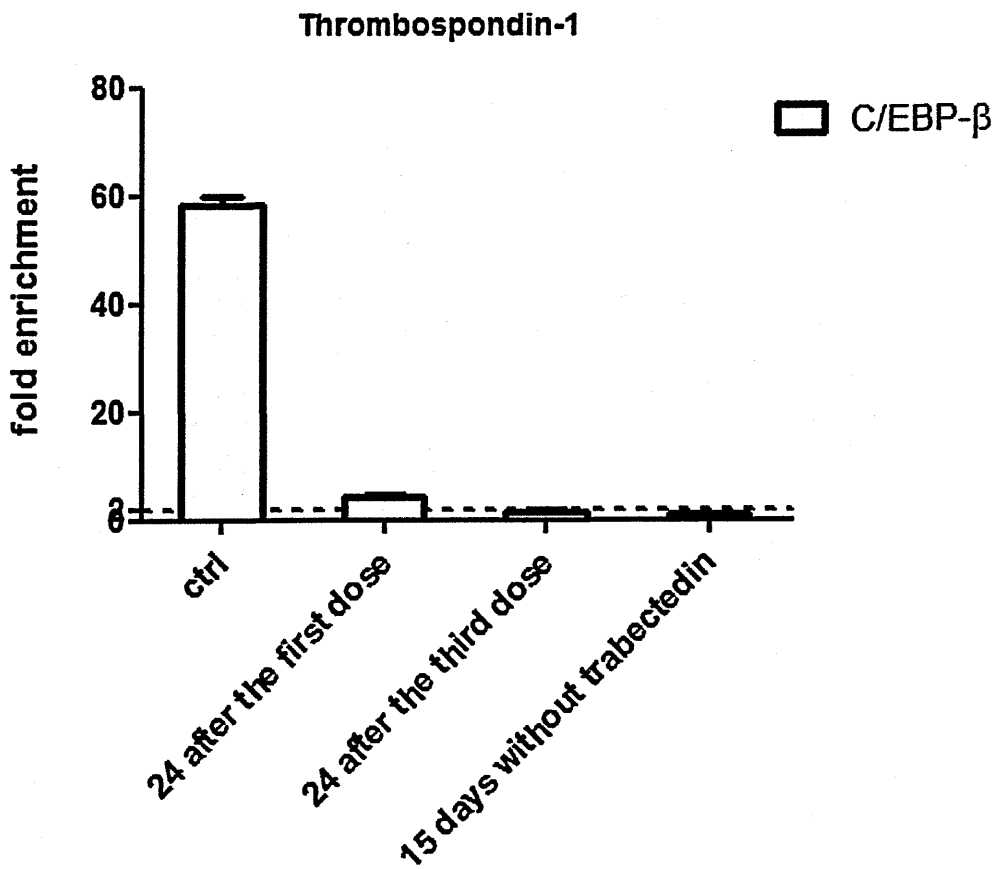

Figure 51: ML015. The promoter region of TSP-1 amplified. Values were measured as fold enrichment over a Flag control antibody in quantitative RT-PCR analysis.

ML004

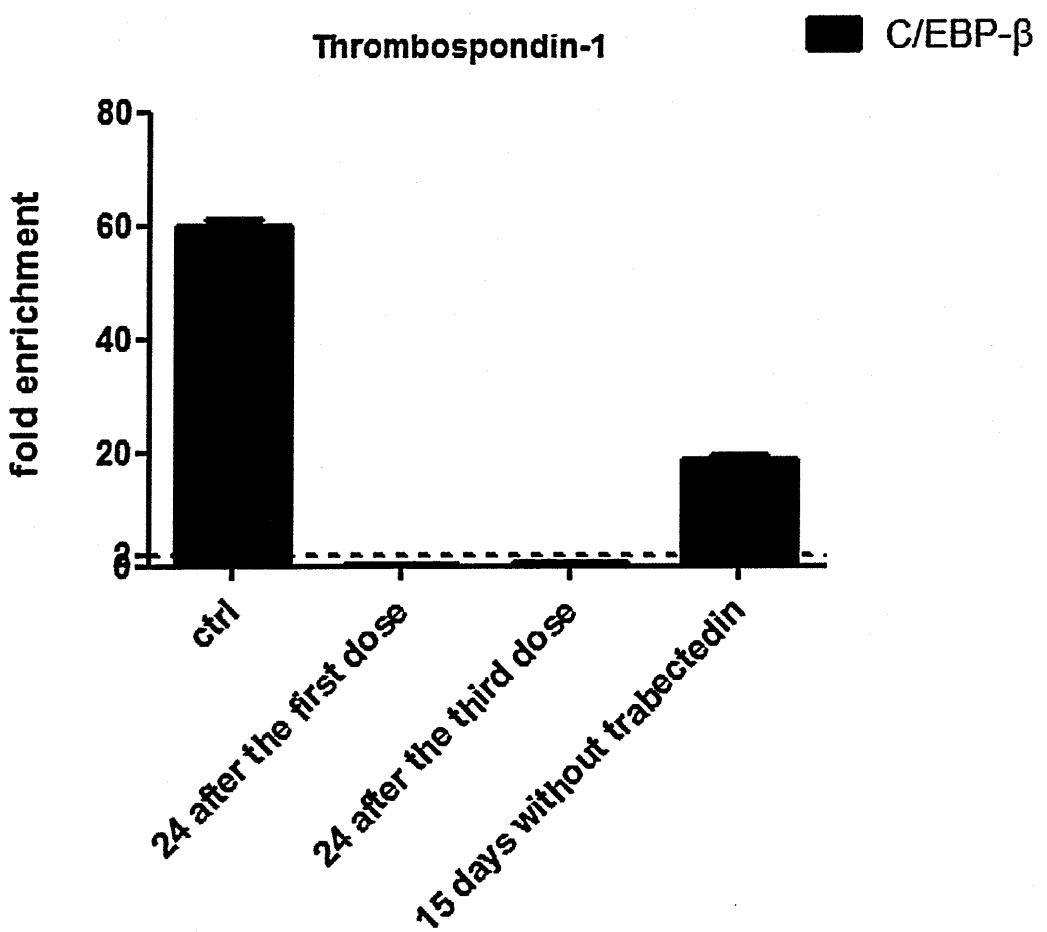

Figure 52 :. ML004. The promoter region of TSP-1 was amplified. Values were measured as fold enrichment over a Flag control antibody in quantitative RT-PCR analysis.

4.4 Methodological design for Chromatin Immunoprecipitation to increase the fold enrichment.

Chromatin immunoprecipitation (ChIP) is a powerful and widely applied technique for detecting the association of individual proteins with specific genomic regions *in vivo*. In this technique, live cells are treated with formaldehyde to generate protein-protein and protein-DNA cross-links between molecules in close proximity on the chromatin template *in vivo*. A whole-cell extract is prepared, and the cross-linked chromatin is sheared by sonication to reduce average DNA fragment size to 500 bp. The resulting materials are immunoprecipitated with an antibody against a desired protein, modified (e.g., acetylated, phosphorylated, methylated) peptide, or epitope (in situations where the protein of interest is epitope-tagged). DNA sequences that directly or indirectly cross-link with a given protein (or modified variant) are selectively enriched in the immunoprecipitated sample [221].

The amounts of specific genomic regions in control and immunoprecipitated samples are determined individually by quantitative PCR. The fold enrichment of certain chromosomal sequences (e.g., presumed binding sites) relative to other chromosomal sequences (e.g., presumed nonbinding sites) provides quantitative information about the relative level of association of a given protein with different genomic regions. Protein association with specific genomic regions can be performed under a variety of conditions (e.g., environmental change, cell-cycle status) and/or in wild-type versus mutant strains. In addition, ChIP can be combined with microarray technology to identify the location of specific proteins on a genome-wide basis [221, 222].

Previously I have described how to perform ChIP on xenograft samples using collagenase enzyme to dissociate the tumour. In order to improve the immunoprecipitation, I have developed an improved ChIP assay by replacing the traditionally used random fragmentation step with a site-specific enzyme digestion using micrococcal enzyme. Instead of dissociating the tumours to obtain a sufficient number of live single cells, I extracted the chromatin directly from the tissue

homogenized by Turax with lysis buffer. After the chromatin was measured by nanodrop, 50 μg was used to be digested by micrococcal enzyme.

The site-specific ChIP allows the immunoprecipitation and enrichment of DNA fragments containing only Transcription Factor Binding Sites. Chromatin is isolated by micrococcal digestion from whole tissue, generating oligonucleosomes which can range in size from mononucleosomes up to 10- to 12 -mers, depending on the time of digestion. The concentration of micrococcal can also be manipulated for the final concentration of chromatin fragments [223].

Figure 53 shows the difference in the two protocols, with sonicated material having an average length of 1.3 kb and careful titration of MNase I-reducing chromatin to single nucleosomes. Binding of FUS-CHOP to two representative CCAAT promoters—PTX3 was monitored by ChIP analysis with a set of core promoter primers. In addition, I compared the efficiency of FUS-CHOP binding in ChIPs performed with sonicated and MNase I-treated chromatins. The 5 to 8-fold enrichment with anti-CHOP and anti-FUS over a control FLAG antibody routinely scored with sonicated material was dramatically enhanced to 2 0 to 30-fold in MNase I ChIPs (figure 54).

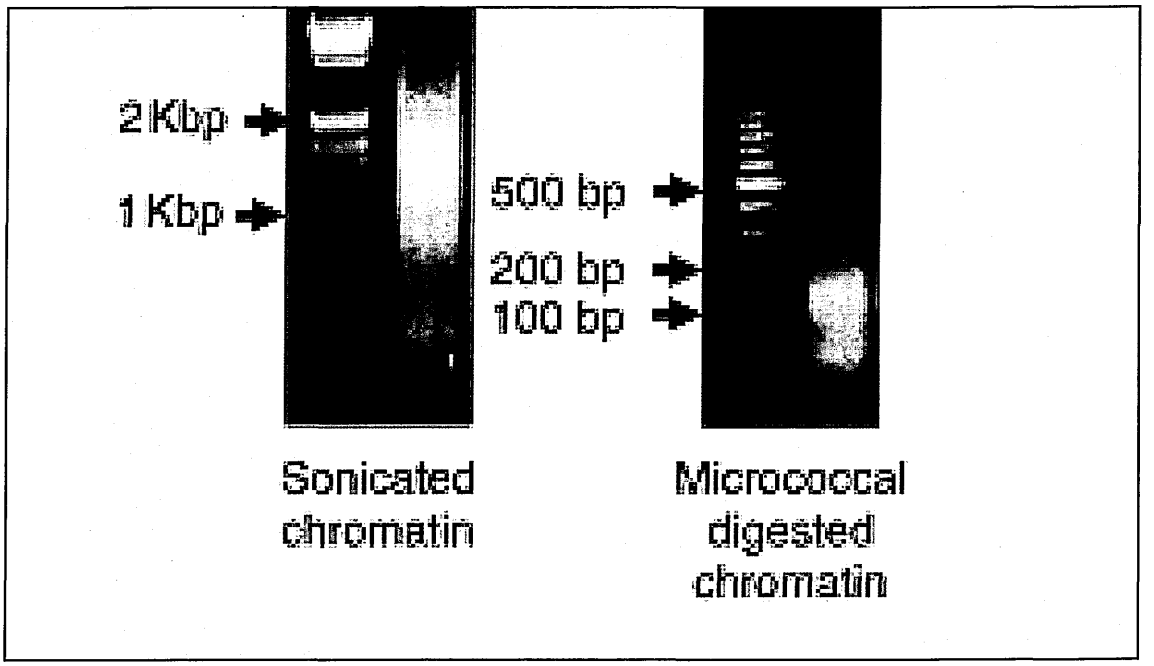

Figura 53: Comparison of chromatin preparations: on the left sonicated, on the right MNase I digested.

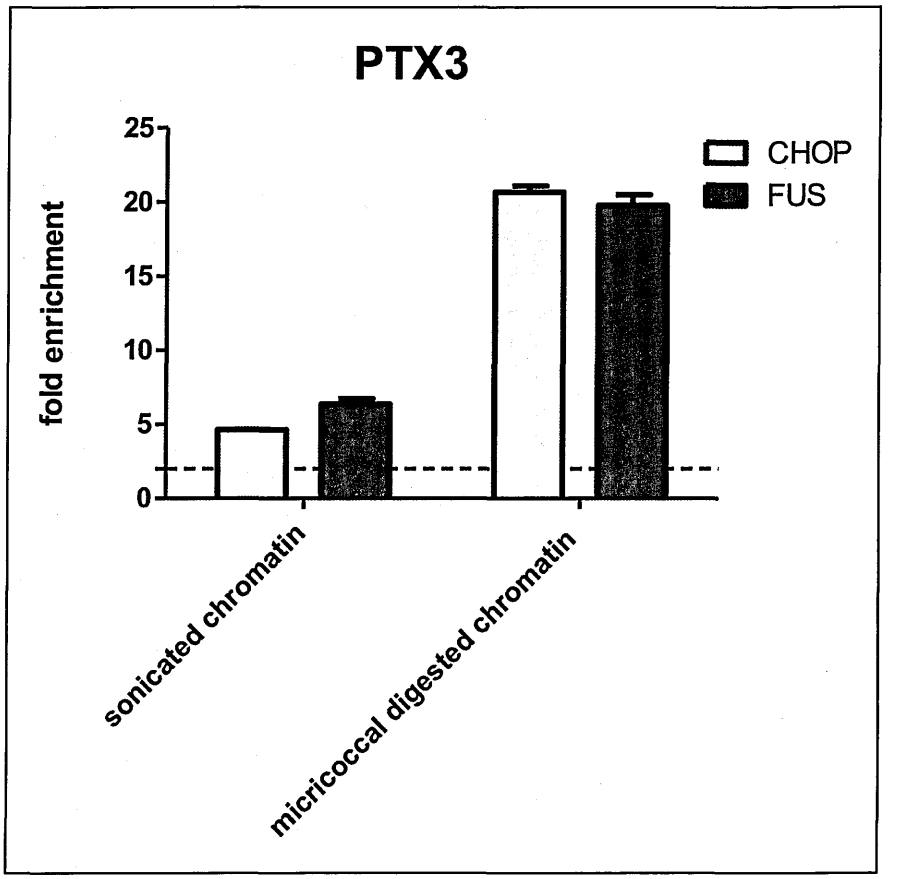

Figura 54: Comparison of ChIP assays performed with sonicated and with MNase I-digested chromatin; enrichment over a negative control antibody (Flag) was measured by quantitative real-time PCR.

Chapter 5

DISCUSSION

Myxoid liposarcoma (ML) accounts for one-third of liposarcomas and represents a morphologic continuum encompassing myxoid and myoxid/round cell variants, the latter characterized by an extent of round cell component >5% [1], [48]. Molecular hallmark of ML is the presence of FUS-CHOP fusion protein. CHOP belongs to and is a negative regulator of the large CAAT/enhancer binding protein family (C/EBP) whose α, β and δ members are master regulator of adipogenesis [54, 224-226]. Clinical studies indicate a peculiar sensitivity of these tumours to the natural marine compound trabectedin. In particular it was shown that trabectedin displayed an objective RECIST response rate of 50% of advanced and previously pretreated ML patients with a median PFS of 17 months, with 90% of patients free of progression at 6 months. Substantial radiological changes in tumour density anticipated tumour shrinkage in 75% of responding patients and were visible in almost 80% of patients having obtained disease stabilization [227]. The surprising finding on the sensitivity of liposarcoma tumours carrying a specific translocation involving a negative regulator of adipogenesis prompted us to investigate the mechanism of action of trabectedin related to this differentiation pathway. One hypothesis was that the activity of trabectedin was related to the functional impairment of the FUS-CHOP oncogene.

I have investigated the molecular mechanism underlying the activity of the anticancer drug trabectedin using 402 -91 cell line carrying type 1 FUS-CHOP fusion (fig 25) as an *in vitro* model. In order to investigate the effects of trabectedin at molecular level, I have treated 402 -91 cells with 5nM or 10 nM of ET-743 for 1 hour and recovered them for 6 and 24 hours with a drug free medium. Initially, I have performed RTPCR to evaluate the expression of genes specifically regulated by FUS-CHOP such as PTX3 and FN-1 after the treatment. I have shown that trabectedin was able to effect both genes' expression already after 1 hour (fig 28, 29) indicating that the drug could affects FUS-CHOP interaction with the DNA. To understand if the compound removed the

chimera from the DNA, I've proceeded with ChIP analysis and found that Trabectedin leads to a 6-10 fold enrichment reduction in 402-91 cells already after 1 hour of treatment. These data confirmed the action of Trabectedin directly on the oncogenic FUS-CHOP chimera. Previous studies [79] indicate that FUS-CHOP arise and function in the uncommitted cells in which FUS-CHOP prevents the development of adipocyte precursors interfering with PPARγ and C/EBPα activities (figure 55, figure 56).

According to this, I have performed RTPCR analyzing the expression of C/EBPβ and C/EBPα. C/EBPβ is considered the early marker of the adipogenesis, and was found that ML is characterized by the accumulation of early adipocytic precursors. I saw that in untreated cells, C/EBPβ was expressed but after treatment there was an increase of 4 fold suggesting that the removal of the chimera could be crucial for the unblock of adipogenesis pathway. Interestingly, I found an increase of 11 fold in C/EBPα expression after the treatment compared to the untreated cells where the Transcription factor was not expressed. Taken together, this study provides evidence that trabectedin treatment might affect the adipogenesis in myxoid liposarcoma harbouring the chimera gene FUS-CHOP type I.

The data presented provide evidence for direct interference of trabectedin with DNA binding of oncogenic FUS-CHOP protein without affecting the chimera protein levels. We speculate that trabectedin binding to the DNA changes the structure of DNA and removes FUS-CHOP from the promoter regions of its targets, resulting in releasing the block of adipogenic differentiation in ML. This is shown by marked increase in the expression of late adipogenic markers in ML cell lines *in vitro*.

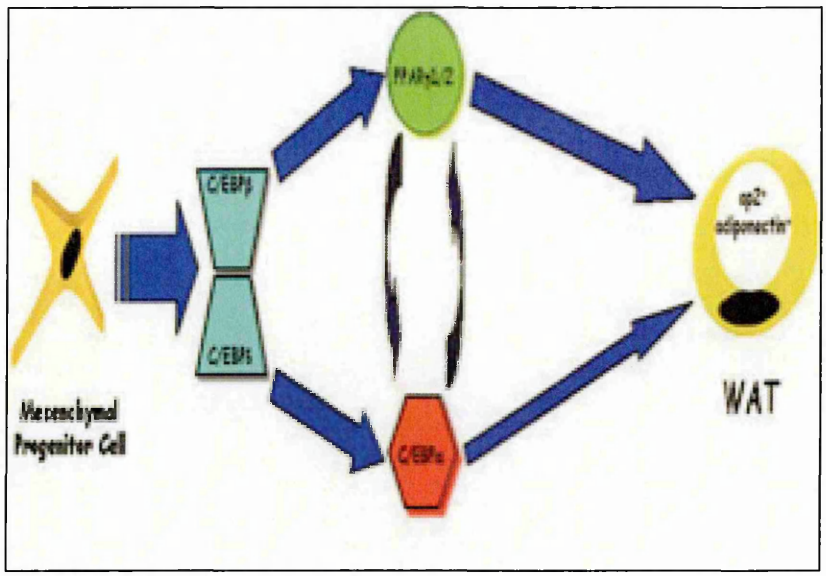

Figure 55: adipogenesis pathway: PPARγ and C/EBP family transcription factor are involved in adypocite differentiation. Transcriptions are expressed in cascade in which C/EBPδ and C/EBPβ, expressed during the first stages of the adipocyte differentiation program, induce the expression of C/EBPα and PPARγ, the master regulator of adypogenesis [79].

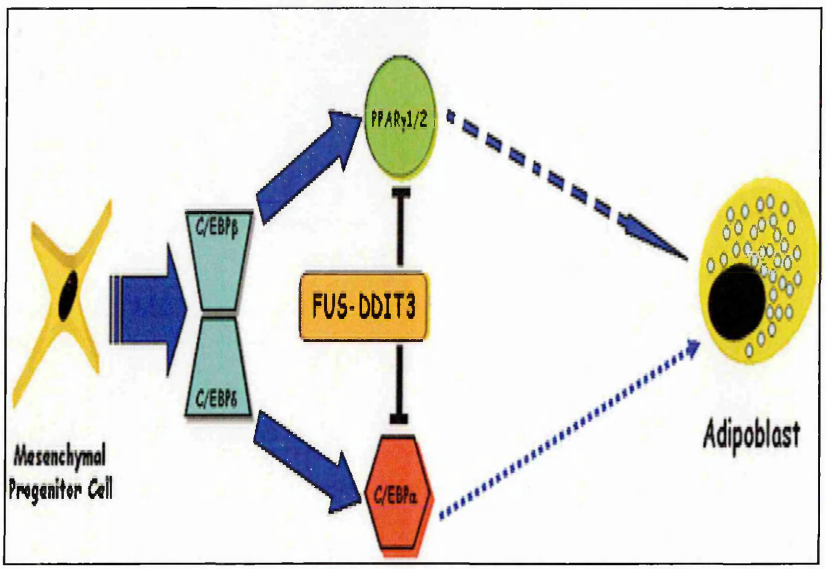

Figure 56: FUS-CHOP blocks the adipocyte differentiation program in mesenchymal cell progenitors by interfering with the PPARγ and C/EBPα activities at the transcriptional level [79].

Since the *in vitro* cell lines do not necessarily mimic the complexity of ML biology *in vivo*, we have developed xenograft models using tumour biopsies from patients with different breakpoints of FUS-CHOP chimera. The present study shows that trabectedin induces the displacement of FUS-CHOP chimera from the promoters of target genes *in vivo*, in human ML growing in mice. This effect was observed giving tolerable therapeutic doses of trabectedin, suggesting that the highly selective antitumour activity of trabectedin associated to the drug ability to induce adipocytic differentiation of ML is related to the ability of the drug to impair the transactivating function of the chimera, that is probably responsible for the block of differentiation. This mechanism appeared to be highly specific as other transcription factors were not affected (e.g. NF-YB [143]), and is likely to be responsible also for the striking antitumour activity of trabectedin in patients with ML. This is suggested by the observation made in tumour biopsies of one patient -who received a relative low dose of trabectedin of 1.1 corresponding to approximately 75% of the recommended dose-showing that the drug was able to displace the chimera from DNA. To our knowledge this is the first report indicating that a small molecule can displace an oncogenic transcription factor *in vivo* from its target DNA sequences, thus specifically modulating the transcription of genes involved in the pathogenesis of a neoplastic disease. Many attempts previously made to identify compounds that selectively block oncogenic transcription factors have failed, although many *in vitro* data have been published using many different molecules including nucleic acids, peptides and also small DNA binding ligands [228, 229]. For example some years ago our group had reported that some natural products that bound in the minor groove in AT rich DNA sequences such as distamycins were able to specifically prevent the binding of some transcription factors to DNA [127, 230-232] and similar data were published for other DNA minor groove binders [231]. However these *in vitro* findings were never confirmed *in vivo*, thus justifying some skepticisms about the

possibility to target transcription factors as a potential anticancer therapy, although it remained theoretically very appealing in consideration of the large number of tumours that are driven by an altered function of transcription factors. The reason why this approach was not successful is related to the fact that, *in vivo*, the complexity of the transcription regulation is much higher than *in vitro*, involving interactions between multiprotein complexes and chromatin and drug design is not feasible because the three dimensional structures of the complexes is not fully elucidated yet. In this respect the finding that trabectedin, a marine natural product that binds in the minor groove of DNA modifying DNA bending with some degree of sequence specificity [127], can specifically block the DNA binding of an oncogenic transcription factor in a specific manner is of great scientific interest and may stimulate the interest in setting up drug discovery programs aimed at identifying new compounds that are directed to the inhibition of transcription factors.

The high level of specificity of the observed mechanism of action of trabectedin in ML is highlighted by the observations that the drug-induced differentiation could be influenced by the breakpoint of the translocations. We found that ML type II xenografts were more sensitive to trabectedin than ML type III ones, these result being in keeping with higher probability of response in patients with type II than with type III chimera [227].

The histological analysis on the xenografts ML015 and ML004 showed that trabectedin induce a cellular component depletion and increase of mature adipoblasts in type II ML, while in type III ML there was not any histological response, indicating that, in our experimental conditions, trabectedin induces maturation in ML carrying FUS-CHOP type II but not in ML carrying FUS-CHOP type III (figure 38, 39). [233]

Previous studies have identified a number of transcription factors involved in adipocyte

differentiation. These include PPARγ and members of the C/EBP family of transcription factors [76]. Many of the components of the gene regulatory network that controls the differentiation of adipocytes have been elucidated in studies of cultured 3T3-L1 preadipocytes and MEFs [74, 75]. These transcription factors are expressed as a cascade in which C/EBPβ and C/EBPδ, expressed during the first stages of the adipocyte differentiation program, induce the expression of C/EBPα and PPARγ the master regulator of adipogenesis. A positive feedback loop mechanism between PPARγ and C/EBPα enhances their activities. This transcriptional cascade finishes with the expression of markers of mature adipocytes such as aP2, adiponectin and adipsin [234]. There are two PPARγ isoforms generated by alternative splicing, PPARγ1 and PPARγ2 , with PPARγ2 being more efficient to induce terminal differentiation *in vitro* [79]. It was recently demonstrated that FUS-CHOP interferes with the PPARγ2 and C/EBPα activities. In addition, it was shown that the regulation of the translation machinery by FUS-CHOP plays an important role in the blockade of adipogenesis associated to liposarcoma development [79]. According to this, I used Western Blot to analyze the expression level of C/EBPα, PPARγ1 and PPARγ2. I found that after trabectedin treatment C/EBPα and PPARγ2 were expressed only in ML015 carrying FUS-CHOP type II (figure 41, 42) but not in ML004 carrying FUS-CHOP type III. Taken together these data provide evidence that trabectedin induces adipocytic differentiation in ML carrying in type II FUS-CHOP but not in ML expressing type III FUS-CHOP.

The different response to trabectedin observed in type II and type III ML could be due to a different ability of the drug to displace the binding of the chimera from target promoters. The experiments done, however, showed that in both type II and type III subtypes tumours after treatment with trabectedin FUS-CHOP was not bound to DNA. Nevertheless when treatment was stopped, the kinetic of reattachment of the chimera to DNA appeared to be different for the two subtypes, being faster for the type III than for

type II. The longer duration of the block of FUS-CHOP might justify the different biological effects that were observed. It might be speculated that the larger size of type III chimera makes the complex of transcription factor-cofactors and DNA more stable. Therefore when the drug is partially cleared from the tumour after some days after treatment, the drug concentrations in tumour cells might be sufficient to prevent the binding of type II but not of type III chimera. Alternatively for some reasons the amount of drug bound to DNA of type II remained longer than on type III, implying that some differences in the DNA repair mechanisms occur.

In the last century anti-cancer therapies concentrated on natural or engineered molecules having the capacity to target the neoplastic cells. Often these tactics do not completely remove the tumour mass and select for resistant clones of cancer cells able to repopulate tumour sites. A new strategy to develop therapies capable of creating a hostile niche for neoplastic cells could be a starting-point. The possibility to contrast cancer cells with a single molecule is obviously naive. A set of different molecules able to target tumour cells, able to normalize the angiogenic network and to restore the correct function of immune cells, could increase the chance of success. The development of the tumour vasculature is crucial for the growth of ML. An experimental study has recently demonstrated that dormancy of liposarcomas is associated with impaired angiogenesis, whereas the acquisition of the angiogenic ability triggers the passage from dormant, poorly vascularized lesions to rapidly growing malignant liposarcomas [215, 216]. Preliminary observations indicate that following treatment with trabectedin tumours appear less vascularized. It is therefore plausible that inhibition of angiogenesis might contribute to the antineoplastic activity of trabectedin on ML. Based on this observations I investigated whether the changes in gene expression caused by trabectedin modifies the host tumour interaction by modulating the angiogenic process. Initially the expression of mRNA levels of VEGF and TSP-1

were checked using 402 -91 cell line. VEGF protein levels did not change whereas TSP-1 protein levels were affected. Afterwards, to forward investigate the effects of trabectedin, TSP-1 protein level was investigated using *in vivo* models. Xenograft samples carrying FUS-CHOP type II has shown a higher response, i.e. increase in TSP-1 levels, compared to xenograft samples carrying FUS-CHOP type III which has shown a lower response, confirming that ML type II was more sensitive to trabectedin compared to ML type III. This sensitivity was demonstrated even at molecular level using ChIP assay.

These findings, therefore, support the idea that to obtain an improved treatment effect in type III ML, the interval between doses should be reduced, and studies are in progress to test this hypothesis in preclinical ML xenograft models.

In summary I have provided evidence that trabectedin has a highly specific mode of action in ML, being able to displace the product of the fusion gene- that represents the hallmark and the pathogenetic lesion of the disease from its target promoters. The functional inactivation of the oncogenic chimera by trabectedin treatment leads to the derepression of the adipocytic differentiation. The duration of the block of the transactivating activity of the chimeric protein seems to be important as highlighted by the differences found in type II and type III ML, a finding of potential clinical importance to attempt different dosage-schedules of the drug according to the molecular characterization of the fusion gene.

Chapter 6:

REFERENCES

1. Sandberg, A.A., *Updates on the cytogenetics and molecular genetics of bone and soft tissue tumors: liposarcoma.* Cancer Genet Cytogenet, 2004. **155**(1): p. 1-24.
2. http://www.istitutotumori.mi.it/.
3. Demetri, G.D., et al., *Soft tissue sarcoma.* J Natl Compr Canc Netw, 2010. **8**(6): p. 630-74.
4. Sauk, J.J., Jr., *Liposarcoma of the head and neck.* J Oral Surg, 1971. **29**(1): p. 38-40.
5. Olsson, H., *An updated review of the epidemiology of soft tissue sarcoma.* Acta Orthop Scand Suppl, 2004. **75**(311): p. 16-20.
6. Slominski, A., et al., *Molecular pathology of soft tissue and bone tumors. A review.* Arch Pathol Lab Med, 1999. **123**(12): p. 1246-59.
7. Kleinerman, R.A., et al., *Risk of soft tissue sarcomas by individual subtype in survivors of hereditary retinoblastoma.* J Natl Cancer Inst, 2007. **99**(1): p. 24-31.
8. Eriksson, M., L. Hardell, and H.O. Adami, *Exposure to dioxins as a risk factor for soft tissue sarcoma: a population-based case-control study.* J Natl Cancer Inst, 1990. **82**(6): p. 486-90.
9. Olsson, H., *A review of the epidemiology of soft tissue sarcoma.* Acta Orthop Scand Suppl, 1999. **285**: p. 8-10.
10. Fletcher, C.D.M., *Soft tissue tumours.* Diagnostic Histopathology of tumours, 1995.
11. Kransdorf, M.J., et al., *Imaging of fatty tumors: distinction of lipoma and well-differentiated liposarcoma.* Radiology, 2002. **224**(1): p. 99-104.

12. Murphey, M.D., L.K. Arcara, and J. Fanburg-Smith, *From the archives of the AFIP: imaging of musculoskeletal liposarcoma with radiologic-pathologic correlation.* Radiographics, 2005. **25**(5): p. 1371-95.

13. Willen, H., M. Akerman, and B. Carlen, *Fine needle aspiration (FNA) in the diagnosis of soft tissue tumours; a review of 22 years experience.* Cytopathology, 1995. **6**(4): p. 236-47.

14. Walaas, L. and L.G. Kindblom, *Lipomatous tumors: a correlative cytologic and histologic study of 27 tumors examined by fine needle aspiration cytology.* Hum Pathol, 1985. **16**(1): p. 6-18.

15. Akerman, M. and A. Rydholm, *Aspiration cytology of lipomatous tumors: a 10-year experience at an orthopedic oncology center.* Diagn Cytopathol, 1987. **3**(4): p. 295-302.

16. Einarsdottir, H., et al., *Accuracy of cytology for diagnosis of lipomatous tumors: comparison with magnetic resonance and computed tomography findings in 175 cases.* Acta Radiol, 2004. **45**(8): p. 840-6.

17. Hisaoka, M., et al., *Detection of TLS/FUS-CHOP fusion transcripts in myxoid and round cell liposarcomas by nested reverse transcription-polymerase chain reaction using archival paraffin-embedded tissues.* Diagn Mol Pathol, 1998. **7**(2): p. 96-101.

18. Enneking, W.F., S.S. Spanier, and M.A. Goodman, *A system for the surgical staging of musculoskeletal sarcoma.* Clin Orthop Relat Res, 1980(153): p. 106-20.

19. Strander, H., I. Turesson, and E. Cavallin-Stahl, *A systematic overview of radiation therapy effects in soft tissue sarcomas.* Acta Oncol, 2003. **42**(5-6): p. 516-31.

20. Lindberg, R.D., et al., *Conservative surgery and postoperative radiotherapy in 300 adults with soft-tissue sarcomas.* Cancer, 1981. **47**(10): p. 2391-7.

21. Rosenberg, S.A., et al., *The treatment of soft-tissue sarcomas of the extremities: prospective randomized evaluations of (1) limb-sparing surgery plus radiation therapy compared with amputation and (2) the role of adjuvant chemotherapy.* Ann Surg, 1982. **196**(3): p. 305-15.

22. Suit, H.D. and C.G. Willett, *Radiation therapy of sarcomas of the soft tissues.* Cancer Treat Res, 1991. **56**: p. 61-74.

23. Suit, H.D., W.O. Russell, and R.G. Martin, *Management of patients with sarcoma of soft tissue in an extremity.* Cancer, 1973. **31**(5): p. 1247-55.

24. Yang, J.C., et al., *Randomized prospective study of the benefit of adjuvant radiation therapy in the treatment of soft tissue sarcomas of the extremity.* J Clin Oncol, 1998. **16**(1): p. 197-203.

25. Kepka, L., et al., *Results of radiation therapy for unresected soft-tissue sarcomas.* Int J Radiat Oncol Biol Phys, 2005. **63**(3): p. 852-9.

26. Slater, J.D., M.D. McNeese, and L.J. Peters, *Radiation therapy for unresectable soft tissue sarcomas.* Int J Radiat Oncol Biol Phys, 1986. **12**(10): p. 1729-34.

27. Tepper, J.E. and H.D. Suit, *Radiation therapy alone for sarcoma of soft tissue.* Cancer, 1985. **56**(3): p. 475-9.

28. Friedman, M. and J.W. Egan, *Irradiation of liposarcoma.* Acta Radiol, 1960. **54**: p. 225-39.

29. Tong, E.C. and S. Rubenfeld, *Cardiac metastasis from myxoid liposarcoma emphasizing its radiosensitivity.* Am J Roentgenol Radium Ther Nucl Med, 1968. **103**(4): p. 792-9.

30. Perry, H. and F.C. Chu, *Radiation therapy in the palliative management of soft tissue sarcomas.* Cancer, 1962. **15**: p. 179-83.

31. Pitson, G., et al., *Radiation response: an additional unique signature of myxoid liposarcoma.* Int J Radiat Oncol Biol Phys, 2004. **60**(2): p. 522-6.

32. Engstrom, K., et al., *Irradiation of myxoid/round cell liposarcoma induces volume reduction and lipoma-like morphology.* Acta Oncol, 2007. **46**(6): p. 838-45.

33. Tierney, J.F., et al., *Adjuvant chemotherapy for soft-tissue sarcoma: review and meta-analysis of the published results of randomised clinical trials.* Br J Cancer, 1995. **72**(2): p. 469-75.

34. Frustaci, S., et al., *Adjuvant chemotherapy for adult soft tissue sarcomas of the extremities and girdles: results of the Italian randomized cooperative trial.* J Clin Oncol, 2001. **19**(5): p. 1238-47.

35. Petrioli, R., et al., *Adjuvant epirubicin with or without Ifosfamide for adult soft-tissue sarcoma.* Am J Clin Oncol, 2002. **25**(5): p. 468-73.

36. Cormier, J.N., et al., *Cohort analysis of patients with localized, high-risk, extremity soft tissue sarcoma treated at two cancer centers: chemotherapy-associated outcomes.* J Clin Oncol, 2004. **22**(22): p. 4567-74.

37. Dei Tos, A.P., *Liposarcoma: new entities and evolving concepts.* Ann Diagn Pathol, 2000. **4**(4): p. 252-66.

38. Evans, H.L., *Atypical lipomatous tumor, its variants, and its combined forms: a study of 61 cases, with a minimum follow-up of 10 years.* Am J Surg Pathol, 2007. **31**(1): p. 1-14.

39. Fletcher, C.D., *The evolving classification of soft tissue tumours: an update based on the new WHO classification.* Histopathology, 2006. **48**(1): p. 3-12.

40. Weiss, S.W. and V.K. Rao, *Well-differentiated liposarcoma (atypical lipoma) of deep soft tissue of the extremities, retroperitoneum, and miscellaneous sites. A*

follow-up study of 92 cases with analysis of the incidence of "dedifferentiation". Am J Surg Pathol, 1992. **16**(11): p. 1051-8.

41. Henricks, W.H., et al., *Dedifferentiated liposarcoma: a clinicopathological analysis of 155 cases with a proposal for an expanded definition of dedifferentiation.* Am J Surg Pathol, 1997. **21**(3): p. 271-81.

42. Conyers, R., S. Young, and D.M. Thomas, *Liposarcoma: molecular genetics and therapeutics.* Sarcoma, 2011. **2011**: p. 483154.

43. Nascimento, A.G., *Dedifferentiated liposarcoma.* Semin Diagn Pathol, 2001. **18**(4): p. 263-6.

44. Elgar, F. and J.R. Goldblum, *Well-differentiated liposarcoma of the retroperitoneum: a clinicopathologic analysis of 20 cases, with particular attention to the extent of low-grade dedifferentiation.* Mod Pathol, 1997. **10**(2): p. 113-20.

45. Hornick, J.L., et al., *Pleomorphic liposarcoma: clinicopathologic analysis of 57 cases.* Am J Surg Pathol, 2004. **28**(10): p. 1257-67.

46. Weiss, S.W., *enzinger and weiss' soft tissue tumors.* edited, St Louis, Mosby, Inc., 2001.

47. Idbaih, A., et al., *Myxoid malignant fibrous histiocytoma and pleomorphic liposarcoma share very similar genomic imbalances.* Lab Invest, 2005. **85**(2): p. 176-81.

48. Frapolli, R., et al., *Novel models of myxoid liposarcoma xenografts mimicking the biological and pharmacologic features of human tumors.* Clin Cancer Res, 2010. **16**(20): p. 4958-67.

49. Schwab, J.H., et al., *Skeletal metastases in myxoid liposarcoma: an unusual pattern of distant spread.* Ann Surg Oncol, 2007. **14**(4): p. 1507-14.

50. ten Heuvel, S.E., et al., *Clinicopathologic prognostic factors in myxoid liposarcoma: a retrospective study of 49 patients with long-term follow-up.* Ann Surg Oncol, 2007. **14**(1): p. 222-9.

51. Canter, R.J., et al., *Why do patients with low-grade soft tissue sarcoma die?* Ann Surg Oncol, 2008. **15**(12): p. 3550-60.

52. Chung, P.W., et al., *Radiosensitivity translates into excellent local control in extremity myxoid liposarcoma: a comparison with other soft tissue sarcomas.* Cancer, 2009. **115**(14): p. 3254-61.

53. Antonescu, C.R., et al., *Prognostic impact of P53 status, TLS-CHOP fusion transcript structure, and histological grade in myxoid liposarcoma: a molecular and clinicopathologic study of 82 cases.* Clin Cancer Res, 2001. **7**(12): p. 3977-87.

54. Crozat, A., et al., *Fusion of CHOP to a novel RNA-binding protein in human myxoid liposarcoma.* Nature, 1993. **363**(6430): p. 640-4.

55. Dal Cin, P., et al., *Additional evidence of a variant translocation t(12;22) with EWS/CHOP fusion in myxoid liposarcoma: clinicopathological features.* J Pathol, 1997. **182**(4): p. 437-41.

56. Sreekantaiah, C., et al., *Trisomy 8 as a nonrandom secondary change in myxoid liposarcoma.* Cancer Genet Cytogenet, 1991. **51**(2): p. 195-205.

57. Miettinen, M., *From morphological to molecular diagnosis of soft tissue tumors.* Adv Exp Med Biol, 2006. **587**: p. 99-113.

58. Bode-Lesniewska, B., et al., *Relevance of translocation type in myxoid liposarcoma and identification of a novel EWSR1-DDIT3 fusion.* Genes Chromosomes Cancer, 2007. **46**(11): p. 961-71.

59. Grosso, F., et al., *Efficacy of trabectedin (ecteinascidin-743) in advanced pretreated myxoid liposarcomas: a retrospective study.* Lancet Oncol, 2007. **8**(7): p. 595-602.

60. Forni, C., et al., *Trabectedin (ET-743) promotes differentiation in myxoid liposarcoma tumors.* Mol Cancer Ther, 2009. **8**(2): p. 449-57.

61. Stolow, D.T. and S.R. Haynes, *Cabeza, a Drosophila gene encoding a novel RNA binding protein, shares homology with EWS and TLS, two genes involved in human sarcoma formation.* Nucleic Acids Res, 1995. **23**(5): p. 835-43.

62. Andersson, M.K., et al., *The multifunctional FUS, EWS and TAF15 proto-oncoproteins show cell type-specific expression patterns and involvement in cell spreading and stress response.* BMC Cell Biol, 2008. **9**: p. 37.

63. Belyanskaya, L.L., P.M. Gehrig, and H. Gehring, *Exposure on cell surface and extensive arginine methylation of ewing sarcoma (EWS) protein.* J Biol Chem, 2001. **276**(22): p. 18681-7.

64. Bertolotti, A., et al., *hTAF(II)68, a novel RNA/ssDNA-binding protein with homology to the pro-oncoproteins TLS/FUS and EWS is associated with both TFIID and RNA polymerase II.* EMBO J, 1996. **15**(18): p. 5022-31.

65. Tan, A.Y. and J.L. Manley, *TLS inhibits RNA polymerase III transcription.* Mol Cell Biol, 2010. **30**(1): p. 186-96.

66. Wang, X.Z., et al., *Signals from the stressed endoplasmic reticulum induce C/EBP-homologous protein (CHOP/GADD153).* Mol Cell Biol, 1996. **16**(8): p. 4273-80.

67. Lekstrom-Himes, J. and K.G. Xanthopoulos, *Biological role of the CCAAT/enhancer-binding protein family of transcription factors.* J Biol Chem, 1998. **273**(44): p. 28545-8.

68. Batchvarova, N., X.Z. Wang, and D. Ron, *Inhibition of adipogenesis by the stress-induced protein CHOP (Gadd153).* EMBO J, 1995. **14**(19): p. 4654-61.

69. Freytag, S.O., D.L. Paielli, and J.D. Gilbert, *Ectopic expression of the CCAAT/enhancer-binding protein alpha promotes the adipogenic program in a variety of mouse fibroblastic cells.* Genes Dev, 1994. **8**(14): p. 1654-63.

70. Wu, Z., et al., *Conditional ectopic expression of C/EBP beta in NIH-3T3 cells induces PPAR gamma and stimulates adipogenesis.* Genes Dev, 1995. **9**(19): p. 2350-63.

71. Wu, Z., et al., *Cross-regulation of C/EBP alpha and PPAR gamma controls the transcriptional pathway of adipogenesis and insulin sensitivity.* Mol Cell, 1999. **3**(2): p. 151-8.

72. Tontonoz, P., et al., *PPARgamma promotes monocyte/macrophage differentiation and uptake of oxidized LDL.* Cell, 1998. **93**(2): p. 241-52.

73. Mansen, A., et al., *Expression of the peroxisome proliferator-activated receptor (PPAR) in the mouse colonic mucosa.* Biochem Biophys Res Commun, 1996. **222**(3): p. 844-51.

74. Rosen, E.D. and O.A. MacDougald, *Adipocyte differentiation from the inside out.* Nat Rev Mol Cell Biol, 2006. **7**(12): p. 885-96.

75. Rosen, E.D. and B.M. Spiegelman, *Molecular regulation of adipogenesis.* Annu Rev Cell Dev Biol, 2000. **16**: p. 145-71.

76. Rosen, E.D., et al., *Transcriptional regulation of adipogenesis.* Genes Dev, 2000. **14**(11): p. 1293-307.

77. Riggi, N., et al., *Expression of the FUS-CHOP fusion protein in primary mesenchymal progenitor cells gives rise to a model of myxoid liposarcoma.* Cancer Res, 2006. **66**(14): p. 7016-23.

78. Perez-Mancera, P.A., et al., *Fat-specific FUS-DDIT3-transgenic mice establish PPARgamma inactivation is required to liposarcoma development.* Carcinogenesis, 2007. **28**(10): p. 2069-73.

79. Perez-Mancera, P.A., et al., *FUS-DDIT3 prevents the development of adipocytic precursors in liposarcoma by repressing PPARgamma and C/EBPalpha and activating eIF4E.* PLoS One, 2008. **3**(7): p. e2569.

80. Thelin-Jarnum, S., et al., *Identification of genes differentially expressed in TLS-CHOP carrying myxoid liposarcomas.* Int J Cancer, 1999. **83**(1): p. 30-3.

81. Cheng, H., et al., *Validation of immature adipogenic status and identification of prognostic biomarkers in myxoid liposarcoma using tissue microarrays.* Hum Pathol, 2009. **40**(9): p. 1244-51.

82. Tao, Y., et al., *Mechanisms of disease: signaling of the insulin-like growth factor 1 receptor pathway--therapeutic perspectives in cancer.* Nat Clin Pract Oncol, 2007. **4**(10): p. 591-602.

83. Negri, T., et al., *Functional mapping of receptor tyrosine kinases in myxoid liposarcoma.* Clin Cancer Res, 2010. **16**(14): p. 3581-93.

84. Andersson, M.K., et al., *Nuclear expression of FLT1 and its ligand PGF in FUS-DDIT3 carrying myxoid liposarcomas suggests the existence of an intracrine signaling loop.* BMC Cancer, 2010. **10**: p. 249.

85. Engstrom, K., et al., *The myxoid/round cell liposarcoma fusion oncogene FUS-DDIT3 and the normal DDIT3 induce a liposarcoma phenotype in transfected human fibrosarcoma cells.* Am J Pathol, 2006. **168**(5): p. 1642-53.

86. Samuels, Y. and V.E. Velculescu, *Oncogenic mutations of PIK3CA in human cancers.* Cell Cycle, 2004. **3**(10): p. 1221-4.

87. Thomas, R.K., et al., *High-throughput oncogene mutation profiling in human cancer.* Nat Genet, 2007. **39**(3): p. 347-51.

88. Barretina, J., et al., *Subtype-specific genomic alterations define new targets for soft-tissue sarcoma therapy.* Nat Genet, 2010. **42**(8): p. 715-21.

89. Cantley, L.C., *The phosphoinositide 3-kinase pathway.* Science, 2002. **296**(5573): p. 1655-7.

90. Momand, J., H.H. Wu, and G. Dasgupta, *MDM2--master regulator of the p53 tumor suppressor protein.* Gene, 2000. **242**(1-2): p. 15-29.

91. Shangary, S., et al., *Temporal activation of p53 by a specific MDM2 inhibitor is selectively toxic to tumors and leads to complete tumor growth inhibition.* Proc Natl Acad Sci U S A, 2008. **105**(10): p. 3933-8.

92. Muller, C.R., et al., *Potential for treatment of liposarcomas with the MDM2 antagonist Nutlin-3A.* Int J Cancer, 2007. **121**(1): p. 199-205.

93. Shangary, S. and S. Wang, *Small-molecule inhibitors of the MDM2-p53 protein-protein interaction to reactivate p53 function: a novel approach for cancer therapy.* Annu Rev Pharmacol Toxicol, 2009. **49**: p. 223-41.

94. Ding, K., et al., *Structure-based design of spiro-oxindoles as potent, specific small-molecule inhibitors of the MDM2-p53 interaction.* J Med Chem, 2006. **49**(12): p. 3432-5.

95. Vassilev, L.T., et al., *In vivo activation of the p53 pathway by small-molecule antagonists of MDM2.* Science, 2004. **303**(5659): p. 844-8.

96. Ringshausen, I., et al., *Mdm2 is critically and continuously required to suppress lethal p53 activity in vivo.* Cancer Cell, 2006. **10**(6): p. 501-14.

97. Tovar, C., et al., *Small-molecule MDM2 antagonists reveal aberrant p53 signaling in cancer: implications for therapy.* Proc Natl Acad Sci U S A, 2006. **103**(6): p. 1888-93.

98. Shapiro, G.I., *Cyclin-dependent kinase pathways as targets for cancer treatment.* J Clin Oncol, 2006. **24**(11): p. 1770-83.

99. De Azevedo, W.F., et al., *Inhibition of cyclin-dependent kinases by purine analogues: crystal structure of human cdk2 complexed with roscovitine.* Eur J Biochem, 1997. **243**(1-2): p. 518-26.

100. Sedlacek, H.H., *Mechanisms of action of flavopiridol.* Crit Rev Oncol Hematol, 2001. **38**(2): p. 139-70.

101. Shapiro, G.I., *Preclinical and clinical development of the cyclin-dependent kinase inhibitor flavopiridol.* Clin Cancer Res, 2004. **10**(12 Pt 2): p. 4270s-4275s.

102. Matranga, C.B. and G.I. Shapiro, *Selective sensitization of transformed cells to flavopiridol-induced apoptosis following recruitment to S-phase.* Cancer Res, 2002. **62**(6): p. 1707-17.

103. Bible, K.C. and S.H. Kaufmann, *Cytotoxic synergy between flavopiridol (NSC 649890, L86-8275) and various antineoplastic agents: the importance of sequence of administration.* Cancer Res, 1997. **57**(16): p. 3375-80.

104. Jung, C.P., M.V. Motwani, and G.K. Schwartz, *Flavopiridol increases sensitization to gemcitabine in human gastrointestinal cancer cell lines and correlates with down-regulation of ribonucleotide reductase M2 subunit.* Clin Cancer Res, 2001. **7**(8): p. 2527-36.

105. Lapenna, S. and A. Giordano, *Cell cycle kinases as therapeutic targets for cancer.* Nat Rev Drug Discov, 2009. **8**(7): p. 547-66.

106. Benson, C., et al., *A phase I trial of the selective oral cyclin-dependent kinase inhibitor seliciclib (CYC202; R-Roscovitine), administered twice daily for 7 days every 21 days.* Br J Cancer, 2007. **96**(1): p. 29-37.

107. Fry, D.W., et al., *Specific inhibition of cyclin-dependent kinase 4/6 by PD 0332991 and associated antitumor activity in human tumor xenografts.* Mol Cancer Ther, 2004. **3**(11): p. 1427-38.

108. Demetri, G.D., et al., *Induction of solid tumor differentiation by the peroxisome proliferator-activated receptor-gamma ligand troglitazone in patients with liposarcoma.* Proc Natl Acad Sci U S A, 1999. **96**(7): p. 3951-6.

109. Sears, I.B., et al., *Differentiation-dependent expression of the brown adipocyte uncoupling protein gene: regulation by peroxisome proliferator-activated receptor gamma.* Mol Cell Biol, 1996. **16**(7): p. 3410-9.

110. Debrock, G., et al., *A phase II trial with rosiglitazone in liposarcoma patients.* Br J Cancer, 2003. **89**(8): p. 1409-12.

111. Workman, P., et al., *Drugging the PI3 kinome: from chemical tools to drugs in the clinic.* Cancer Res, 2010. **70**(6): p. 2146-57.

112. Folkes, A.J., et al., *The identification of 2-(1H-indazol-4-yl)-6-(4-methanesulfonyl-piperazin-1-ylmethyl)-4-morpholin-4-yl-t hieno[3,2-d]pyrimidine (GDC-0941) as a potent, selective, orally bioavailable inhibitor of class I PI3 kinase for the treatment of cancer.* J Med Chem, 2008. **51**(18): p. 5522-32.

113. Raynaud, F.I., et al., *Biological properties of potent inhibitors of class I phosphatidylinositide 3-kinases: from PI-103 through PI-540, PI-620 to the oral agent GDC-0941.* Mol Cancer Ther, 2009. **8**(7): p. 1725-38.

114. Ihle, N.T., et al., *Mutations in the phosphatidylinositol-3-kinase pathway predict for antitumor activity of the inhibitor PX-866 whereas oncogenic Ras is a dominant predictor for resistance.* Cancer Res, 2009. **69**(1): p. 143-50.

115. O'Brien, C., et al., *Predictive biomarkers of sensitivity to the phosphatidylinositol 3' kinase inhibitor GDC-0941 in breast cancer preclinical models.* Clin Cancer Res, 2010. **16**(14): p. 3670-83.

116. Di Nicolantonio, F., et al., *Deregulation of the PI3K and KRAS signaling pathways in human cancer cells determines their response to everolimus.* J Clin Invest, 2010. **120**(8): p. 2858-66.

117. Cecchi, F., D.C. Rabe, and D.P. Bottaro, *Targeting the HGF/Met signalling pathway in cancer.* Eur J Cancer, 2010. **46**(7): p. 1260-70.

118. Eder, J.P., et al., *A phase I study of foretinib, a multi-targeted inhibitor of c-Met and vascular endothelial growth factor receptor 2.* Clin Cancer Res, 2010. **16**(13): p. 3507-16.

119. Adams, J. and P.J. Elliott, *New agents in cancer clinical trials.* Oncogene, 2000. **19**(56): p. 6687-92.

120. Schwartsmann, G., et al., *Marine organisms as a source of new anticancer agents.* Lancet Oncol, 2001. **2**(4): p. 221-5.

121. da Rocha, A.B., R.M. Lopes, and G. Schwartsmann, *Natural products in anticancer therapy.* Curr Opin Pharmacol, 2001. **1**(4): p. 364-9.

122. Cragg, G.M., D.J. Newman, and R.B. Weiss, *Coral reefs, forests, and thermal vents: the worldwide exploration of nature for novel antitumor agents.* Semin Oncol, 1997. **24**(2): p. 156-63.

123. D'Incalci, M., *Some hope from marine natural products.* Ann Oncol, 1998. **9**(9): p. 937-8.

124. Scheuer, P.J., *From the rainforest to the reef: searching for bioactive natural products in the mid-Pacific.* Med Res Rev, 1994. **14**(5): p. 487-503.

125. Pettit, G.R., et al., *Antineoplastic components of marine animals.* Nature, 1970. **227**(5261): p. 962-3.

126. Rinehart, K.L., *Antitumor compounds from tunicates.* Med Res Rev, 2000. **20**(1): p. 1-27.

127. Pommier, Y., et al., *DNA sequence- and structure-selective alkylation of guanine N2 in the DNA minor groove by ecteinascidin 743, a potent antitumor compound from the Caribbean tunicate Ecteinascidia turbinata.* Biochemistry, 1996. **35**(41): p. 13303-9.

128. Cvetkovic, R.S., D.P. Figgitt, and G.L. Plosker, *Et-743.* Drugs, 2002. **62**(8): p. 1185-92; discussion 1193-4.

129. Gago F., H.L.H., *Devising a structural basis for the potent cytotoxic effects of ecteinascidin 743.* . Demeunynck M, Bailly C, Wilson WD, editors. Small molecule DNA and RNA binders: from synthesis to nucleic acid complexes. Weinheim (Germany), 2002: p. 643-75

130. Hurley, L.H. and M. Zewail-Foote, *The antitumor agent ecteinascidin 743: characterization of its covalent DNA adducts and chemical stability.* Adv Exp Med Biol, 2001. **500**: p. 289-99.

131. D'Incalci, M. and C.M. Galmarini, *A review of trabectedin (ET-743): a unique mechanism of action.* Mol Cancer Ther, 2010. **9**(8): p. 2157-63.

132. Takebayashi, Y., et al., *Poisoning of human DNA topoisomerase I by ecteinascidin 743, an anticancer drug that selectively alkylates DNA in the minor groove.* Proc Natl Acad Sci U S A, 1999. **96**(13): p. 7196-201.

133. Damia, G., et al., *Unique pattern of ET-743 activity in different cellular systems with defined deficiencies in DNA-repair pathways.* Int J Cancer, 2001. **92**(4): p. 583-8.

134. D'Incalci, M., et al., *The combination of yondelis and cisplatin is synergistic against human tumor xenografts.* Eur J Cancer, 2003. **39**(13): p. 1920-6.

135. Zewail-Foote, M., et al., *The inefficiency of incisions of ecteinascidin 743-DNA adducts by the UvrABC nuclease and the unique structural feature of the DNA*

adducts can be used to explain the repair-dependent toxicities of this antitumor agent. Chem Biol, 2001. **8**(11): p. 1033-49.

136. Soares, D.G., et al., *Replication and homologous recombination repair regulate DNA double-strand break formation by the antitumor alkylator ecteinascidin 743.* Proc Natl Acad Sci U S A, 2007. **104**(32): p. 13062-7.

137. Tavecchio, M., et al., *Role of homologous recombination in trabectedin-induced DNA damage.* Eur J Cancer, 2008. **44**(4): p. 609-18.

138. Guirouilh-Barbat, J., C. Redon, and Y. Pommier, *Transcription-coupled DNA double-strand breaks are mediated via the nucleotide excision repair and the Mre11-Rad50-Nbs1 complex.* Mol Biol Cell, 2008. **19**(9): p. 3969-81.

139. Shao, L., et al., *Ecteinascidin-743 drug resistance in sarcoma cells: transcriptional and cellular alterations.* Biochem Pharmacol, 2003. **66**(12): p. 2381-95.

140. Bonfanti, M., et al., *Effect of ecteinascidin-743 on the interaction between DNA binding proteins and DNA.* Anticancer Drug Des, 1999. **14**(3): p. 179-86.

141. D'Incalci, M., et al., *Unique features of the mode of action of ET-743.* Oncologist, 2002. **7**(3): p. 210-6.

142. KW., S., *ET-743: more than an innovative mechanism of action*

. Anticancer Drugs 2002. **13[Suppl 1]**(:S3–6.).

143. Minuzzo, M., et al., *Interference of transcriptional activation by the antineoplastic drug ecteinascidin-743.* Proc Natl Acad Sci U S A, 2000. **97**(12): p. 6780-4.

144. Jin, S., et al., *Ecteinascidin 743, a transcription-targeted chemotherapeutic that inhibits MDR1 activation.* Proc Natl Acad Sci U S A, 2000. **97**(12): p. 6775-9.

145. Martinez EJ, C.E., Owa T., *Antitumor activity- and gene expression-based profiling of ecteinascidin Et 743 and phtha- lascidin Pt 650.* Chem Biol 2001

, 2001. **146**: p. 1-10

146. Synold, T.W., I. Dussault, and B.M. Forman, *The orphan nuclear receptor SXR coordinately regulates drug metabolism and efflux.* Nat Med, 2001. **7**(5): p. 584-90.

147. Aune, G.J., et al., *Von Hippel-Lindau-coupled and transcription-coupled nucleotide excision repair-dependent degradation of RNA polymerase II in response to trabectedin.* Clin Cancer Res, 2008. **14**(20): p. 6449-55.

148. Li, W.W., et al., *Sensitivity of soft tissue sarcoma cell lines to chemotherapeutic agents: identification of ecteinascidin-743 as a potent cytotoxic agent.* Clin Cancer Res, 2001. **7**(9): p. 2908-11.

149. Erba, E., et al., *Ecteinascidin-743 (ET-743), a natural marine compound, with a unique mechanism of action.* Eur J Cancer, 2001. **37**(1): p. 97-105.

150. Germano, G., A. Mantovani, and P. Allavena, *Targeting of the innate immunity/inflammation as complementary anti-tumor therapies.* Ann Med, 2011. **43**(8): p. 581-93.

151. Porta, C., E. Riboldi, and A. Sica, *Mechanisms linking pathogens-associated inflammation and cancer.* Cancer Lett, 2011. **305**(2): p. 250-62.

152. Allavena, P., et al., *Anti-inflammatory properties of the novel antitumor agent yondelis (trabectedin): inhibition of macrophage differentiation and cytokine production.* Cancer Res, 2005. **65**(7): p. 2964-71.

153. Germano, G., et al., *Antitumor and anti-inflammatory effects of trabectedin on human myxoid liposarcoma cells.* Cancer Res, 2010. **70**(6): p. 2235-44.

154. Negus, R.P., et al., *The detection and localization of monocyte chemoattractant protein-1 (MCP-1) in human ovarian cancer.* J Clin Invest, 1995. **95**(5): p. 2391-6.

155. Balkwill, F., *Cancer and the chemokine network.* Nat Rev Cancer, 2004. **4**(7): p. 540-50.

156. Mantovani, A., et al., *Cancer-related inflammation.* Nature, 2008. **454**(7203): p. 436-44.

157. Conti, I. and B.J. Rollins, *CCL2 (monocyte chemoattractant protein-1) and cancer.* Semin Cancer Biol, 2004. **14**(3): p. 149-54.

158. Bingle, L., N.J. Brown, and C.E. Lewis, *The role of tumour-associated macrophages in tumour progression: implications for new anticancer therapies.* J Pathol, 2002. **196**(3): p. 254-65.

159. Condeelis, J. and J.W. Pollard, *Macrophages: obligate partners for tumor cell migration, invasion, and metastasis.* Cell, 2006. **124**(2): p. 263-6.

160. Solinas, G., et al., *Tumor-associated macrophages (TAM) as major players of the cancer-related inflammation.* J Leukoc Biol, 2009. **86**(5): p. 1065-73.

161. Strieter, R.M., *Chemokines: not just leukocyte chemoattractants in the promotion of cancer.* Nat Immunol, 2001. **2**(4): p. 285-6.

162. Raman, D., et al., *Role of chemokines in tumor growth.* Cancer Lett, 2007. **256**(2): p. 137-65.

163. Karin, M., *Nuclear factor-kappaB in cancer development and progression.* Nature, 2006. **441**(7092): p. 431-6.

164. Ishihara, K. and T. Hirano, *IL-6 in autoimmune disease and chronic inflammatory proliferative disease.* Cytokine Growth Factor Rev, 2002. **13**(4-5): p. 357-68.

165. Klein, B., et al., *Paracrine rather than autocrine regulation of myeloma-cell growth and differentiation by interleukin-6.* Blood, 1989. **73**(2): p. 517-26.

166. Naugler, W.E. and M. Karin, *The wolf in sheep's clothing: the role of interleukin-6 in immunity, inflammation and cancer.* Trends Mol Med, 2008. **14**(3): p. 109-19.

167. Willeke, F., et al., *Overexpression of a member of the pentraxin family (PTX3) in human soft tissue liposarcoma.* Eur J Cancer, 2006. **42**(15): p. 2639-46.

168. Garlanda, C., et al., *Pentraxins at the crossroads between innate immunity, inflammation, matrix deposition, and female fertility.* Annu Rev Immunol, 2005. **23**: p. 337-66.

169. Clark, M.A., et al., *Soft-tissue sarcomas in adults.* N Engl J Med, 2005. **353**(7): p. 701-11.

170. Casali, P.G., R. Sanfilippo, and M. D'Incalci, *Trabectedin therapy for sarcomas.* Curr Opin Oncol, 2010. **22**(4): p. 342-6.

171. Brandon, E.F., et al., *In-vitro cytotoxicity of ET-743 (Trabectedin, Yondelis), a marine anti-cancer drug, in the Hep G2 cell line: influence of cytochrome P450 and phase II inhibition, and cytochrome P450 induction.* Anticancer Drugs, 2005. **16**(9): p. 935-43.

172. van Kesteren, C., et al., *Pharmacokinetics and pharmacodynamics of the novel marine-derived anticancer agent ecteinascidin 743 in a phase I dose-finding study.* Clin Cancer Res, 2000. **6**(12): p. 4725-32.

173. Beumer, J.H., et al., *Trabectedin (Yondelis, formerly ET-743), a mass balance study in patients with advanced cancer.* Invest New Drugs, 2005. **23**(5): p. 429-36.

174. Forouzeh B, H.M., Denis L, et al, *Phase I and pharmacokinetic study of ET-743, a minor groove DNA binder administered weekly to patients with advanced cancer. Proc Am Soc Clin Oncol.* Proc Am Soc Clin Onco, 2001. **20**: p. Abstract #373.

175. Ryan, D.P., et al., *Phase I and pharmacokinetic study of ecteinascidin 743 administered as a 72-hour continuous intravenous infusion in patients with solid malignancies.* Clin Cancer Res, 2001. **7**(2): p. 231-42.

176. Taamma, A., et al., *Phase I and pharmacokinetic study of ecteinascidin-743, a new marine compound, administered as a 24-hour continuous infusion in patients with solid tumors.* J Clin Oncol, 2001. **19**(5): p. 1256-65.

177. Villalona-Calero, M.A., et al., *A phase I and pharmacokinetic study of ecteinascidin-743 on a daily x 5 schedule in patients with solid malignancies.* Clin Cancer Res, 2002. **8**(1): p. 75-85.

178. Christinat, A. and S. Leyvraz, *Role of trabectedin in the treatment of soft tissue sarcoma.* Onco Targets Ther, 2009. **2**: p. 105-13.

179. Yovine, A., et al., *Phase II study of ecteinascidin-743 in advanced pretreated soft tissue sarcoma patients.* J Clin Oncol, 2004. **22**(5): p. 890-9.

180. Le Cesne, A., et al., *Phase II study of ET-743 in advanced soft tissue sarcomas: a European Organisation for the Research and Treatment of Cancer (EORTC) soft tissue and bone sarcoma group trial.* J Clin Oncol, 2005. **23**(3): p. 576-84.

181. Garcia-Carbonero, R., et al., *Phase II and pharmacokinetic study of ecteinascidin 743 in patients with progressive sarcomas of soft tissues refractory to chemotherapy.* J Clin Oncol, 2004. **22**(8): p. 1480-90.

182. Morgan JA, L.C.A., Chawla S, et al;, *Yondelis Sarcoma Study Group. Randomized phase II study of trabectedin in patients with liposarcoma and leiomyosarcoma (L-sarcomas) after failure of prior anthracylines (A) and ifosfamide (I).* J Clin Oncol., 2007. **25(june 20 Supplement**(18S, ASCO Annual Meeting Proceedings Part I Vol 25, No 18S (June 20 Supplement), 10060.).

183. Blay, J.Y., et al., *A phase II study of ET-743/trabectedin ('Yondelis') for patients with advanced gastrointestinal stromal tumours.* Eur J Cancer, 2004. **40**(9): p. 1327-31.

184. Grosso, F., et al., *Steroid premedication markedly reduces liver and bone marrow toxicity of trabectedin in advanced sarcoma.* Eur J Cancer, 2006. **42**(10): p. 1484-90.

185. Huygh, G., et al., *Ecteinascidin-743: evidence of activity in advanced, pretreated soft tissue and bone sarcoma patients.* Sarcoma, 2006. **2006**: p. 56282.

186. Grosso. Seattle, W.t.C.m., Nov 1–3, 2007. Abstract # 900 2007., *Trabectedin in Soft Tissue Sarcomas (STS) carrying a chromo- somal translocation: an exploratory analysis.* . 2007. **Nov 1–3, 2007. Abstract # 900 2007.**

187. M., D., *Final results of a phase II trial of 3-hr infusion trabectedin in patients with recurrent sarcomas.* Istanbul, Turkey: 31st ESMO Congress Sept 29 – Oct 3, 2006. Abstract # 524P 2006.

188. Casali, P.G., et al., *Some lessons learned from imatinib mesylate clinical development in gastrointestinal stromal tumors.* J Chemother, 2004. **16 Suppl 4**: p. 55-8.

189. Demetri, G.D., et al., *Efficacy and safety of sunitinib in patients with advanced gastrointestinal stromal tumour after failure of imatinib: a randomised controlled trial.* Lancet, 2006. **368**(9544): p. 1329-38.

190. Choi, H., et al., *CT evaluation of the response of gastrointestinal stromal tumors after imatinib mesylate treatment: a quantitative analysis correlated with FDG PET findings.* AJR Am J Roentgenol, 2004. **183**(6): p. 1619-28.

191. Panagopoulos, I., et al., *A novel FUS/CHOP chimera in myxoid liposarcoma.* Biochem Biophys Res Commun, 2000. **279**(3): p. 838-45.

192. Grohar, P.J., et al., *Ecteinascidin 743 interferes with the activity of EWS-FLI1 in Ewing sarcoma cells.* Neoplasia, 2011. **13**(2): p. 145-53.

193. Garcia-Carbonero, R., et al., *Ecteinascidin-743 (ET-743) for chemotherapy-naive patients with advanced soft tissue sarcomas: multicenter phase II and pharmacokinetic study.* J Clin Oncol, 2005. **23**(24): p. 5484-92.

194. Grosso, F., et al., *Trabectedin in myxoid liposarcomas (MLS): a long-term analysis of a single-institution series.* Ann Oncol, 2009. **20**(8): p. 1439-44.

195. Hollebecque, A., et al., *Inadequacy of size-based response criteria to assess the efficacy of trabectedin among metastatic sarcoma patients.* Invest New Drugs, 2010. **28**(4): p. 529-30.

196. Demetri, G.D., et al., *Efficacy and safety of trabectedin in patients with advanced or metastatic liposarcoma or leiomyosarcoma after failure of prior anthracyclines and ifosfamide: results of a randomized phase II study of two different schedules.* J Clin Oncol, 2009. **27**(25): p. 4188-96.

197. Ganjoo, K.N. and S.R. Patel, *Trabectedin: an anticancer drug from the sea.* Expert Opin Pharmacother, 2009. **10**(16): p. 2735-43.

198. Schoffski, P., et al., *Clinical impact of trabectedin (ecteinascidin-743) in advanced/metastatic soft tissue sarcoma.* Expert Opin Pharmacother, 2008. **9**(9): p. 1609-18.

199. Carter, N.J. and S.J. Keam, *Trabectedin : a review of its use in the management of soft tissue sarcoma and ovarian cancer.* Drugs, 2007. **67**(15): p. 2257-76.

200. Gronchi, A., et al., *Phase II clinical trial of neoadjuvant trabectedin in patients with advanced localized myxoid liposarcoma.* Ann Oncol, 2012. **23**(3): p. 771-6.

201. Nielsen, O.S., et al., *Effect of high-dose ifosfamide in advanced soft tissue sarcomas. A multicentre phase II study of the EORTC Soft Tissue and Bone Sarcoma Group.* Eur J Cancer, 2000. **36**(1): p. 61-7.

202. Lorigan, P., et al., *Phase III trial of two investigational schedules of ifosfamide compared with standard-dose doxorubicin in advanced or metastatic soft tissue sarcoma: a European Organisation for Research and Treatment of Cancer Soft Tissue and Bone Sarcoma Group Study.* J Clin Oncol, 2007. **25**(21): p. 3144-50.

203. Donald, S., et al., *Complete protection by high-dose dexamethasone against the hepatotoxicity of the novel antitumor drug yondelis (ET-743) in the rat.* Cancer Res, 2003. **63**(18): p. 5902-8.

204. Donald, S., et al., *Comparison of four modulators of drug metabolism as protectants against the hepatotoxicity of the novel antitumor drug yondelis (ET-743) in the female rat and in hepatocytes in vitro.* Cancer Chemother Pharmacol, 2004. **53**(4): p. 305-12.

205. Puchalski, T.A., et al., *Pharmacokinetics of ecteinascidin 743 administered as a 24-h continuous intravenous infusion to adult patients with soft tissue sarcomas: associations with clinical characteristics, pathophysiological variables and toxicity.* Cancer Chemother Pharmacol, 2002. **50**(4): p. 309-19.

206. Skorupa, A., et al., *Fatal rhabdomyolysis as a complication of ET-743 (Yondelis) chemotherapy for sarcoma.* Cancer Biol Ther, 2007. **6**(7): p. 1015-7.

207. Meco, D., et al., *Effective combination of ET-743 and doxorubicin in sarcoma: preclinical studies.* Cancer Chemother Pharmacol, 2003. **52**(2): p. 131-8.

208. Riccardi, A., et al., *Combination of trabectedin and irinotecan is highly effective in a human rhabdomyosarcoma xenograft.* Anticancer Drugs, 2005. **16**(8): p. 811-5.

209. Takahashi, N., et al., *Sequence-dependent enhancement of cytotoxicity produced by ecteinascidin 743 (ET-743) with doxorubicin or paclitaxel in soft tissue sarcoma cells.* Clin Cancer Res, 2001. **7**(10): p. 3251-7.

210. von Mehren, M., et al., *A phase I study of the safety and pharmacokinetics of trabectedin in combination with pegylated liposomal doxorubicin in patients with advanced malignancies.* Ann Oncol, 2008. **19**(10): p. 1802-9.

211. Aune, G.J., T. Furuta, and Y. Pommier, *Ecteinascidin 743: a novel anticancer drug with a unique mechanism of action.* Anticancer Drugs, 2002. **13**(6): p. 545-55.

212. Marchini, S., et al., *Molecular characterisation of two human cancer cell lines selected in vitro for their chemotherapeutic drug resistance to ET-743.* Eur J Cancer, 2005. **41**(2): p. 323-33.

213. Erba, E., et al., *Cell cycle phase perturbations and apoptosis in tumour cells induced by aplidine.* Br J Cancer, 2002. **86**(9): p. 1510-7.

214. Minuzzo, M., et al., *Selective effects of the anticancer drug Yondelis (ET-743) on cell-cycle promoters.* Mol Pharmacol, 2005. **68**(5): p. 1496-503.

215. Achilles, E.G., et al., *Heterogeneity of angiogenic activity in a human liposarcoma: a proposed mechanism for "no take" of human tumors in mice.* J Natl Cancer Inst, 2001. **93**(14): p. 1075-81.

216. Almog, N., et al., *Prolonged dormancy of human liposarcoma is associated with impaired tumor angiogenesis.* FASEB J, 2006. **20**(7): p. 947-9.

217. Taraboletti, G., et al., *Antiangiogenic and antitumor activity of IDN 5390, a new taxane derivative.* Clin Cancer Res, 2002. **8**(4): p. 1182-8.

218. Taraboletti, G., et al., *Antiangiogenic activity of aplidine, a new agent of marine origin.* Br J Cancer, 2004. **90**(12): p. 2418-24.

219. Kang, J.H., et al., *CCAAT box is required for the induction of human thrombospondin-1 gene by trichostatin A.* J Cell Biochem, 2008. **104**(4): p. 1192-203.

220. Goransson, M., et al., *Myxoid liposarcoma FUS-DDIT3 fusion oncogene induces C/EBP beta-mediated interleukin 6 expression.* Int J Cancer, 2005. **115**(4): p. 556-60.

221. O'Neill, L.P. and B.M. Turner, *Immunoprecipitation of native chromatin: NChIP.* Methods, 2003. **31**(1): p. 76-82.

222. O'Neill, L.P., M.D. VerMilyea, and B.M. Turner, *Epigenetic characterization of the early embryo with a chromatin immunoprecipitation protocol applicable to small cell populations.* Nat Genet, 2006. **38**(7): p. 835-41.

223. Gatta, R. and R. Mantovani, *NF-Y substitutes H2A-H2B on active cell-cycle promoters: recruitment of CoREST-KDM1 and fine-tuning of H3 methylations.* Nucleic Acids Res, 2008. **36**(20): p. 6592-607.

224. Aman, P., *Fusion genes in solid tumors.* Semin Cancer Biol, 1999. **9**(4): p. 303-18.

225. Goransson, M., M. Wedin, and P. Aman, *Temperature-dependent localization of TLS-CHOP to splicing factor compartments.* Exp Cell Res, 2002. **278**(2): p. 125-32.

226. Ron, D. and J.F. Habener, *CHOP, a novel developmentally regulated nuclear protein that dimerizes with transcription factors C/EBP and LAP and functions as a dominant-negative inhibitor of gene transcription.* Genes Dev, 1992. **6**(3): p. 439-53.

227. Grosso, F., *Trabectedin in Soft Tissue Sarcamos (STS) carrying a chromosomal traslocation: an explory analysis.* . 2007.

228. Hurley, L.H., *DNA and its associated processes as targets for cancer therapy.* Nat Rev Cancer, 2002. **2**(3): p. 188-200.

229. Broggini, M. and M. D'Incalci, *Modulation of transcription factor--DNA interactions by anticancer drugs.* Anticancer Drug Des, 1994. **9**(4): p. 373-87.

230. Dervan, P.B. and R.W. Burli, *Sequence-specific DNA recognition by polyamides.* Curr Opin Chem Biol, 1999. **3**(6): p. 688-93.

231. Broggini, M., et al., *DNA sequence-specific adenine alkylation by the novel antitumor drug tallimustine (FCE 24517), a benzoyl nitrogen mustard derivative of distamycin.* Nucleic Acids Res, 1995. **23**(1): p. 81-7.

232. Chiang, S.Y., et al., *Effects of minor groove binding drugs on the interaction of TATA box binding protein and TFIIA with DNA.* Biochemistry, 1994. **33**(23): p. 7033-40.

233. Yeh, W.C., et al., *Cascade regulation of terminal adipocyte differentiation by three members of the C/EBP family of leucine zipper proteins.* Genes Dev, 1995. **9**(2): p. 168-81.

234. Lin, F.T., et al., *A 30-kDa alternative translation product of the CCAAT/enhancer binding protein alpha message: transcriptional activator lacking antimitotic activity.* Proc Natl Acad Sci U S A, 1993. **90**(20): p. 9606-10.

Chapter 7 :

APPENDIX

7.1 Abbreviations

ATM ataxia-telangiectasia mutated

ATR ataxia-telangiectasia mutated and rad3-related bZIP basic leuzine zipper region

CDK cyclin dependent kinase

cDNA complementary deoxyribonucleic acid

CHK checkpoint kinase 2

C/EBP CCAAT/enhancer binding protein

CHOP C/EBP homologous protein

CT computed tomography

CR complete responde

CHOP DNA-damage-inducible transcript 3 (DDIT3,

GADD153)

DDLS dedifferentiated liposarcoma

DNA deoxyribonucleic acid

EGFP enhanced green fluorescent protein

EGFR epidermal growth factor receptor

ECOG PS, Eastern Cooperative Oncology Group performance status.

EWS Ewing sarcoma

FNA fine needle aspiration

FUS fusion (TLS)

GADD153 growth arrest and damage-inducible153

IBMX 3-Isobutyl-I-methylxanthin

IFN-" interferon-gamma

IHC immunohistochemistry

IL interleukin

ML myxoid liposarcoma

MM maintenance medium

MR minor response

MRI magnetic resonance imaging

PCNA proliferating cell nuclear antigen

pCR pathologic complete response

PD progression desease

PDGFR platelet derived growth factor receptor

PFS progression free survival

PLS pleomorphic liposarcoma

PPAR peroxisome proliferator-activated receptor pRB retinoblastoma protein

PR partial response

RCLS round cell liposarcoma

RNA ribonucleic acid

RT-PCR reverse transcription-polymerase chain reaction RXR retinoid X receptor

SCID severe combined immune deficient 8

SD stable disease

TNF-α tumour necrosis factor alpha

TLS translocated in liposarcoma (FUS) UVB ultraviolet B

VEGFR vascular endothelial growth factor receptor WDLS well-differentiated liposarcoma

WHO World Health Organization

---

iiii